ANALYSIS OF INTEGRAL MEMBRANE PROTEIN POM34P IN NUCLEAR PORE COMPLEX STRUCTURE AND FUNCTION

By

Mi Miao

Dissertation

Submitted to the Faculty of the

Graduate School of Vanderbilt University

in partial fulfillment of the requirements

for the degree of

DOCTOR OF PHILOSOPHY

in

Cell and Developmental Biology

May, 2007

Nashville, Tennessee

Approved:

Professor Susan R. Wente

Professor Kathleen L. Gould

Professor James R. Goldenring

Professor Todd R. Graham

To my parents and sister for their infinite support

ACKNOWLEDGEMENTS

At the end of my study in graduate school at Vanderbilt University, I am particularly grateful to my dissertation mentor Dr. Susan R. Wente for her academic guidance and career support. The path in science is a long and sort of “torturous” journey that needs great enthusiasm and persistence. Dr. Susan R. Wente always encouraged me and helped me to establish goals and pursue them with continuous effort. She gave me a chance to work in the nuclear pore complex field and provided the opportunity to let me chase my dreams. She is an excellent mentor and encourages me to stand high and overlook the direction with fundamental significance. I have often been very impressed by her sharp insight to the biological nature in science, which greatly inspires me to think in depth. I am educated to be independent but open for discussion, be thoughtful but critical to scientific concepts, and be goal-directed but cooperative with colleagues. After four years of work in the lab, I grew as a scientific researcher. The effort and patience from Dr. Susan R. Wente made all this possible.

I also owe many thanks for my thesis committee members, including Dr. Kathleen Gould, Dr. James Goldenring, Dr. Todd Graham, and previous committee member Dr. David Greenstein. The process of proposing questions, testing hypotheses, and interpretating results is critical in leading to an academic success, and also needs patience. The truth is often discovered from troubleshooting the experiments and analyzing the subtle differences in repeating the experiments. My committee members gave me great instructions and helped me in developing my graduate school study, which

would benefit all my life. I appreciate very much to their effort and encouragement when I am about to become an independent scientific researcher at this moment.

I am so grateful to my labmates, who have been working with me for four years. The many discussions with them effectively expanded my knowledge level and sparked ideas. Our laboratory is composed of multiple international persons, I am lucky to make friends with them and have the opportunity to talk about many topics, which led to a joyful life in graduate school. They showed great love and concern when I was in need of their help, which made me feel like a family. Vanderbilt University provided a delightful environment to study and work, and I will miss the golden time I spent here.

My family is always giving me endless encouragement wherever I am going and whenever I am talking with them. Their intellectual and emotional support accompanied me through the entire graduate school. My father and mother have shown me how to see life and cope with difficulties. I appreciate all their love and efforts throughout my path in pursuing the doctoral degree overseas. My sister is such a wonderful person who always cheers me up and chats with me. She and her beloved husband, as well as my newborn nephew, gave me much support and concern. I am grateful to all these above and would take them as precious treasure in the life.

TABLE OF CONTENTS

Page

LIST OF TABLES

LIST OF FIGURES

Chapter III

Chapter IV

LIST OF ABBREVIATIONS

3-AT	3-aminotriazole
Δ	Null
AL	Annulate lamellae
C	Carboxyl
cfu	Colony forming unit
Cub	C-terminal moiety of ubiquitin
DAPI	4′,6-diamidino-2-phenylindole
$DiOC_6$	3,3′-Dihexyloxacarbocyanineiodide
ER	Endoplasmic reticulum
feSEM	Field emission scanning electron microscopy
FG	Phenylalanine–glycine
GLFG	Glycine–leucine–phenylalanine–glycine
iFRAP	Inverse fluorescence recovery after photobleaching
IIF	Indirect immunofluorescence
INM	Inner nuclear membrane
Kap	Karyopherins
N	Amino
NE	Nuclear envelope
NEBD	NE break down
NEM	N-ethylmaleimide
NES	Nuclear export signal

NLS	Nuclear localization signal
NPC	Nuclear pore complex
Nub	N-terminal moiety of ubiquitin
Nup	Nucleoporin
ONM	Outer nuclear membrane
PMSF	Phenylmethylsulfonyl fluoride
Pom	Pore membrane proteins
pos	Pom synthetic lethal
RanGAP	Ran GTPase-activating protein
RanGEF	Ran guanine nucleotide exchange factor
RNP	Ribonucleoprotein
SPB	Spindle pole body
TEM	Thin section electron microscopy
TM	Transmembrane
VLCFA	Very long chain fatty acid
WGA	Wheat germ agglutinin

CHAPTER I

INTRODUCTION

In eukaryotes, the nuclear envelope (NE) separates the nucleus from the cytoplasm and facilitates the highly specialized compartmentalization of genetic information. All intranuclear activities, such as DNA replication, gene transcription, ribosome biosynthesis *etc*., rely on the successful trafficking of biomolecules across the NE. This nucleocytoplasmic transport is mediated through the nuclear pore complex (NPC), which is embedded at the site where the outer nuclear membrane (ONM) and inner nuclear membrane (INM) join together. The precise regulation of bidirectional transport across the nuclear pore requires complete and functional NPCs. A normal budding yeast nucleus contains approximately 200 NPCs while a vertebrate cell nucleus has on the order of 2000 NPCs (MAUL *et al.* 1972; WINEY *et al.* 1997). The whole complex has a predicted mass of ~44 MDa in *Saccharomyces cerevisiae* and 60 MDa in vertebrates (CRONSHAW *et al.* 2002; ROUT *et al.* 2000). In-depth proteomics studies of NPCs from budding yeast and mammalian cells have revealed a proteinaceous complex consisting of ~30 different protein components (CRONSHAW *et al.* 2002; ROUT *et al.* 2000), termed nucleoporins (Nups). A highly regulated process is required to organize these various Nups into a functional complex. To study how the Nups assemble and insert into the NE during the NPC assembly will improve the understanding of NPC structural organization and its function in nucleocytoplasmic transport.

Morphological study of NPCs

Electron microscopy of freeze-etched rat kidney cell nuclei demonstrated that NPCs are not distributed evenly in the NE (MAUL *et al.* 1971). The pore-to-pore space ranges from approximately 130 nm to 620 nm. In most cell types NPCs are localized in such a random manner. This unequal distribution pattern at the nuclear surface may reflect the accommodation of highly active transport events adjacent to certain intranuclear compartments, or preferential localization correlated to sub- and peri-nuclear supportive structures.

Ultrastructural studies (reviewed by SUNTHARALINGAM and WENTE 2003) suggested that NPCs are organized with 8-fold radial symmetric architecture relative to the perpendicular axis across the NE, with a tripartite mode along the NE plane. As demonstrated in Fig 1-1, its central framework, composed of a spoke-ring complex, is joined by eight fibrils on the cytoplasmic side and one nuclear basket on the intranuclear side. The central framework consists mainly of 8 spokes sandwiched by a cytoplasmic ring and a nuclear ring structure. A channel wherein nuclear transport takes place is embraced in the middle. Electron microscopy often reveals a central plug in the framework. However, its molecular nature is still controversial (STOFFLER *et al.* 2003). As part of the transport path through the NE, the cytoplasmic filaments and nuclear basket play a role in the docking of transport cargos. The overall NPC structure is evolutionally conserved between *S. cerevisiae* and higher eukaryotes, although the vertebrate NPC is larger and might contain additional core substructures (ADAM 2001). The structural similarity indicates that they might have a conserved mechanism in molecular organization and function.

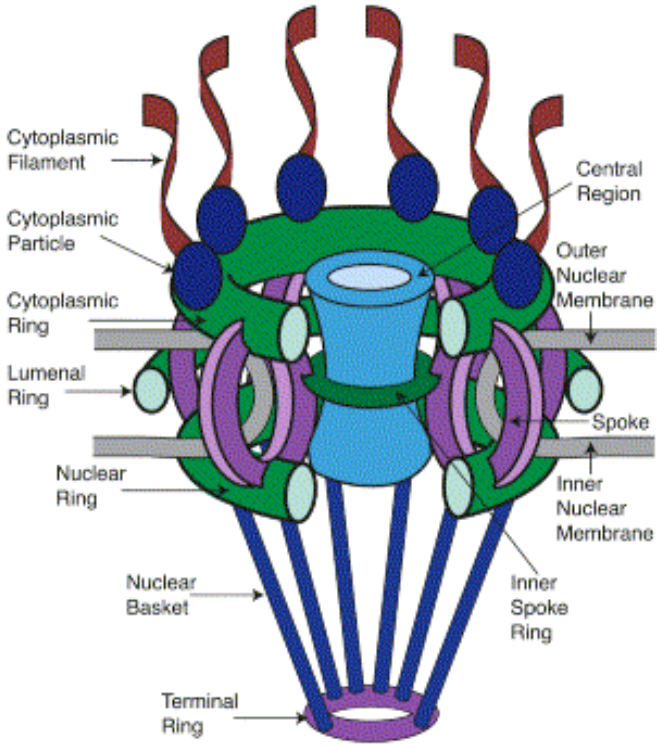

Figure 1-1: Schematic diagram of NPC structure and composition (reprinted from SUNTHARALINGAM and WENTE 2003). The representative NPC from vertebrates is depicted. It is embedded in the NE with cytoplasmic side positioned on top and nuclear side on bottom. Corresponding names of substructure are labeled. The overall NPC is also in 8-fold symmetry related to the perpendicular axis across the NE. A portion of structure is removed for clarity.

This ring-like central framework is embedded inside of the NE pore, which is 25-30 nm thick in budding yeast (YANG *et al.* 1998) and 50-60 nm thick in vertebrates (GOLDBERG and ALLEN 1996; PANTE and AEBI 1996). The overall dimensions of NPCs from amphibian are about ~120 nm in width along the NE plane, and ~180 nm in length perpendicular to the NE plane. The tomographic 3-D reconstruction of vertebrate NPCs has observed eight distinct "handles" which might reside in the NE lumen (STOFFLER *et al.* 2003). These "handles" protrude from the NPC framework and extend beyond the adjacent nuclear membrane. They are presumably formed by integral membrane proteins. It is conceivable that these membrane proteins are playing a critic role in NPC anchorage. In vertebrates there is a lamina structure underneath the nuclear membrane that provides a physical support and flexible platform for NE morphology. The lamina network may also interact with the nuclear face of NPCs and act as an anchor (HAWRYLUK-GARA *et al.* 2005; SMYTHE *et al.* 2000). However, there is no homolog of lamina components identified in *S. cerevisiae* so far.

Nucleoporins: the building blocks for NPCs

The ~ 30 Nups can be divided into two general categories, FG-Nups and non-FG Nups. The former group is named after its phenylalanine-glycine (FG) motif repeats and primarily functions in the nucleocytoplasmic transport process. The latter group is generally involved in forming the NPC framework. Interestingly, only one third of all *S. cerevisiae* Nups are encoded by essential genes, suggesting that there is extensive functional redundancy among NPC components. This is evident from the various genetic relationships among Nups. Consistent with the architectural similarity between *S.*

cerevisiae and metazoan NPCs, most Nups share a certain level of sequence homology (MANS *et al.* 2004).

In agreement with the modular structure of NPCs, the Nups form several different subcomplexes that can be biochemically isolated (summarized in Fig 1-2). Technical improvements, such as TAP-tagged purification followed by mass spectrometry analysis, or FRET assay, have allowed the NPC subcomplex list to be refined (DAMELIN and SILVER 2002; LUTZMANN *et al.* 2005). Several Nups are included in multiple subcomplexes. It is noteworthy that these interactions might be unstable and dynamic in response to different NPC functional requirements (LUSK *et al.* 2002). The Nup85p-Nup120p subcomplex in budding yeast is analogous to Nup107-Nup160 subcomplex in vertebrates, and plays a critical role in NPC assembly (LUTZMANN *et al.* 2005; WALTHER *et al.* 2003a, discussed in following sections). The Nup188p and Nup170p subcomplexes in budding yeast are both composed of large molecular mass Nups, and contribute to approximately 25% of the total NPC mass (AITCHISON *et al.* 1995). These two Nup subgroups are speculated to form a bulky NPC framework and provide a structural base for assembly of peripheral components.

Among all Nup molecules identified in *S. cerevisiae*, only three are defined as pore membrane proteins (POMs), *i.e.*, yNdc1p, Pom152p, and Pom34p. yNdc1p is the only membrane protein encoded by essential gene and has a dual distribution between the spindle pole body (SPB) and NPC (CHIAL *et al.* 1998). Pom152p and Pom34p are both dispensable for cell viability and are exclusively localized to NPCs (ROUT *et al.* 2000). The integral membrane Nups in vertebrates are vNdc1, POM121, and gp210. Of them, only vNdc1 shares primary sequence homology and adopts the same membrane topology

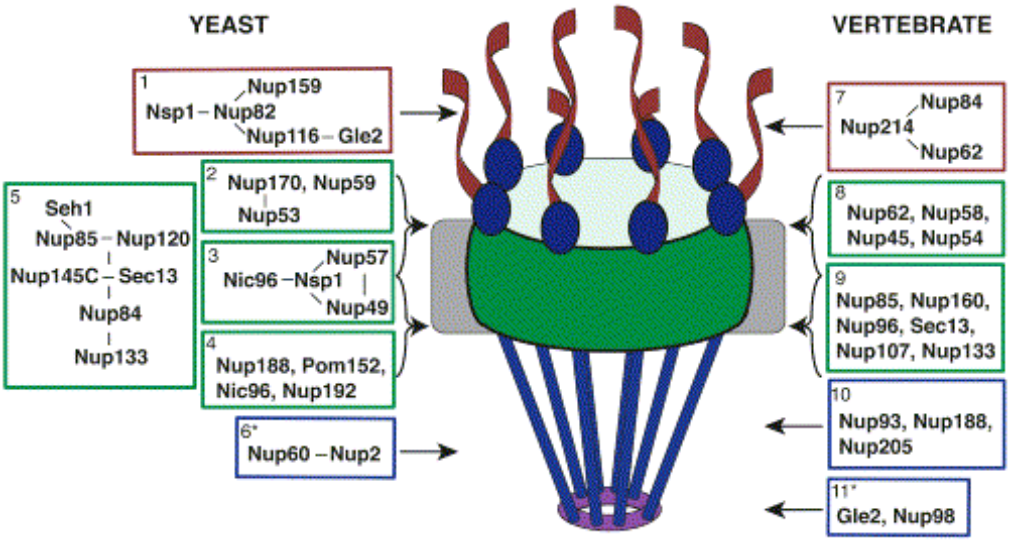

Figure 1-2: Nups form subcomplexes inside of the NPC (reprinted from SUNTHARALINGAM and WENTE 2003). The NPC is depicted with its cytoplasmic side on top and its intranuclear side at bottom. Nups from the same subcomplex are included in a single box. Various subcomplexes from *S. cerevisiae* and vertebrate cell are listed at left and right side, respectively. The dashes indicate the defined interaction, whereas the commas indicate less defined association.

as its *S. cerevisiae* counterpart (LAU *et al.* 2006; MANSFELD *et al.* 2006). The membrane orientation of all Poms in NPCs has been defined (Fig1-3). Strikingly, many metazoan species lack one of the NPC membrane proteins (MANS *et al.* 2004). Moreover, even cells from different human tissues do not necessarily contain all three Poms (OLSSON *et al.* 2004), implying a functional redundancy between these three membrane proteins. Combined RNAi treatment against one or two integral membrane Nups in HeLa cells also caused additive defects in NPC structural organization (MANSFELD *et al.* 2006).

Although morphological studies with electron microscopy have suggested that Poms may bridge the NPC architecture and nuclear membrane (STOFFLER *et al.* 2003), limited information is known about the physical interaction between Poms and peripheral Nups. This is probably due to the highly hydrophobic motifs contained in integral membrane Nups and the consequent difficulty in biochemical characterization. In budding yeast, Pom152p is reported to form a complex with Nup188p (NEHRBASS *et al.* 1996). A recent study has revealed that vNdc1 interacts with Nup53, implying a role in recruiting the Nup53-Nup93 subcomplex for NPC biogeneration (MANSFELD *et al.* 2006). The role of Poms in anchoring peripheral Nups was well demonstrated in a recent report (STAVRU *et al.* 2006b). Ectopic localization of POM121 to mitochondria recruits the FG-Nups, as well as several structural Nups including Nup62, Nup205, Nup98, and Nup358, to the mitochondrial membrane, suggesting that POM121 may be sufficient to assemble a portion of NPC substructures. More effort is required to dissect the physical network between Poms and other Nups. There are also interactions between Nups and adjacent subcellular supporting structures. For example, Nup153 directly interacts with lamin B in

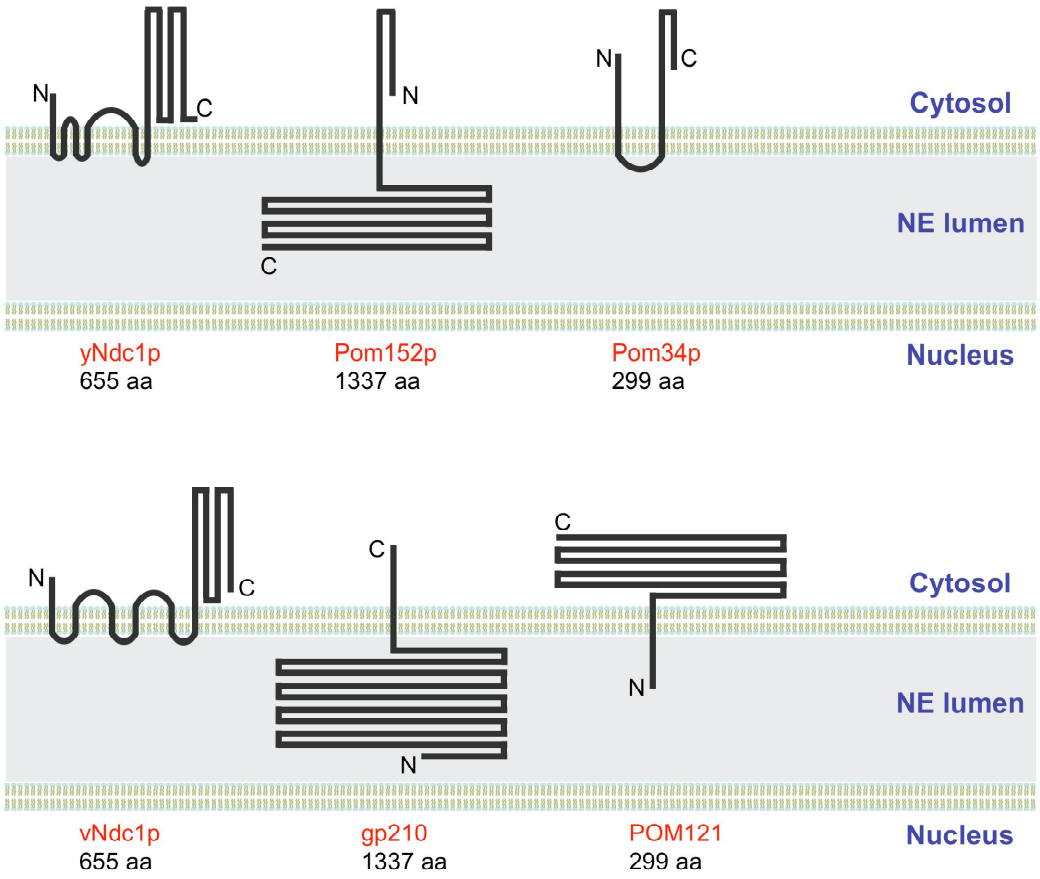

Figure 1-3: The schematic diagram of the topological orientation of Poms in *S. cerevisiae* and vertebrates. In top panel, three integral membrane Nups from budding yeast cell are depicted relative to their membrane integration topology. N- and C-terminus orientation of each protein are labeled. In the bottom panel, three integral membrane Nups from vertebrate cells are depicted in a similar manner.

vertebrates (SMYTHE *et al.* 2000), indicating the potential for multiple mechanisms operating to anchor NPCs to the NE.

In the past two decades, numerous *NUP* mutants have been generated and used to study the structural organization of the NPC. Particularly, several mutants with defective NE morphology have been isolated. At the restrictive temperature, the nuclear membrane of *nup116* null (Δ) cells protrudes at the cytoplasmic side of NPC and seals over the top of the pore complex. Nuclear export continues in these cells and cargo accumulates underneath the sealed NE to generate a "herniation-like" abnormality. The molecular nature of this perturbation is still unknown (WENTE and BLOBEL 1993). Overexpression of *NUP53* leads to another type of membrane defect, highly proliferated intranuclear double membrane stacks. This double membrane lamellae, adjacent to the INM, is characterized by transcisternal pores and association of Pom152p and Ndc1p. However, there is no electron dense material apparent in the pores. When *NUP170* is deleted from the *NUP53*-overexpressing cells, the membrane stacks are not observed (MARELLI *et al.* 2001). In vertebrates, overproduction of POM121 or Nup153 induces the generation of annulate lamellae (AL, see below) in the cytosol containing well assembled pore complexes (DAIGLE *et al.* 2001). These intriguing observations suggest a close relationship between nuclear membrane morphology and NPC components.

Computational and biochemical efforts have been conducted to seek the evolutionary ancestor of NPCs (DEVOS *et al.* 2004). Secondary structure prediction has revealed that a subset of budding yeast Nups, *e.g.*, the Nup84p-Nup120p subcomplex, are composed of β-propeller and α-solenoid motifs. This motif organization, particularly the N-terminal β-propeller followed by an α-solenoid, is distinctive and also found in the heavy chain of

clathrin. The similar motif arrangement implies a common evolutionary origin. Interestingly, Sec13p is a shared component between NPC and COPII trafficking vesicles. In vertebrates, the COPI coatomer complex is targeted to NE through Nup358 and Nup153 and involved in NE break down (NEBD) at the entry to mitosis (LIU *et al.* 2003; PRUNUSKE *et al.* 2006). Considering the highly curved membrane surface at both the nuclear pore domain and trafficking vesicles, these lines of evidence may implicate that they share a common structure stabilization mechanism.

Nucleocytoplasmic transport through the NPC

As the only portal access embedded inside the NE, NPCs play an essential role in nucleocytoplasmic trafficking. There are two types of nuclear transport mediated through the NPCs, namely nonselective transport and selective transport. The nonselective transport is conducted by passive diffusion down a concentration gradient. Metal ions, small metabolites, and a portion of biomolecules use this mechanism to reach an equal distribution across the nuclear membrane. Several studies have indicated that the molecular size limit of passive diffusion is about 40 kD. The permeability of NPCs is impaired in several Nup mutants (GALY *et al.* 2003; SHULGA *et al.* 2000), suggesting that the structural integrity of NPCs is critical for a biologically appropriate permeability limit.

Multiple large biomolecules use the selective nuclear transport mechanism to traffic across the nuclear membrane. The enzymes for DNA replication and transcription, various transcription factors as well as histones are imported into the nucleus. Ribosomes, mRNA as well as tRNA are exported into the cytoplasm. This process is energy

dependent and facilitated by two basic categories of molecules, the karyopherins (Kaps) and the RanGTPase cycle components. The detailed process is described in Fig 1-4. The Kaps refer to a family of 14 different transporters that recognize the nuclear localization signal (NLS) and/or nuclear export signal (NES) harbored in the cargo molecules (reviewed by CHOOK and BLOBEL 2001). Different cargo has a specific binding affinity for a certain type of Kap. The RanGTPase cycle is critical in providing the energy and dictating the directionality of the transport processes (reviewed by GORLICH and KUTAY 1999). In *S. cerevisiae*, the RanGTPase is encoded by *GSP1* and *GSP2*. The spatial segregation of GTP-bound Ran inside the nucleus and GDP-bound Ran in the cytoplasm is achieved by a guanine nucleotide exchange factor (RanGEF) Prp20p that is restricted to the nucleus, and a GTPase-activating protein (RanGAP) Rna1p restricted to cytosol, respectively. The import of RanGDP into the nucleus also requires the Ntf2p import factor. The switch between GTP-bound Ran and GDP-bound Ran leads to the association or release of cargo molecules from Kaps at specific locations, and hence the directed nuclear transport.

The FG-Nups are a subset of Nups that specifically interact with the Kaps during passage through the NPCs. Various biochemical experiments have detected direct physical interactions between them (ALLEN *et al.* 2001; PYHTILA and REXACH 2003). In a systematic study to pinpoint the necessity of FG motifs in nuclear transport, multiple FG repeats in combination were deleted to examine the effect on a series of Kap-mediated transport pathways (STRAWN *et al.* 2001). This study revealed that the mass of FG-Nups was not crucial for the cell viability or the nuclear pore permeability barrier. However, certain FG-repeats harbored in some Nups played more important roles than the rest in

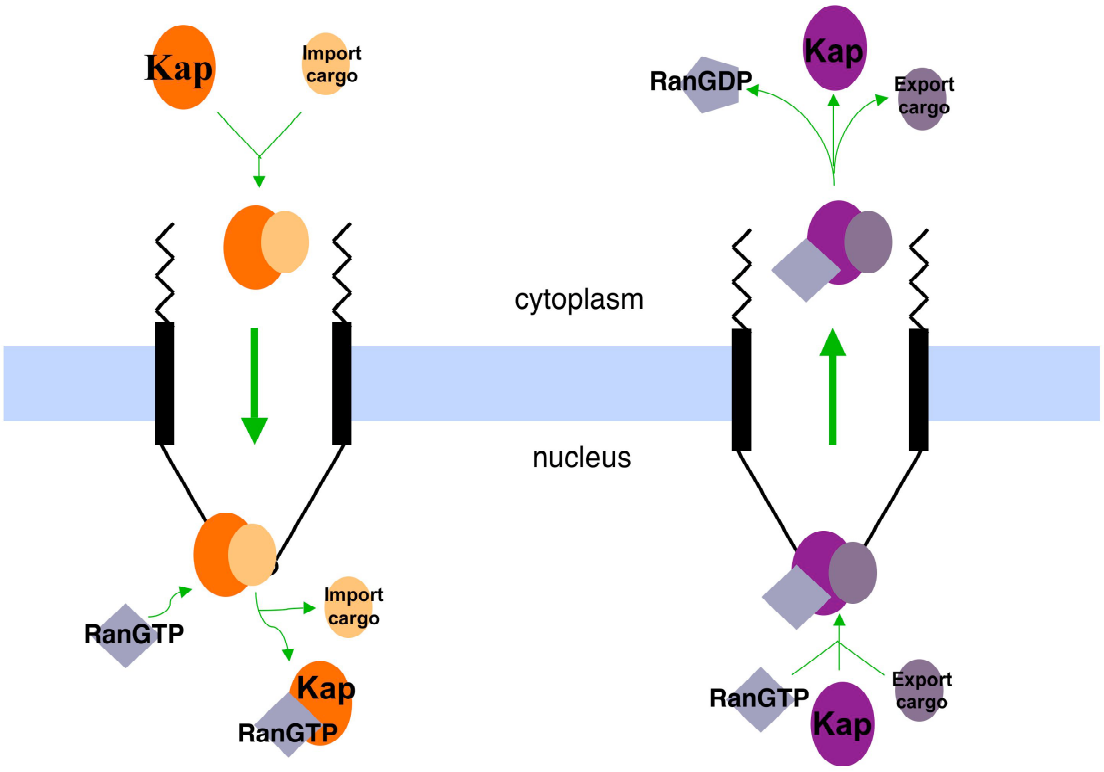

Figure 1-4: The nucleocytoplasmic transport cycle. (A) During import, the Kaps recognize the NLS sequence contained in the import cargo molecules and bind to the cargo at the cytoplasm. The Kap-cargo complex is imported through the NPC. In the nucleus, binding of RanGTP to Kaps leads to the disassociation of Kap-cargo complex. (B) During export, the Kaps binds to both NES-containing export cargo and RanGTP in the nucleus, and the RanGTP-Kap-Cargo complex is exported through the NPC. In the cytoplasm, hydrolysis of RanGTP to RanGDP results in the dissociation of Kap-cargo complex. The hydrolysis of RanGTP to RanGDP and the regeneration of RanGTP are facilitated by the cytoplasmically localized RanGAP and the nuclearly localized RanGEF, respectively. The chemical gradient of RanGTP across the NE determines the directionality of nulceocytoplasmic transport.

nucleocytoplasmic transport process, suggesting a heterogeneity of FG repeats in forming a transport passage. Moreover, different Kap-mediated transport pathways were affected by the deletion of different FG motif combinations, indicating the existence of multiple transport pathways through the NPCs.

Dynamic NPC architecture organization

NPC assembly is a dynamic process that occurs throughout the cell cycle. In metazoan cells undergoing an open mitosis, the NPCs disassemble along with the NE at the entry into mitosis, and then reassemble on the surface of nascent chromatin at the exit from mitosis. This stage of NPC assembly, called postmitotic assembly, is a process coordinated with the reformation of the nuclear membrane. However, NPCs are of lowest abundance at the end of mitosis. To accommodate the high volume of nuclear transport during the cell cycle, the biogenesis of NPCs continues through interphase and reaches its highest level before the onset of the next mitosis. In HeLa cells, NPC levels almost double from early G1 to the end of cell cycle (MAUL *et al.* 1972). This stage of NPC assembly in metazoan, termed interphase assembly, requires insertion of proteinaceous structures into an intact NE and may utilize a mechanism distinct from postmitotic NPC assembly. On the other hand, in single cell eukaryotes undergoing a closed mitosis, *e.g.*, *S. cerevisiae*, the NE remains intact during the entire cell cycle (WINEY *et al.* 1997). All NPC assembly events occur in the enclosed double nuclear membrane. At this point, it is postulated that budding yeast cells may utilize a mechanism analogous to that used by metazoans in assembling Nups during interphase.

It is noteworthy that NPC assembly not only takes place at the NE, but also occurs in the cytosol within certain type of cells. These NPCs are contained in cytoplasmic membrane stacks, named AL, which are frequently observed in rapidly dividing cells including those from embryonic or tumor tissue. Pore complexes in AL are very similar in composition and structure to NPCs in the NE except for lack of uniform bipolar arrangement along the NE (IMREH and HALLBERG 2000; SUNTHARALINGAM and WENTE 2003). These pore complexes are considered to be a storage form of NPCs to accommodate the functions of fast-growing cell. However, exchange between the two types of pore complexes still needs to be experimentally determined.

Ultrastructural research of NPCs demonstrated that the NPC is not in a rigid form. In NRK cells, NPCs undergo elastic conformational changes on the nucleus of migrating cells (DAIGLE *et al.* 2001). The dynamic organization of NPCs is also evident from the subtle structural modifications observed during nuclear transport. The cytoplasmic filaments bend over to interact with the import cargos (PANTE and AEBI 1996). The nuclear basket is rearranged to adapt to the export of Balbiani ring ribonucleoprotein (RNP) particles (KISELEVA *et al.* 1996). Several studies also suggested that the NPC is able to adjust the functional pore size to accommodate the transport of large cargo (FELDHERR *et al.* 2001; PANTE and KANN 2002). These observations support a flexible NPC architecture. In budding yeast, NPCs exhibit free lateral mobility on the surface of nuclear membrane (BUCCI and WENTE 1997). However, NPCs in higher eukaryotes are restrained to individual foci (DAIGLE *et al.* 2001), probably due to the close connection between NPCs and the underlying lamina network.

Once assembled, the overall structure of the NPC is stable and has a very low turnover rate (DAIGLE *et al.* 2001). Nonetheless, its components are not all in stationary association with the pore complex. Inverse fluorescence recovery after photobleaching (iFRAP) analysis has been widely used to determine the association kinetics of individual Nups within NPCs (RABUT *et al.* 2004). According to studies with NRK cells, 19 Nups tested could be sorted into three distinct categories. The first group of Nups have a residence time in the NPC of over 35 hours and barely disassociate during the cell cycle. This group includes most components of the Nup107-Nup160 subcomplex, as well as Nup214, Nup93 and ALADIN, which are proposed to form the NPC scaffold. The second group of Nups have a residence time in the range of several minutes and fast disassociation from NPCs. This group, which includes gp210, Nup153, and Nup50, is proposed to be more involved in the transport function of the NPC. Other Nups with median disassociation rates may be more likely to act as structural adaptors between the core framework and peripheral substructure. This group of Nups include Pom121, Nup62, Nup58, hCG1, Nup35 and Nup98.

The stepwise process of NPC assembly

To study NPC assembly events taking place in metazoans, a *Xenopus in vitro* nuclear reconstitution system is widely used to imitate the postmitotic condition inside of cells. The membrane-free cytosolic fraction and membrane vesicles fraction have been prepared from *Xenopus* eggs, and loaded onto the decondensed *Xenopus* sperm chromatin to observe the assembly of NE and NPC. Previous studies have showed that the membrane vesicles bind to the sperm chromatin and fuse to form a closed double nuclear

membrane (MACAULAY and FORBES 1996). These vesicles are speculated to contain Pom and other NE membrane proteins. Those integral membrane proteins are likely to induce the generation of nascent nuclear pore across the NE. Along with the enclosure of NE, peripheral Nups are recruited and assembled into a mature pore complex. This proposed stepwise process of NPC assembly is summarized in Fig1-5.

The NE/NPC assembly process observed in the *Xenopus in vitro* nuclear reconstitution system can be blocked by several reagents (MACAULAY and FORBES 1996). Pretreatment of membrane vesicles with the alkylating agent N-ethylmaleimide (NEM) blocks the fusion step needed to form a complete NE. Adding the Ca^{2+} chelator BAPTA causes the inhibition of *de novo* NPC assembly, as indicated by fused nuclear membranes devoid of nuclear pores. However, application of GTPγS inhibits both the membrane vesicle fusion step and the following NPC assembly step occurring at the enclosed nuclear membranes. The application of these block reagents helps to define the order of NPC assembly events and dissect the underlying mechanism.

Several studies with *S. cerevisiae* have revealed factors involved in NPC assembly. In a genetic screen aimed at identifying novel *S. cerevisiae* mutants defective in NPC assembly, several conditional alleles encoding RanGTPase cycle components have been identified (RYAN *et al.* 2003). These mutations include alleles of *NTF2*, *RNA1*, *PRP20* and *GSP1*. All of the mutant strains show mislocalization of Nup-GFP fusion proteins at the nonpermissive temperature. Treatment of cells with protein synthesis inhibitor cycloheximide indicates that Nup mislocalization is due to a defective NPC assembly process, but not a degradation of preexisting NPCs. Ultrastructural studies have detected several abnormalities, such as extended cytoplasmic membrane stretches, lobulated

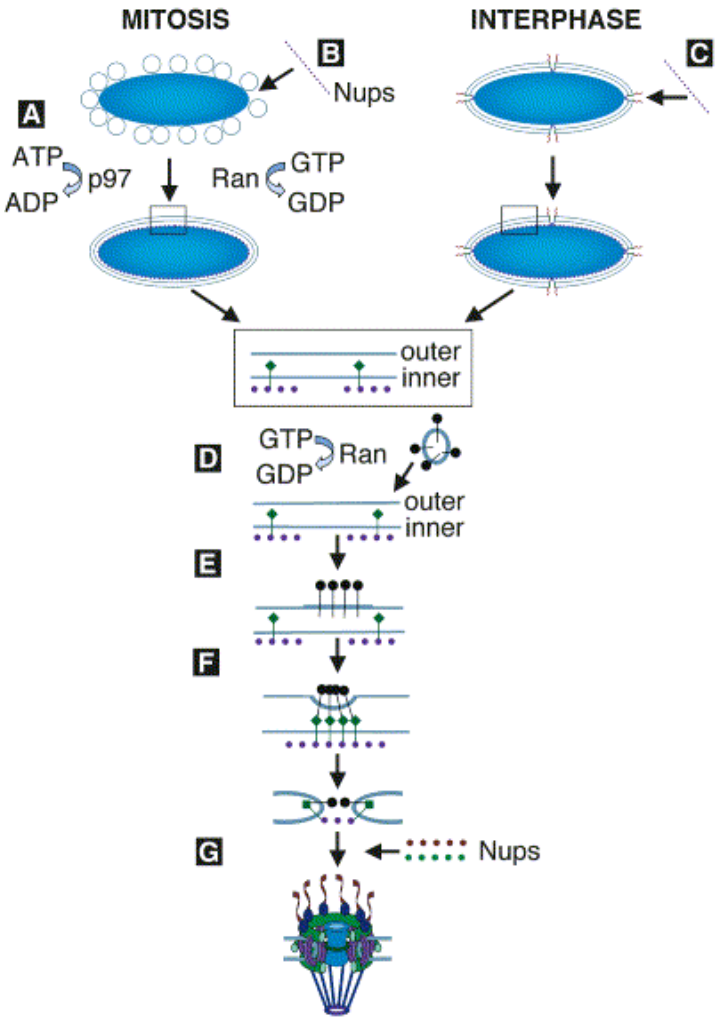

Figure 1-5: Stepwise assembly of the NPC (reprinted from SUNTHARALINGAM and WENTE 2003). The entire postmitotic and interphase NPC assembly pathways are depicted. (A) In vertebrate cells undergoing open mitosis, membrane vesicles bind to chromatin and fuse to form an enclosed NE by the end of mitosis. RanGTPase and p97 ATPase are suggested to be involved in this step. (B) A portion of Nups is preassociated with nascent chromatin before NE enclosure. (C) At interphase, or in *S. cerevisiae* undergoing closed mitosis, a portion of Nups is hypothesized to be imported into nucleus through preexisting NPC. (D) The Nup and Pom containing cytoplasmic vesicles are speculated to fuse with complete NE in both vertebrate and budding yeast cells. The RanGTPase cycle is suggested to be involved in this step. (E) The fusion of Nup and Pom-containing vesicles results in enriched Nup concentration at certain NE sites. (F) Integral membrane proteins are hypothesized to trigger or facilitate the fusion event between outer and inner nuclear membranes and form a nuclear pore. (G) More Nups are recruited to the newly generated nuclear pore and assembled into a mature NPC.

nuclear region, and invaginated NE. More notably, there is an accumulation of 80-100 nm vesicles in the cytosol, particularly with the mutant allele *prp20-G282S* (encoding a *S. cerevisiae* form of RanGEF). Gold-conjugated immunoelectron microscopy demonstrated that these vesicles are indeed associated with mislocalized Nups. In light of the subcellular fractionation studies of vesicle composition, it is hypothesized that these vesicles are Nup-enriched assembly intermediates ready to be recruited to the NE for NPC assembly.

A recent report has suggested that *KAP95*, encoding the *S. cerevisiae* homolog of importin β1, also plays a role in NPC assembly (RYAN *et al.* 2006). Using the conditional allele *kap95-E126K*, the Nup-GFP fusion proteins are mislocalized at the restrictive temperature. This mutant allele causes several intracellular membrane defects at the ultrastructural level. Extended and distorted membrane stacks are seen both in the nucleus and cytosol. Electron dense material, presumably NPCs, is found in between the intranuclear membrane stacks, or underneath the INM without full penetrance across the NE. However, vesicle accumulation is not as predominant as in the *prp20-G282S* mutant. Interestingly, the deletion of the RanGTP binding domain in Kap95p results in a dominant negative effect, *i.e.*, the alteration of GFP-Nup localization, suggesting a functional link between Kap95p and RanGTP in NPC assembly.

In agreement with this, the coordinative effect between RanGTPase and importin β is also observed in vertebrates (HAREL *et al.* 2003a; WALTHER *et al.* 2003b). In the *Xenopus in vitro* assembly system, RanGTP and importin β act as positive and negative regulators, respectively, in NE membrane vesicle fusion and the subsequent NPC assembly steps. Their antagonistic relationship is evidenced by the inhibitory effect of importin β in NE

vesicle fusion being reversed by adding RanQ69L, a mutant unable to hydrolyze GTP. It was suggested that RanGTP is required to release several Nups, including Nup107, Nup153, and Nup358, from association with importin β, and then target them to the chromatin surface for NPC assembly (WALTHER *et al.* 2003b). Overproduction of RanGTP or depletion of importin β leads to the formation of AL with pore complexes, suggesting that the balance between RanGTP and importin β is necessary for NE/NPC biogenesis. Further studies (HAREL *et al.* 2003a) showed that the NPC assembly step blocked by importin β comes after the GTPγS and BAPTA sensitive steps. But the negative effect of importin β in NPC assembly process is not reversed by excess RanGTP, indicating that the relationship between RanGTP and importin β is more complicated in the NPC assembly step than in the NE formation step.

Although the postmitotic NE/NPC assembly process can be experimentally divided into two phases, *i.e.*, NE membrane vesicle fusion and NPC assembly, these two steps are related and happen rapidly upon the exit from mitosis. For instance, the integral membrane Nups might be included in the NE membrane vesicles. Depletion of this subset of Nups prevents the formation of a complete NE. Moreover, several Nups are recruited to the periphery of nascent chromatin in the absence of fragmented NE membrane vesicles. This group of Nups includes the Nup107-Nup160 subcomplex, Nup153 and POM121. It is still unclear whether the fusion step in forming the NE precedes Nup recruitment in forming the NPC, or alternatively, whether the essential preassociation of Nups with chromatin triggers the subsequent NE membrane vesicle fusion.

A key group of Nups in vertebrates, the Nup107-Nup160 subcomplex, is attracting increased attention in the NPC assembly field (HAREL *et al.* 2003b; WALTHER *et al.*

2003a). This subset of Nups is recruited to *Xenopus* sperm chromatin earlier than other NPC components including the FG-Nups, and even before the enclosure of the nuclear membrane. Immunodepletion of this subcomplex of Nups leads to a closed NE devoid of NPC structures on the chromatin surface, as examined by field emission scanning electron microscopy (feSEM). Consistent with this, decreasing the expression level of several components of this complex in HeLa cells results in the lack of FxFG-Nups signals around the nuclear rim, and reduces the NPC density about 3 fold. These observations suggested that the Nup107-Nup160 subcomplex is essential for subsequent NPC assembly, probably providing the seeding foci to define the NPC assembly site. In budding yeast there is a subcomplex of conserved homologs, *i.e.*, Nup84p-Nup120p subcomplex. Deletion mutants of four individual Nups from this subcomplex have an NPC clustering phenotype (reviewed by DOYE and HURT 1997). Most combinations of two mutant alleles from this complex result in the synthetic lethality. It is postulated that this subgroup might play a conserved role in NPC assembly.

Interphase NPC assembly in vertebrates takes place on the continuous nuclear membrane, similar to the assembly events that happen in budding yeast cells. Although there is a lack of NE membrane vesicle fusion step at this stage, the above regulatory molecules may also be involved. The identification of NPC assembly defects in *S. cerevisiae* RanGTPase cycle and *KAP95* mutants is a strong indication of a unified mechanism for NPC assembly between budding yeasts and higher eukaryotes. Besides, Poms might diffuse through the continuous network of ER/NE to reach the critical assembly site, and soluble Nups might be imported through preexisting NPCs for access to chromatin. These potential mechanisms are speculated to recapitulate the events

occurring during postmitotic assembly. The NPC structures assembled at the postmitotic phase are not different from the ones assembled during interphase, suggesting that two stages of NPC assembly may converge through a common assembly pathway.

The role of integral membrane Nups in NPC assembly

Several intermediate structures of the stepwise NPC assembly process have been observed in the *Xenopus in vitro* assembly system through feSEM studies (GOLDBERG *et al.* 1997). As shown in Fig 1-6, these structures, named "star-ring", "thin-ring", *etc*. are speculated to be partially assembled NPCs at nuclear membranes. When NPC biogenesis is blocked by wheat germ agglutinin (WGA) or BAPTA, the proportion of assembly intermediates greatly increases. Interestingly, "dimple-like" membrane deformations are also observed on the ONM, presumably at the site where NPC assembly initiates. Based on these discoveries, a hypothesis related to the "porogenic" events is proposed (GOLDBERG *et al.* 1997). In order to generate a pore in the continuous nuclear membrane, the ONM and INM are pulled in close opposition to favor a final fusion event. The newly generated nuclear pore is unstable and is in dynamic transition until further recruitment of peripheral Nups. The assembly of peripheral Nups occurs in stepwise manner and thus allows various incomplete pore complexes to be visualized, particularly when the process is blocked with chemical reagents. It is assumed that integral membrane proteins are playing significant roles in both the ONM-INM fusion and subsequent Nup anchorage processes.

The three Poms from vertebrates are contained in different vesicle populations as indicated from the membrane vesicle fractionation with *Xenopus* egg extract (MANSFELD

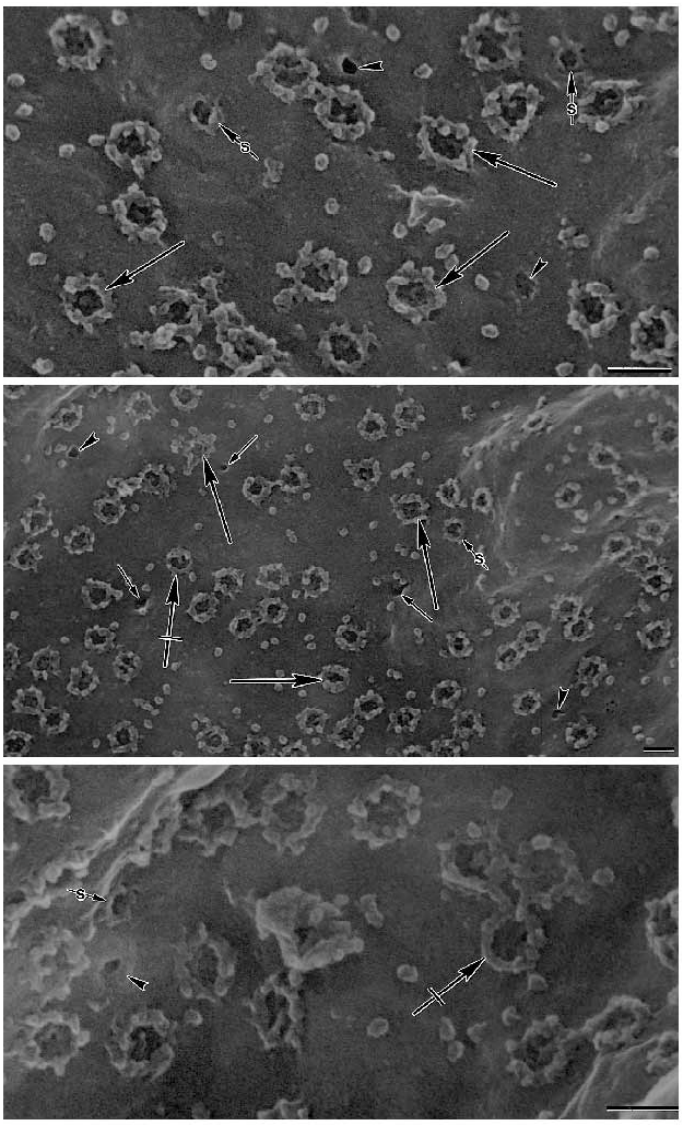

Figure 1-6: Morphology of NPC assembly intermediates (reprinted from GOLDBERG *et al.* 1997). In the *Xenopus in vitro* nucleus reconstitution system, the NE and NPCs formed on the surface of sperm chromatin were fixed 40 min after initiation of assembly, and visualized by feSEM. Mature NPCs (large arrows), dimples (small arrows), stabilizing pores (arrowheads), star-rings (arrows marked 's'), and late intermediates (crossed arrows). Bars, 100nm.

et al. 2006). POM121-containing vesicles are able to bind the decondensed sperm chromatin, suggesting a role in postmitotic NPC assembly. Immunodepletion of POM121 from membrane or removal of POM121-containing vesicles effectively reduces the formation of a complete NE as well as NPCs at sperm chromatin periphery. However, removal of gp210 does not lead to any detectable effect. The defect with POM121 depletion is rescued by adding back recombinant POM121 (ANTONIN *et al.* 2005). Several studies illustrate that POM121 is recruited early to the nascent chromatin surface, even before the enclosure of the NE (BODOOR *et al.* 1999). Interestingly, the inhibition of NE fusion by POM121 depletion is suppressed by codepletion of the Nup107-Nup160 complex, suggesting a coordinative effect between membrane proteins and soluble Nups in postmitotic NE/NPC biogenesis (ANTONIN *et al.* 2005). However, contradictory results were reported regarding whether there is an NPC assembly defect in mammalian cells after RNAi treatment against POM121, probably due to the different target sequences and cell types selected in the experiments (ANTONIN *et al.* 2005; STAVRU *et al.* 2006b). The weak binding affinity of gp210 to sperm chromatin and its late recruitment to the nuclear periphery suggests that it might be involved in a late stage of NPC assembly, or mediate the nuclear transport function of NPCs.

vNdc1 is a multipass transmembrane protein. Its unique topological orientation may provide a broad surface for interaction with other soluble factors. This protein is essential for NPC assembly according to several *in vivo* and *in vitro* investigations (MANSFELD *et al.* 2006; STAVRU *et al.* 2006a). vNdc1-containing vesicles exist in similar or overlapping vesicle fractions as POM121-containing vesicles in *Xenopus* egg extract. *In vitro* NE/NPC formation with the sperm chromatin is blocked if vNdc1 is depleted from the

membrane fraction. Elimination of vNdc1 expression in mammalian cells and *C. elegans* leads to decreased FG-Nup assembly at the nuclear rim. Although the depletion of vNdc1 or POM121 has a similar defect in NE/NPC formation, their function is not exchangeable, as evidenced by the inability of one Pom to rescue the other. Interestingly, gp210 knockdown significantly attenuates the FG-Nup localization to the nuclear rim when combined with vNdc1 knockdown in HeLa cells. The combination of vNdc1 and POM121 knockdown results in a small nucleus in addition to the FG-Nups assembly defect (MANSFELD *et al.* 2006). These observations suggest that Poms might function in a synergistic manner during NPC biogenesis process.

A conditional allele from *S. cerevisiae*, *ndc1-39*, shows defects in the incorporation of a GFP-Nup49 fusion protein into NPCs at the restrictive temperature. It also has an enhanced growth defect when combined with another NPC assembly mutant, *nic96-1* (LAU et al. 2004). However the precise function of yNdc1p in the NPC is still unclear, probably due to its dual role in both SPB and NPC structural organization. *POM152* is a nonessential gene and has a synthetic lethal relationship with several genes encoding components from the Nup170p subcomplex and Nup188p subcomplex. Thin section EM studies of *pom152*Δ *nup170*Δ double mutant cells showed a long stretch of nuclear membrane devoid of detectable NPCs and massive invaginated NE into the cytosol, suggesting that Pom152p is important in maintaining NE morphology in certain mutant backgrounds (AITCHISON *et al.* 1995; NEHRBASS *et al.* 1996). When yNdc1p and Pom152p are co-depleted, Nup159p, Nup59p, as well as Nup60p have reduced signals at the nuclear periphery and increased signals in the cytoplasm, and nuclear import function is perturbed. Ultrastructural studies revealed that a major portion of nuclear pores lack

electron dense material, and occasionally there exist enlarged pores with vacant structure (MADRID *et al.* 2006). Pom34p is a newly identified integral membrane Nup (ROUT *et al.* 2000). Its function was first characterized in this thesis study.

Disassembly of NPC during mitosis

As discussed previously, the overall structure of the NPC is stable during the cell cycle in both *S. cerevisiae* and higher eukaryotes. However, it disassembles rapidly at the entry into mitosis in metazoans which undergo an open mitosis. As with other mitotic events, this process is triggered by the mitotic cyclin complex, Cdk1-cyclinB (MPF). The phosphorylation of Nups is critical to induce the disassembly of NPCs. Consensus phosphorylation sites are found in the primary sequences of several vertebrate Nups. Further analysis reveals that some Nups, *e.g.*, Nup214/CAN, Nup358, Nup153, and gp210 (FAVREAU *et al.* 1996), do indeed undergo phosphorylation at the initial stage of mitosis. In agreement with this, NPC reassembly at mitotic exit requires phosphatases. Inhibition of major protein phosphatases PP1 and PP2A in *Drosophila* embryos leads to rapid disassembly of the NPC (ONISCHENKO *et al.* 2005).

The above NPC disassembly event is correlated with NEBD. However, NPC disassembly generally happens prior to NEBD. feSEM and thin section electron microscopy (TEM) studies with *Drosophila* embryos indicate that NPC disassembly is fundamentally a reversal of assembly, but in a more rapid manner (KISELEVA *et al.* 2001). The peripheral substructures, *e.g.*, the cytoplasmic filaments and the central plug, are removed at the very beginning, leaving the "star ring" structure as a dominant form on the NE. The "star ring" is finally removed before the closure of the pore. Morphological

studies of starfish oocytes showed that the passive diffusion limit of nuclear pores increases during the disassembly process (LENART *et al.* 2003). The evidence from *Aspergillus nidulans* shows that a subset of Nups is disassembled from the NPC in mitosis, whereas the core substructure stays associated with the nuclear pore (DE SOUZA *et al.* 2004; OSMANI *et al.* 2006). Interestingly, the Pom152p homolog in *Aspergillus nidulans* remains associated with the residual pore complex, suggesting a role of integral membrane Nups in maintaining the core NPC structure. This partial disassembly of NPCs in some fungal species undergoing closed mitoses indicates that the step-wise disassembly hypothesis may be a common feature conserved during evolution.

These previous studies support the hypothesis that integral membrane proteins, whether *bona fide* NPC components or not, are playing a crucial role in NPC biogenesis and function. The goal of this dissertation is to test this hypothesis by examining the function of integral membrane proteins in NPC structural organization. In chapter II, Pom34p, a recently identified *S. cerevisiae* NPC integral membrane Nup, was characterized through a combination of genetics and morphology study approaches. In chapter III, the relationship between *POM34* and *POM152* has been investigated, and a synthetic lethal screen approach was used in an attempt to reveal novel assembly factors. In chapter IV, a modified yeast two hybrid screen is discussed. Moreover, future research directions with NE/NPC integral membrane proteins have been proposed. This combined work sheds light into the role of membrane proteins in NPC assembly and contribute to the understanding of general mechanisms in forming a pore-like structure in subcellular membranes.

CHAPTER II

THE INTEGRAL MEMBRANE PROTEIN POM34P FUNCTIONALLY LINKS NUCLEOPORIN SUBCOMPLEXES

Introduction

In eukaryotic cells, translocation of macromolecules across organellar membranes requires specialized protein complexes embedded at the sites of entry and/or exit (SCHNELL and HEBERT 2003). Nucleocytoplasmic transport is mediated through nuclear pore complexes (NPCs) anchored in a nuclear envelope (NE) pore. These NPCs are formed from the assembly of at least 30 nucleoporins (Nups), in multiple copies each, that are organized in biochemically discrete subcomplexes and localized to specific NPC substructures (FAHRENKROG and AEBI 2003; SUNTHARALINGAM and WENTE 2003). In sum, NPCs have a predicted mass of ~44 MDa in *Saccharomyces cerevisiae* and 60 MDa in vertebrates (CRONSHAW *et al.* 2002; ROUT *et al.* 2000). Three-dimensional morphology studies have observed close contact between the proteinaceous NPC structure and surrounding NE (pore membrane), supporting models wherein nuclear *po*re *m*embrane proteins (Poms) play key roles in organizing NPC architecture (ALLEN *et al.* 2000; BECK *et al.* 2004; STOFFLER *et al.* 2003). Moreover, the interactions between integral membrane proteins in the lumen are speculated to promote fusion of the inner and outer nuclear membranes for formation of the nuclear pore in the intact NE (GOLDBERG *et al.* 1997). The mechanisms by which the membrane fusion and subsequent

This chapter is adapted from "The integral membrane protein Pom34p functionally links nucleoporin subcomplexes. Miao M, Ryan KJ, Wente SR. Genetics 2006 172(3): 1441-57"

recruitment of distinct NPC subcomplexes occur have not been fully elucidated.

Two out of three vertebrate Poms have been well characterized: gp210 and Pom121. Both are type I transmembrane proteins with single membrane-spanning segments and their amino (N)-terminal regions positioned in the NE lumen (GREBER *et al.* 1990; HALLBERG *et al.* 1993; SODERQVIST and HALLBERG 1994; WOZNIAK *et al.* 1989). However, they share no sequence homology and likely play distinct roles in NPC structure and function. Most of the gp210 mass is lumenally localized. In contrast, the majority of Pom121 is exposed to the cytosolic/pore side of the membrane. After integration into the endoplasmic reticulum (ER), gp210 and Pom121 are sorted to the nuclear pore membrane by lateral diffusion through the functionally continuous ER (IMREH *et al.* 2003; YANG *et al.* 1997). During postmitotic NE reformation in mammalian cells, Pom121 is recruited to the nuclear periphery at a very early stage, while the recruitment of gp210 occurs relatively late (BODOOR *et al.* 1999). Fluorescence recovery after photobleaching experiments with interphase NPCs has shown that gp210 is notably dynamic with a relatively rapid exchange rate at NPCs. In contrast, Pom121 is markedly stable with a much slower exchange rate (ERIKSSON *et al.* 2004; RABUT *et al.* 2004). Finally, in a recent study of mitotic *in vitro* NPC/NE assembly (ANTONIN *et al.* 2005), inhibition of Pom121 function or depletion of Pom121-containing vesicles blocks membrane vesicle fusion around chromatin. Depletion of gp210 vesicles does not perturb assembly. However, it is unknown whether Pom121 is sufficient for pore formation and whether this is linked to gp210 roles in NPC structure and function. Taken together, Pom121 likely plays a central role in regulating NE/NPC biogenesis and anchorage of the NPC in the NE.

Whereas the majority of the peripheral Nups are structurally or functionally conserved across species (SUNTHARALINGAM and WENTE 2003), gp210 and Pom121 do not possess any significant sequence similarity with proteins predicted from the open reading frames annotated in the *S. cerevisiae* genome. Instead, three distinct Poms have been identified in budding yeast: Ndc1p, Pom152p, and Pom34p (CHIAL *et al.* 1998; ROUT *et al.* 2000; WOZNIAK *et al.* 1994). Ndc1p is the only Pom encoded by an essential gene, harbors six or seven potential membrane-spanning regions, and is localized to both NPCs and spindle pole bodies (CHIAL *et al.* 1998). Unlike Ndc1p, both Pom152p and Pom34p reside exclusively within the NPC (ROUT *et al.* 2000; WOZNIAK *et al.* 1994). Pom152p is a type II integral membrane protein with a single transmembrane segment and the majority of the protein positioned in the NE lumen (TCHEPEREGINE *et al.* 1999). Several studies have revealed roles for Ndc1p and Pom152p in NPC molecular organization. A conditional *ndc1-39* allele has genetic interactions with another NPC assembly mutant *nic96-1*, and at the restrictive temperature *ndc1-39* cells have defects in incorporating Nup49p into the NPC (LAU *et al.* 2004). Although *POM152* is dispensable for cell growth, the *pom152* null (Δ) mutant results in lethality when combined with mutants allelic to *NUP170*, *NUP188*, *NUP59*, or *NIC96* (AITCHISON *et al.* 1995; NEHRBASS *et al.* 1996). The *pom152*Δ *nup170*Δ double mutant has massive NE extensions and invaginations and long stretches of NE without detectable NPCs.

Pom34p was discovered in a comprehensive proteomics study of enriched S. cerevisiae NPCs, and localization and biochemistry results have indicated that Pom34p is a novel NPC constituent (ROUT *et al.* 2000). However, its function in NPC structure and function remains uncharacterized. In this report, we have conducted a series of

experiments to define the membrane topology of Pom34p. Using genetic approaches, we have demonstrated that Pom34p has broad functional interactions with other Nups. By dissecting the functional domains of Pom34p and examining the influence on NPC structure in the context of nup mutants, we provide evidence that Pom34p is involved in the molecular organization of NPC.

Materials and methods

Yeast strains

The *S. cerevisiae* strains were grown in either rich (YPD: 1% yeast extract, 2% peptone, 2% glucose) or synthetic minimal (SM) media lacking appropriate amino acids and supplemented with 2% glucose. 5-Fluoroorotic acid (5-FOA; United States Biological) was used at a concentration of 1.0 mg/ml. Kanamycin resistance (KAN^R) was selected on medium containing 200 μg/ml G418 (United States Biological). Yeast transformations were performed using the lithium acetate method (ITO *et al.* 1983), and general yeast manipulations were conducted as described elsewhere (Sherman et al. 1986).

All *S. cerevisiae* strains used in this work are listed in Table 2-1. Unless indicated otherwise, the null (Δ) mutants used in these studies were obtained from Research Genetics (Birmingham, AL). The *pom34*Δ::*spHIS5* strain was made according to the method of (BAUDIN *et al.* 1993) with pGFP-HIS5 (gift from J. Aitchison) as template and two 80-mer oligonucleotides (1314, GTG CTA ATA GTA ATA ATG ATA GAA ATA ATA ACA ATT AAT AAG ATG GTT ATG ATG AAC GGT GAA GCT CAA

AAA CTT ATT; 1316, ATA CTT ATT TCC AAA CTA TTG GTA ATG GTT GCC GCT AAT CAT ATG TAA AAT ATA AAT AGG AGC TGA CGG TAT CGA TAA GCT T). PCR amplification generated a *GFP-spHIS5* fragment flanked on one end by ～60 bp of sequence with homology 138–82 bp upstream of the *POM34* coding region and on the other end by ～60 bp of sequence with homology 50–110 bp downstream. The resulting fragment contained the full-length *Schizosaccharomyces pombe HIS5* (homologous to *S. cerevisiae HIS3*) and a *GFP* sequence that lacked a promoter. The fragment was transformed and integrated into diploid SWY595 cells. The resulting heterozygous diploid was sporulated, and tetrads were dissected to obtain viable haploid null strains (SWY2565 and SWY2566). PCR was used to confirm the integration.

Plasmids and cloning

Cloning of wild-type *POM34*: The plasmids used in this work are described in Table 2-2.

Epitope-tagged *POM34*: Using pSW1516 as a template with forward primer 1668 (introducing *Spe*I and sequence encoding the myc epitope before the sequence for the fourth amino acid of Pom34p) and reverse primer 1653, PCR was used to generate a fragment that was digested with *Spe*I/*Sac*I and ligated with the promoter sequence of pSW3186, resulting in pSW3193 (*myc-POM34*).

Construction of *SUC2*-fused genes: A fragment encoding a c-myc fusion to Suc2p (*myc-SUC2*) was obtained using PCR and the template pSW939 with the following oligonucleotide pairs: forward primer 1681 (introducing *Spe*I and sequence for the myc epitope before the sequence for *SUC2*) and reverse primer 1703 (introducing *Spe*I after

the *SUC2* sequence) or forward primer 1679 (introducing *Sac*I and the sequence encoding for the myc epitope before the *SUC2* sequence) and reverse primer 1682 (introducing *Sac*I and the sequence encoding for the myc epitope after the *SUC2* sequence). The resulting *myc-SUC2* or *myc-SUC2-myc* sequences were digested with either *Spe*I or *Sac*I and inserted in frame into pSW3193 or pSW3188, respectively, generating plasmids with the gene fusions *myc-SUC2-myc-POM34* (encoding Suc2p^{myc}-Pom34p) (pSW3189) or *POM34-myc-SUC2-myc* (encoding Pom34p-Suc2p^{myc}) (pSW3190). A 5.26-kb fragment encoding the full-length *POM152* plus its flanking 800-bp promoter and 440-bp terminator regions was cloned into the *Pst*I sites of pRS315 and pRS425 to obtain pSW3191 and pSW863, respectively. The coding sequence of *POM152* (pSW3191) for amino acids 1026–1337 was removed by *Sac*I digestion and replaced in frame by the above PCR product *myc-SUC2-myc* (from primers 1682 and 1679 with the pSW939 template). The resulting pSW3192 encoded a Pom152p-myc-Suc2p-myc (Pom152p-Suc2p^{myc}) fusion protein.

Deletion of transmembrane segment 1 or transmembrane segment 2: The sequence-encoding protein A (containing four tandem repeats of IgG-binding domain) was obtained by PCR using the template pFA6a-CTAP-MX6 (TASTO *et al.* 2001). The *Sac*II/*Sac*I-digested PCR product was cloned in frame into pSW3188 to yield pSW3195, which encodes Pom34p-PrA. Using pSW3195 as a template, a *pom34* DNA fragment lacking the coding region for potential transmembrane segment (TM)1 was amplified by PCR, using the primers 1688, 5′-AATTA CCC GGG AAC AAC ACT CAT GTT GGG AGA C-3′ and 1691, 5′-ATATA CCC GGG CGT CTC CAT TTC CTT GTT TAC-3′ (exogenous *Sma*I sites underlined). Similarly, the TM2 deletion fragment was amplified

with the primers 1690, 5′-AATTA CCC GGG AAA GTA AGT GAT TTG AAT CTC-3′ and 1689, 5′-ATATA CCC GGG TTC TGC ATT CAA CCA ACT GAA C-3′(with exogenous *Sma*I sites underlined). The *Sma*I-digested PCR products were ligated to generate pSW3196 (TM1Δ-PrA) and pSW3197 (TM2Δ-PrA), respectively. The resulting deletion proteins had TM1 (residues 62–85) or TM2 (residues 129–153) replaced by proline and glycine derived from an exogenous *Sma*I restriction site.

Other *POM34* constructs: The following oligonucleotides were used to generate the *POM34* deletion/truncation variants: 1657, 5′-ATATA GAG CTC TTA GAG ATT CAA ATC ACT TAC TTT-3′ (exogenous *Sac*I site underlined); 1652, 5′-AATTA ACT AGT GTA AAC AAG GAA ATG GAG ACG-3′(exogenous *Spe*I site underlined); 1691; 1690; and the vector-based T3 and T7. Using template pSW1516 and combinations of these primers, DNA fragments of various truncation forms of *POM34* were obtained by PCR and cloned into pRS425 or pSW3187 to generate pSW3036, pSW3042, pSW3198, and pSW3199. *pom34*-Δ*C* (sequence for residues 161–299 deleted), *pom34*-Δ*N* (residues 4–54 deleted), *pom34*-Δ*N*Δ*C* (residues 4–54 and 161–299 deleted), and *pom34*-Δ*TM* (residues 62–153 deleted) were obtained, respectively.

Protein manipulation

Biochemical fractionation: Fifty milliliters of cells grown to midlog phase (OD600 = 0.4–0.5) in SM-leu/2% glucose were harvested by centrifugation. All of the following steps were in the presence of 1× protease inhibitor cocktail (Roche Applied Science, Indianapolis). Cell pellets were pretreated (100 mM Tris, pH 9.4 and 10 mM DTT) for 10 min at room temperature, washed in spheroplast wash buffer [SWB: 1.2 M sorbitol, 20

mM HEPES, pH 7.4, and 0.5 mM phenylmethylsulfonyl fluoride (PMSF)], and then resuspended in 1 ml SWB with 0.1 mg/ml zymolyase 20T and 0.1 ml glusulase for 1.5 hr at 30˚C. After spheroplasting, cells were washed twice with 1.2 M sorbitol, 20 mM PIPES, pH 6.5, 1 mM $MgCl_2$, and 0.5 mM PMSF; resuspended in 1 ml lysis buffer (20 mM HEPES, pH 7.4, 5 mM $MgCl_2$, and 0.5 mM PMSF); and incubated on ice for 20 min with occasional vortexing. The resulting total (T) lysate was centrifuged at 14,000 × g at 4˚C for 45 min to yield a low-speed supernatant (S1) and postnuclear pellet (P1) fractions. For alkaline extraction, the P1 fraction was resuspended in extraction buffer (20 mM HEPES, pH 7.5, 5 mM $MgCl_2$, 150 mM NaCl, 0.5 mM PMSF, and 0.1 M Na_2CO_3, pH 11), incubated on ice for 20 min, and pelleted at 14,000 × g at 4˚C for 45 min. The resulting supernatant (S2) was combined with the prior S1, yielding the total S fraction. Equivalent amounts of the T lysate and S1 or S were precipitated with trichloroacetic acid (TCA) for analysis with corresponding equivalents of the P1 or P2 fractions. All fractions were separated by electrophoresis in SDS polyacrylamide gels for immunoblot analysis. Immunoblotting was conducted with the following antibodies: rabbit anti-Snl1p (1:100, HO *et al.* 1998), rabbit anti-Nup145C (1:100, EMTAGE *et al.* 1997), mouse monoclonal anti-myc (9E10, 1:500; Covance), rabbit anti-mouse (IgG, 1:1000; ICN Pharmaceuticals), rabbit anti-Nup116 glycine–leucine–phenylalanine–glycine (GLFG) (1:2500, BUCCI and WENTE 1998), rabbit anti-Nsp1p (1:2500, NEHRBASS *et al.* 1990), mouse monoclonal anti-Pgk1p (mAb22C5, 1:1000; Molecular Probes, Eugene, OR), and mouse monoclonal anti-Nop1p (mAb D77, 1:25; ARIS and BLOBEL 1988).

Endoglycosidase H treatment: Fifty milliliters of budding yeast cells were harvested at midlog phase. Whole-cell lysates were prepared by glass bead lysis in 350 µl lysis

buffer (20 mM Tris, pH 6.5, 5 mM $MgCl_2$, 2% Triton X-100, 150 mM NaCl) supplemented with 1× protease inhibitor mixture and 0.5 mM PMSF. The cells were vortexed vigorously for 12 min (1 min on, 2 min rest on ice) and then centrifuged at ~200 × g for 10 min. Fifty microliters of the resulting supernatant were added to 150 μl 0.1 M sodium phosphate buffer (pH 5.6), 0.5 mM PMSF, and digested with 15 milliunits endoglycosidase H (Endo H) (Roche Molecular Biochemicals) at 37˚C for 4 hr. For mock samples, the Endo H was eliminated. Samples were precipitated with TCA and separated by electrophoresis in SDS polyacrylamide gels for analysis by immunoblotting.

Fluorescence microscopy

Indirect immunofluorescence experiments were performed as described previously (WENTE *et al.* 1992), following a 10-min fixation in 3.7% formaldehyde and 10% methanol. The fixed cells were incubated for 16 hr at 4˚C with mAb414 (1:2 tissue culture supernatant, DAVIS and BLOBEL 1986), mouse monoclonal mAb118C3 against Pom152p (1:2 tissue culture supernatant, STRAMBIO-DE-CASTILLIA *et al.* 1995), or affinity-purified rabbit polyclonal against the Nup116GLFG region (1:800, BUCCI and WENTE 1998). Bound antibody was detected by incubation with Alexa 594-conjugated goat anti-mouse IgG (1:400 dilution) or Alexa 594-conjugated goat anti-rabbit IgG (1:300) for 60 min at room temperature. The cells were stained with 0.05 μg/ml 4′,6-diamidino-2-phenylindole (DAPI) before visualizing under the fluorescence microscope (model BX50; Olympus, Lake Success, NY) using an Uplan 100×/1.3 objective. Images were captured using a digital camera (Photometrics Cool Snap HQ; Roper Scientific)

with MetaVue software (Universal Imaging, West Chester, PA). Images were processed using Adobe Photoshop 7.0.

Results

Pom34p is a double-pass transmembrane protein with both the N and the carboxy (C) terminus located on the cytosolic/pore side.

Hydropathy analysis of the Pom34p amino acid sequence identified two hydrophobic regions that could potentially serve as transmembrane segments (Figure 2-1A). In the 299-residue sequence, these extended from amino acid residues 64 to 84 (TM1) and 132 to 153 (TM2), respectively. Depending on whether one or both of these transmembrane domains are bona fide, there are six possible topology models for Pom34p relative to nuclear pore membranes (Figure 2-1B). To define the Pom34p membrane topology, we used a combination of approaches that have been established in previous studies of *S. cerevisiae* ER membrane proteins. The fusion of Suc2p to protein regions is a common strategy for detecting localization in the ER/NE lumen (KIM *et al.* 2003; SENGSTAG 2000). The Suc2p fusion allows extensive N-linked glycosylation when lumenally localized, with a coincident Endo H-sensitive increase in molecular mass. Cytoplasmic Suc2p localization yields a nonglycosylated protein. To analyze Pom34p topology, we fused Suc2p, flanked by c-myc epitope tags, to either the N or the C terminus of wild-type Pom34p ($Suc2p^{myc}$-Pom34p and Pom34p-$Suc2p^{myc}$, respectively). As controls, we confirmed that the fusion proteins were functional by testing for their complementation of *pom34*Δ double mutants (see below).

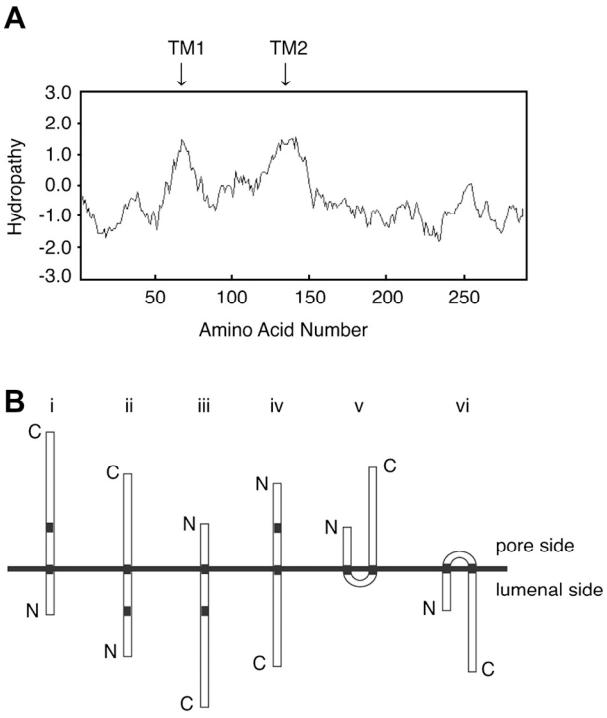

Figure 2-1: Pom34p has two predicted transmembrane domains. (A) Kyte–Doolittle hydropathy analysis (with a 20-amino-acid window size) (KYTE and DOOLITTLE 1982) of Pom34p revealed two spans (arrows) extending from amino acid residues 64 to 84 (TM1) and 132 to 153 (TM2) with significant hydropathic character and length to be transmembrane segments. (B) Six possible topological models for Pom34p relative to the pore membrane are shown. N, amino; C, carboxy.

To determine whether the N and/or C terminus of Pom34p is located on the lumenal side of the ER/NE membrane, the glycosylation status of Pom34p fusions was assessed. Cell lysates were prepared from a *pom34*Δ strain that harbored plasmids encoding either Suc2p^{myc}-Pom34p or Pom34p-Suc2p^{myc}, treated with Endo H, and analyzed by immunoblotting. As controls, the glycosylation states of a Pom152p-Suc2p^{myc} fusion in *pom152*Δ cells and a Snl1p-Suc2p fusion in *snl1*Δ cells were monitored. Pom152p and Snl1p have opposite topologies with the C terminus sequestered in the ER/NE lumen and cytosol, respectively (HO *et al.* 1998; TCHEPEREGINE *et al.* 1999). The Pom152p-Suc2p^{myc} fusion was sensitive to Endo H digestion as reflected by the migration shift (Figure 2-2A, lanes 3 and 4). On the other hand, the apparent molecular mass of Snl1p–Suc2p was not affected by Endo H treatment (Figure 2-2A, lanes 1 and 2). In comparison, the Suc2p^{myc}-Pom34p and Pom34p-Suc2p^{myc} fusion proteins both migrated with a predicted mass of ～93 kDa. Strikingly, their status was not sensitive to Endo H treatment (Figure 2-2A, lanes 5–8). Therefore the Suc2p domain was not glycosylated when fused at either the N or the C terminus of Pom34p. This suggested that both N- and C-terminal regions of Pom34p are exposed to the cytoplasm.

To examine if the Pom34p fusion proteins were targeted to the membrane, alkaline extraction experiments were performed. Cell lysates from *pom34*Δ strains expressing different fusions were extracted with 0.1 M sodium carbonate (pH 11), and supernatant (S) and pellet (P) fractions were separated by centrifugation and analyzed by immunoblotting. All the Pom34p topology reporter proteins were resistant to extraction and remained associated with the pellet fraction in a manner similar to the integral membrane protein control Snl1p. In contrast, the peripheral nucleoporin Nup145C was

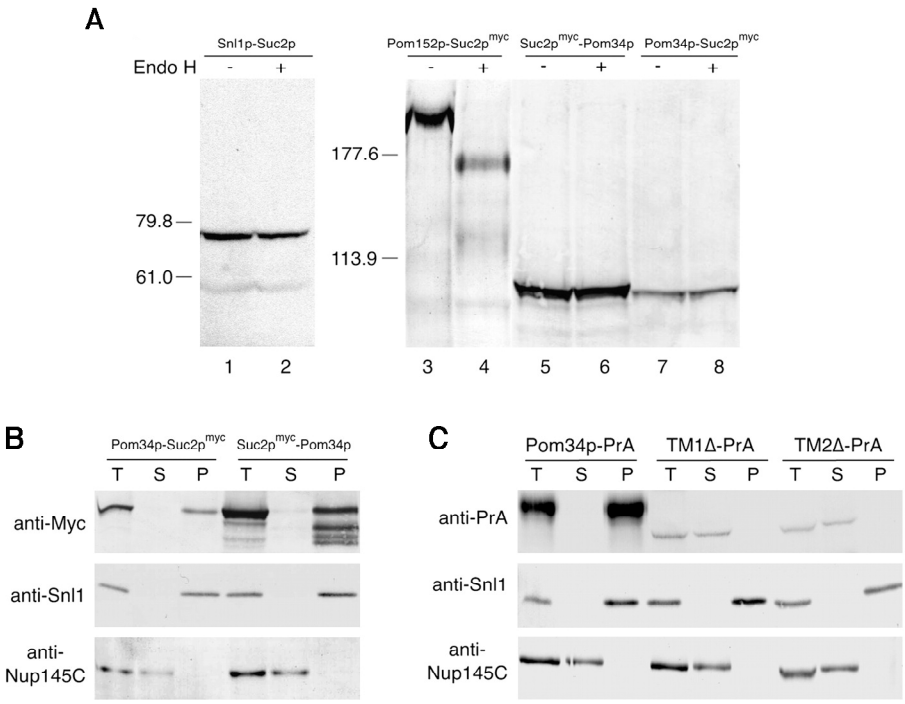

Figure 2-2: Pom34p is a double-pass integral membrane protein with the N- and the C-terminal regions exposed to the cytosol/pore. (A) Cell extracts from strains expressing Snl1p-Suc2p (pSW939) (lanes 1 and 2), Pom152p-Suc2p^{myc} (pSW3192) (lanes 3 and 4), Suc2p^{myc}-Pom34p (pSW3189) (lanes 5 and 6), or Pom34p-Suc2p^{myc} (pSW3190) (lanes 7 and 8) were either mock digested (–) or treated with Endo H (+) and analyzed by immunoblotting using rabbit anti-Snl1p (lanes 1 and 2) or mouse monoclonal 9E10 (anti-c-Myc) (lanes 3–8). Molecular mass markers are indicated in kilodaltons. (B) Spheroplast lysates from the *pom34*Δ strain expressing Suc2p^{myc}-Pom34p (pSW3189), Pom34-Suc2p^{myc} (pSW3190) were alkali extracted and separated into supernatant (S indicates S1 and S2) and pellet (P indicates P2) fractions by centrifugation. Fractions were analyzed by immunoblotting with the mouse monoclonal 9E10 (anti-myc), rabbit anti-Snl1p or with rabbit anti-Nup145C antibodies. (C) Spheroplast lysates from *pom34*Δ cells expressing Pom34p-PrA, TM1Δ-PrA (lacking the TM1), or TM2Δ-PrA (lacking the TM2) were alkali extracted and separated into S and P fractions by centrifugation as in B. Fractions were analyzed by immunoblotting with rabbit anti-mouse (anti-protein A), rabbit anti-Snl1p, or rabbit anti-Nup145C antibodies.

extracted (Figure 2-2B). We also tested the role of each of the two transmembrane segments in targeting Pom34p to the membrane. In-frame internal deletions of the sequence encoding each respective transmembrane segment were constructed in the context of a Pom34p–Protein A (PrA) C-terminal fusion. This resulted in TM1Δ-PrA (amino acids 62–85 deleted) and TM2Δ-PrA (amino acids 129–153 deleted). The mutants were expressed in a *pom34*Δ strain, cell lysates were prepared, and alkaline extraction experiments were conducted. The wild-type Pom34p-PrA was exclusively present in the pellet fraction (Figure 2-2 C). In contrast, both TM1Δ-PrA and TM2Δ-PrA were extracted from the membrane/pellet fraction and found in the supernatant. We concluded that the membrane integration of Pom34p is dependent on both transmembrane segments.

The *pom34*Δ mutant has genetic interactions with a specific subset of mutants in genes encoding nucleoporins

There are at least six major biochemically defined nucleoporin subcomplexes in the NPC (as shown in Fig 1-2): the Nup84 subcomplex (Nup84p-Nup85p-Nup120p-Nup133p-Nup145C-Seh1p-Sec13p) (LUTZMANN *et al.* 2002; SINIOSSOGLOU *et al.* 2000; SINIOSSOGLOU *et al.* 1998), the Nup82 subcomplex (Nsp1p–Nup82p-Nup159p-Nup116p-Gle2p) (BAILER *et al.* 2000; BAILER *et al.* 1998; BELGAREH *et al.* 1998; GRANDI *et al.* 1995a; HO *et al.* 2000; HURWITZ *et al.* 1998), the Nic96 subcomplex (Nic96p-Nsp1p-Nup49p-Nup57p) (GRANDI *et al.* 1993; GRANDI *et al.* 1995b; SCHLAICH *et al.* 1997), the Nup188 subcomplex (Nic96p-Nup188p-Nup192p-Pom152p) (KOSOVA *et al.* 1999; NEHRBASS *et al.* 1996; ZABEL *et al.* 1996), the Nup170 subcomplex (Nup170p-Nup53p-Nup59p) (MARELLI *et al.* 1998), and the Nup60-Nup2 subcomplex (DENNING *et al.* 2001; DILWORTH *et al.* 2001). To test for *POM34* genetic interactions with genes encoding

other NPC components, we assembled a full panel of selected haploid *nup* mutants including at least two representatives from each of these defined NPC subcomplexes. For all the strain constructions, a haploid *pom34*Δ mutant was mated pairwise with mutant alleles of each of the *NUP* genes, and the resulting heterozygous diploids were sporulated and dissected to yield double-mutant *pom34*Δ *nup* haploids. If viable double-mutant haploid strains were not obtained, a *URA3/CEN* plasmid harboring wild-type *POM34* was transformed into the corresponding heterozygous diploids. Plasmid-rescued, double-mutant haploids were isolated and tested for growth on media containing 5-FOA. Strains that are dead in the absence of the *URA3* plasmid will not grow on 5-FOA, and those were scored as synthetically lethal double mutants. All viable double-mutant haploids were tested for growth at 16.5˚C, 23˚C, 30˚C, 34˚C, and 37˚C on YPD media and compared with the growth of the corresponding single mutants. The results are summarized in Table 2-3.

A *pom152*Δ synthetic lethal screen by Wozniak and coworkers identified four *nup* mutants that require *POM152* for viability: *nup59-40*, *nup170-21*, *nup188-4*, and *nic96-7* (AITCHISON *et al.* 1995; NEHRBASS *et al.* 1996). We speculated that *POM34* might have genetic interactions with the same *NUP* genes as *POM152*. Consistent with our hypothesis, *pom34*Δ shared most of the same synthetic lethal interactions reported for *pom152*Δ, including lethality with *nup59*Δ, *nup170*Δ, and *nup188*Δ. In addition, we identified three other mutants that were lethal in the *pom34*Δ genetic background: *nup82-3* (*nle4-1*), *nup159-1* (*rat7-1*), and *gle2*Δ. In some cases, the double mutants were viable but had conditional growth phenotypes at temperatures permissive for the respective single-mutants' growth. Enhanced lethality defects were detected when *pom34*Δ was

combined with *nup120*Δ, *nup116*Δ, or *nup57-E17* mutants. Notably, we did not detect genetic interactions with the *nup* alleles corresponding to nucleoporins localized exclusively to the nucleoplasmic NPC face (Nup1p, Nup2p, Nup60p) (ROUT *et al.* 2000). These results revealed that *POM34* genetically interacts with a wide range of *NUP*s representing multiple distinct NPC subcomplexes.

N- and C-terminal domains of Pom34p are required for distinct NPC subcomplexes

On the basis of the topology analysis, the two transmembrane segments divide Pom34p into at least three distinctive domains: the cytosolic/pore N- and C-terminal regions and the lumenal loop region. To evaluate which of these regions are required for function, a panel of deletion/truncation mutants was generated (Figure 2-3A). Plasmids expressing the respective deletion mutants were transformed into six synthetic lethal double-mutant strains that require wild-type *POM34/URA3/CEN* for viability. Functional complementation was assayed by replica plating from SM–leu to media containing 5-FOA. Deletion of both the N- and the C-terminal regions (Pom34pΔNΔC) or an internal deletion of both transmembrane spans and the lumenal loop region (Pom34p-ΔTM) abolished function in all the double-mutant strains tested (Figure 2-3B). In contrast, production of the Pom34p-ΔN or Pom34p-ΔC deletions complemented the *nup170*Δ, *nup159-1* (*rat7-1*), and *nup82-3* (*nle4-1*) double-mutant strains when expressed from high-copy *LEU2/2μ* plasmids (Figure 2-3B, columns 2, 5, and 6) but not from low-copy *LEU2/CEN* plasmids (data not shown). This high-copy suppression of some double-mutant combinations suggested that the N- or the C-terminal region could replace its opposite end in some, but not all, functions. Interestingly, the production of Pom34p-ΔC

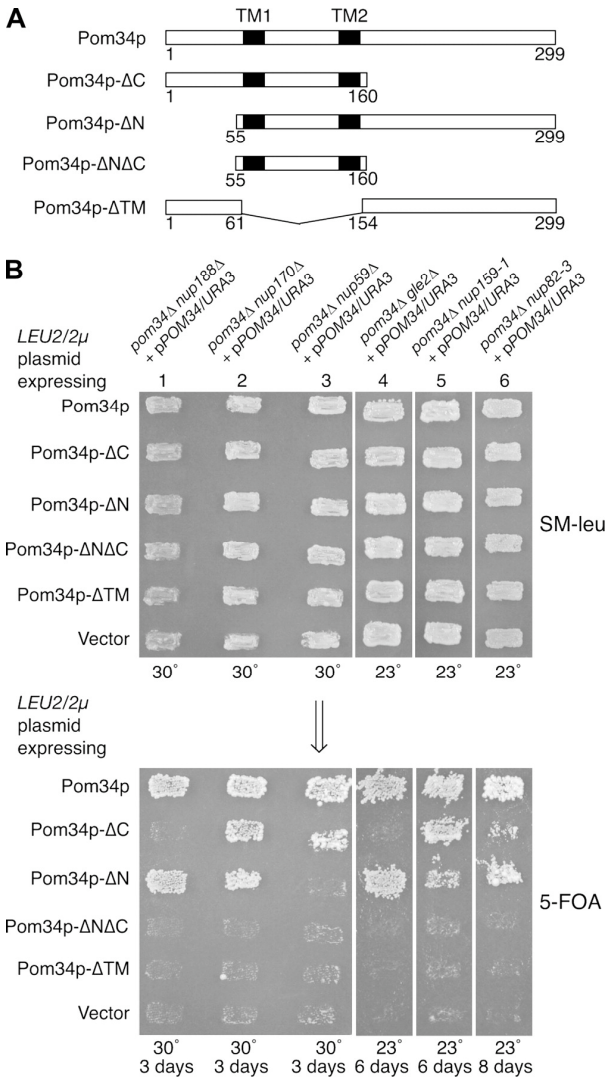

Figure 2-3: Functional analysis of Pom34p domains. (A) Schematics of the Pom34p structural regions and related deletion/truncation polypeptides are shown. (B) Synthetic lethal double mutants harboring a *POM34/URA3/CEN* plasmid (low copy) were transformed with the wild-type *POM34/LEU2/2μ* plasmid, the respective mutant *pom34/LEU2/2μ* plasmids (high copy), and empty vector. Transformants were patched on SM-leu (top) at 30˚C (lanes 1–3) or 23˚C (lanes 4–6) for 2 days and then replica plated onto 5-FOA media (bottom) and incubated for the indicated days at the same temperature.

and Pom34p-ΔN also showed allele-specific complementation. Pom34p-ΔC did not rescue the viability of *pom34*Δ *nup188*Δ and *pom34*Δ *gle2*Δ mutants whereas Pom34p-ΔN did (Figure 2-3B, columns 1 and 4). Furthermore, Pom34p-ΔN did not support growth of the *pom34*Δ *nup59*Δ strain (Figure 2-3B, column 3) whereas Pom34p-ΔC did. Thus, the N-terminal region was required in the *nup59*Δ cells and the C-terminal region in *nup188*Δ and *gle2*Δ cells. Overall, these complementation results reveal possible distinct functions for the N- and the C-terminal Pom34p regions with particular peripheral Nups in the NPC.

NPC structure and function are perturbed in the *pom34*ΔN *nup188*Δ double mutant

Although the viability of some *pom34*Δ synthetic lethal double mutants was rescued by overproduction of Pom34p-ΔN or Pom34p-ΔC, the growth rates of the complemented strains were significantly slower at all temperatures tested when compared to complementation by wild-type Pom34p (data not shown). We focused on the *pom34*Δ *nup188*Δ + p*pom34*Δ*N/2μ* strain (henceforth designated *pom34*Δ*N nup188*Δ) as it had an exacerbated growth defect at elevated temperatures. Others have reported, and we have independently tested, that the *nup188*Δ single mutant does not have any apparent defects in the NPC localization of FG Nups (NEHRBASS *et al.* 1996; ZABEL *et al.* 1996). We speculated that the slowed growth of *pom34*Δ*N nup188*Δ cells might reflect perturbations of NPC structure and function by the combined absence of the Pom34p N-terminal domain and Nup188p. To test this hypothesis, microscopy was performed to detect any defects in the *pom34*Δ *nup188*Δ mutant strain harboring either a wild-type *POM34* or a mutant *pom34*Δ*N/LEU2/2μ* plasmid. Thin-section electron microscopy showed no

ultrastructural differences in the *pom34*Δ *nup188*Δ cells complemented with either wild-type Pom34p or Pom34p-ΔN (data not shown). To evaluate possible effects on individual Nup localization, indirect immunofluorescence microscopy was conducted with these same strains. Fixed budding yeast cells were labeled with mouse monoclonal antibodies recognizing FG Nups (mAb414), affinity-purified rabbit anti-Nup116GLFG antibodies, or mouse monoclonal anti-Pom152p antibodies (mAb118C3). In *pom34*Δ *nup188*Δ cells harboring the wild-type *POM34* plasmid, the fluorescence staining for all three antibodies was predominantly confined to the nuclear rim in a punctate pattern (Figure2-4, left column). The anti-Pom152p staining in the *pom34*Δ*N nup188*Δ cells was similar to that in the *POM34* complemented strain (Figure 2-4, bottom right). However, the FG and GLFG staining in the majority of the *pom34*ΔN *nup188*Δ cells was no longer concentrated at the nuclear rim. Instead, most of the signal was diffuse throughout the cytoplasm and in some cases appeared as cytoplasmic foci (Figure 2-4, top right and middle right). Overproduction of Pom34p-ΔN in wild-type cells or in a *nup188*Δ single mutant had no effect on GLFG staining (Figure 2-5). In addition, GFP-tagged Nup145p, Nup159p, Nup170p, Nup188p, and Pom152p were not displaced from the NPC when Pom34p-ΔN was expressed in otherwise wild-type cells (Figure 2-6). These results suggested that a subset of the NPC proteins, the FG Nups, was specifically mislocalized in the absence of Nup188p and the N-terminal region of Pom34p.

To further characterize the FG Nup mislocalization phenotype, subcellular fractionation was conducted with lysates from wild-type, *pom34*Δ *nup188*Δ + p*POM34*, and *pom34*Δ*N nup188*Δ strains. Total crude cell lysates were separated by centrifugation into S1 and P1 fractions. Samples of the fractions were analyzed by immunoblotting with

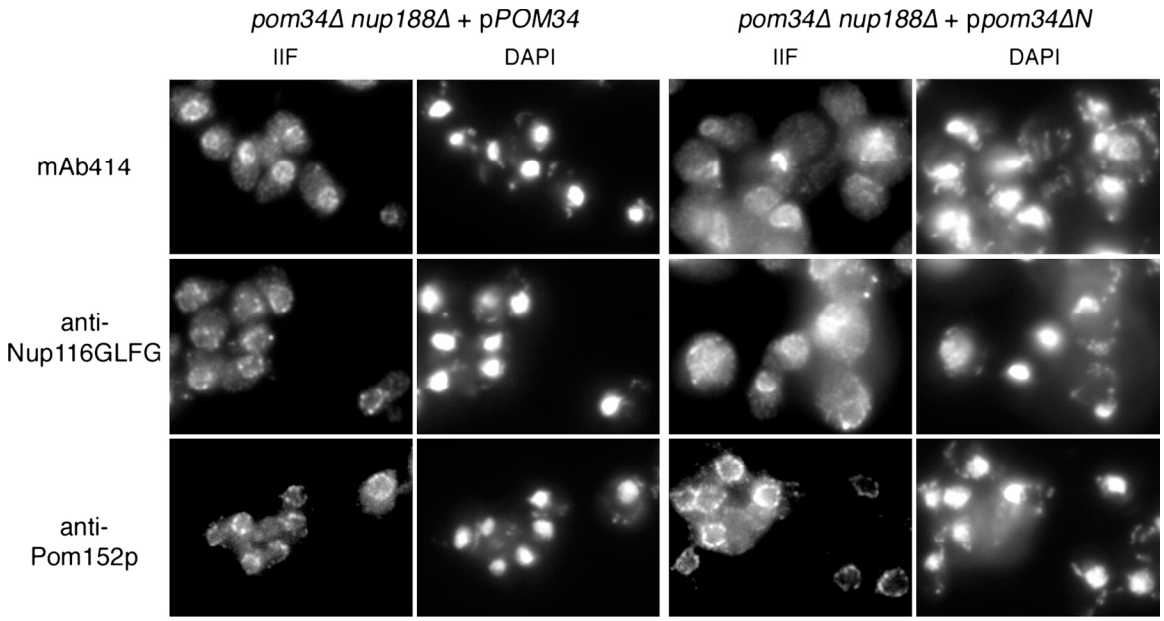

Figure 2-4: FG Nups mislocalize in the *pom34*Δ*N nup188*Δ mutant strain. Cells in early log phase were processed for indirect immunofluorescence microscopy with mouse monoclonal mAb414, rabbit anti-Nup116GLFG, or mouse monoclonal mAb118C3 (anti-Pom152p) antibodies. Nuclei were detected by DAPI staining.

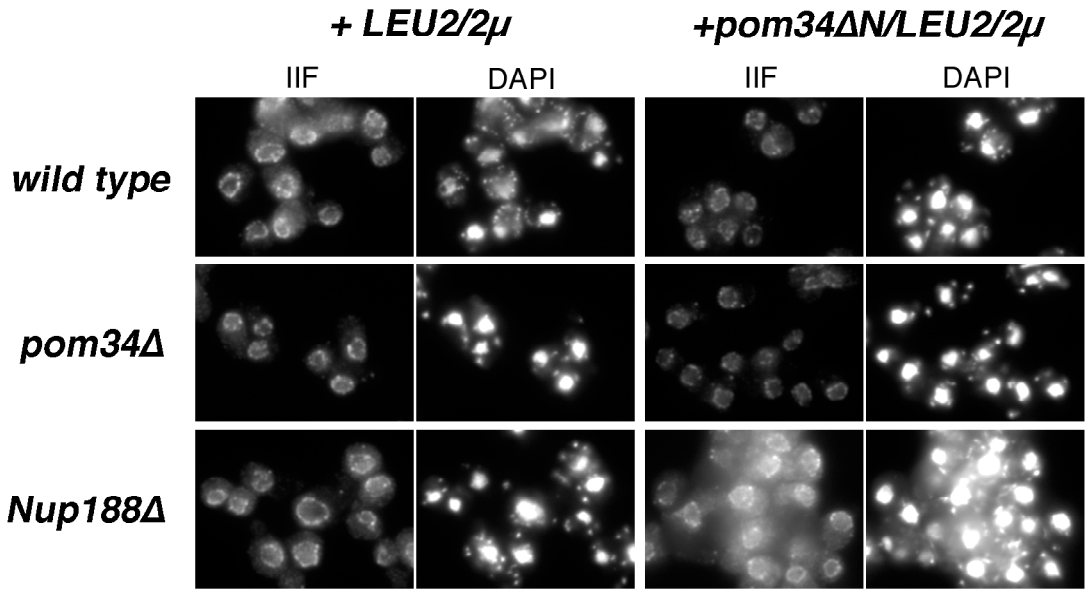

Figure 2-5: Overexpressing *pom34ΔN/LEU2/2μ* does not affect the localization of GLFG-containing Nups. *pom34ΔN/LEU2/2μ* or empty vector was transformed into *nup188Δ*, *pom34Δ*, or wild type budding yeast strains. The cells in early to mid-log phase at 30˚C were processed for indirect immunofluorescence microscopy with rabbit anti-Nup116GLFG antibody. Nuclei were detected by DAPI staining.

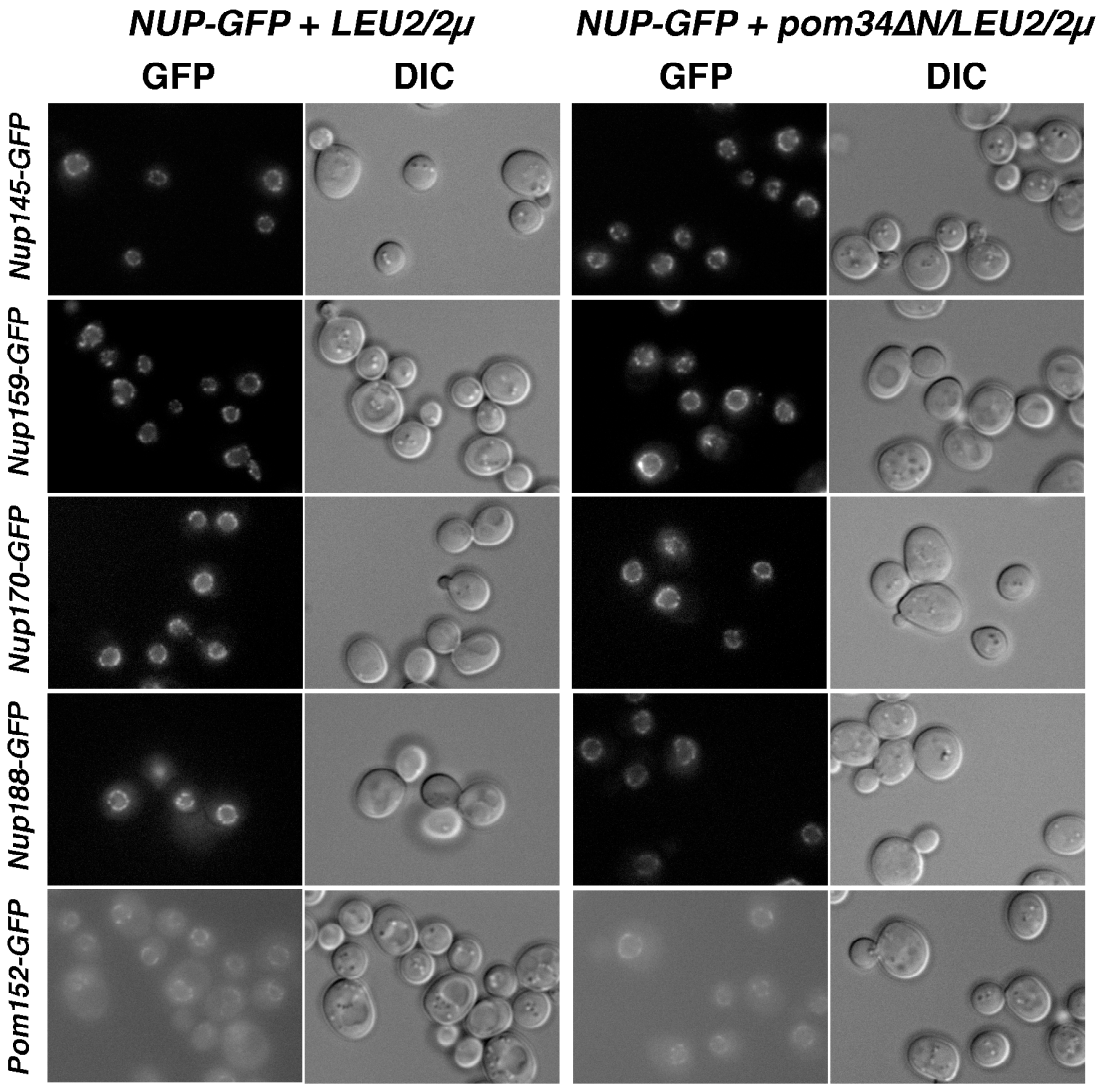

Figure 2-6: Overexpressing *pom34ΔN* does not affect the structural Nups localization. *pom34ΔN/LEU2/2μ* plasmid or empty vector was transformed into several Nup-GFP strains. Cells growing at early to mid log phase at 30˚C were visualized for fluorescence signals. The corresponding DIC images were shown.

controls for cytoplasmic (anti-Pgk1p) and nuclear (anti-Nop1p) proteins that fractionate in the S1 and the P1, respectively. Immunoblotting was used to monitor the Nup fractionation with anti-Nup116GLFG detecting four GLFG Nups, anti-Nsp1p recognizing both Nup2p and Nsp1p, and anti-Nup145C for a non-FG polypeptide. In fractions from the wild-type and the *pom34*Δ *nup188*Δ + p*POM34* cells, all the Nups were predominantly distributed in the P1 fraction (Figure 2-7, lanes 1–6). In contrast, the distribution of FG Nups in the S1 and P1 fractions was quite different in lysates from the *pom34*Δ*N nup188*Δ mutant. Significant fractions of Nup116p, Nup100p, Nup57p, Nup49p, and Nup2p were recovered in the S1 fraction (Figure 2-7, lanes 7–9). Interestingly, the effect on Nsp1p was not as dramatic as for the above FG Nups, with the majority of Nsp1p still in the P1 fraction. Nup145C also was not changed and was exclusively in the P1 fraction. Taken together, these data suggested that a specific subset of Nups is perturbed in the *pom34*Δ*N nup188*Δ, resulting in diminished NPC localization.

To directly test the role of Pom34p in NPC function, we conducted nucleocytoplasmic transport assays. A series of green fluorescence protein (GFP)-conjugated reporters harboring nuclear localization sequences (NLS) and/or nuclear export sequences (NES) for distinct transport pathways were expressed in the cells. These included cNLS-GFP for Kap60p–Kap95p import, Nab2-NLS-GFP for Kap104p import, Pho4-NLS-GFP_3 for Kap121p (Pse1p) import, and NLS-NES-GFP_2 for shuttling by Kap60p-Kap95p import and Xpo1p (Crm1p, Kap124p) export (as reviewed in CHOOK and BLOBEL 2001). The steady-state localizations for the GFP-reporters were examined by direct fluorescence microscopy (Figure 2-8). All three import reporters showed nuclear accumulation in the control *pom34*Δ *nup188*Δ + p*POM34* strain, and the shuttling

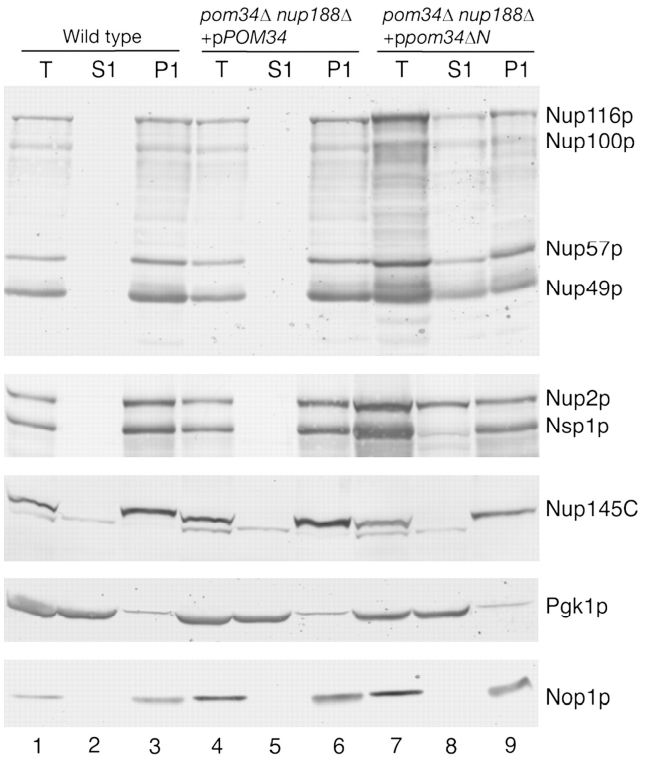

Figure 2-7: Subcellular fractionation of the *pom34*Δ*N nup188*Δ mutant shows increased levels of FG Nups in the cytoplasm. Spheroplast lysates from wild type (SWY518), *pom34*Δ *nup188*Δ + p*POM34* (SWY3489), and *pom34*Δ *nup188*Δ + p*pom34*Δ*N* (SWY3490) were prepared and separated into soluble (S1) and insoluble pellet (P1) fractions at a low speed centrifugation. Fractions were analyzed by immunoblotting with rabbit anti-Nup116GLFG, rabbit anti-Nsp1p, rabbit anti-Nup145C, mouse monoclonal mAb22C5 (anti-cytoplasmic protein Pgk1p), and mouse monoclonal mAb D77 (anti-nucleolar protein Nop1p) antibodies. The anti-Nup116GLFG antibody recognizes Nup116p, Nup100p, Nup57p, and Nup49p. The anti-Nsp1p antibody recognizes Nup2p in addition to Nsp1p.

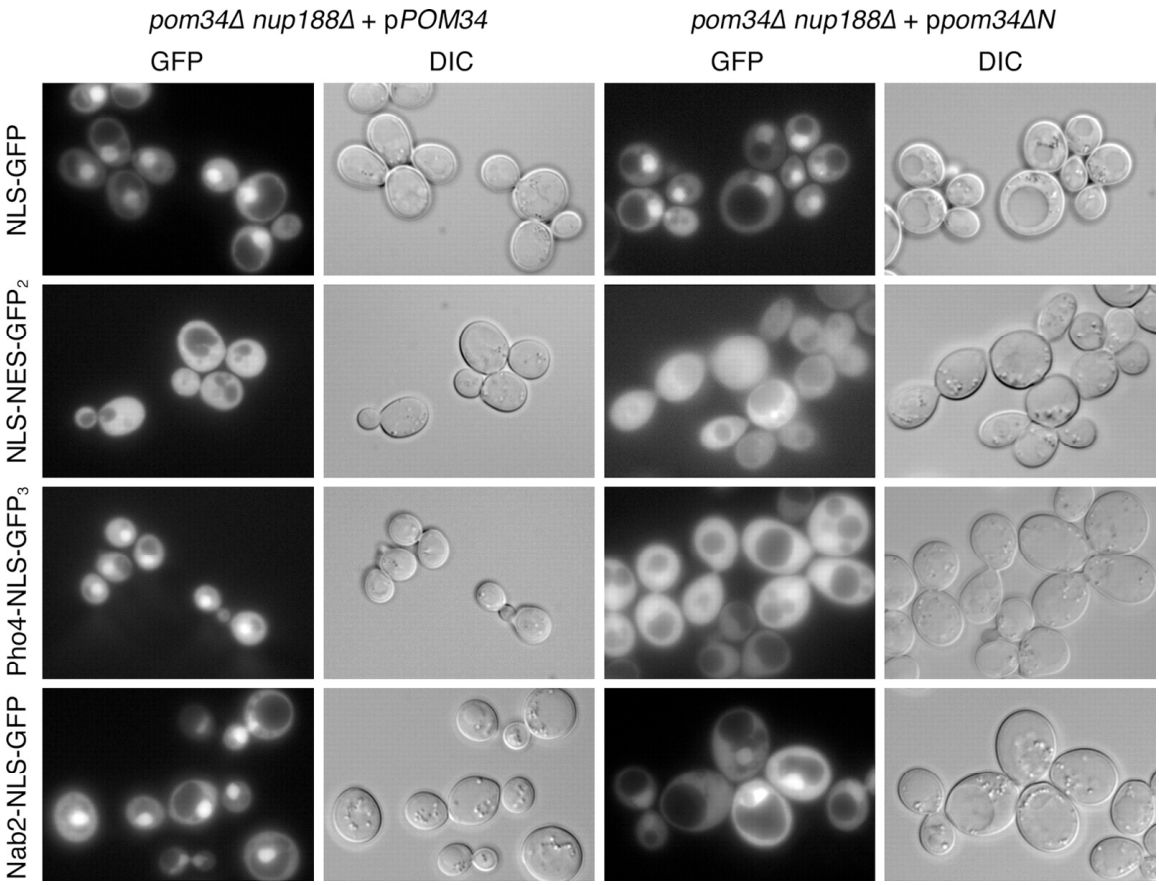

Figure 2-8: Analysis of nucleocytoplasmic transport in the *pom34*Δ*N nup188*Δ mutant reveals defects in Kap121p and Kap104p-mediated import. Cells growing at 30˚C in early log phase were visualized by direct fluorescence microscopy for steady-state localization of GFP fluorescence. The four GFP reporters analyzed include NLS-GFP (for Kap95p import), NLS-NES-GFP_2 (for Xpo1p export), Pho4-NLS-GFP_3 (for Kap121p), and Nab2-NLS-GFP (for Kap104p). The corresponding DIC images are shown.

NLS-NES-GFP_2 also had no detectable perturbations and showed steady-state cytoplasmic localization (Figure 2-8, left column). The steady-state localizations of cNLS-GFP and NLS-NES-GFP_2 in the *pom34*Δ*N nup188*Δ mutant cells were similar to that in the complemented *pom34*Δ *nup188*Δ + p*POM34* double mutant (Figure 2-8, first and second rows, respectively). However, in the *pom34*Δ*N nup188*Δ mutant cells, the steady-state nuclear levels of Pho4-NLS-GFP_3 were significantly altered with increased cytoplasmic localization and markedly diminished nuclear accumulation (Figure 2-8, third row, right column). There was a similar, although less severe, change in Nab2-NLS-GFP with increased cytoplasmic localization. This indicated import defects in karyopherin transport pathways. Thus, specific FG Nups and transport pathways were perturbed in the *pom34*Δ*N nup188*Δ mutant cells.

Discussion

To gain insight into the function of nuclear pore membrane proteins, we have conducted experiments to define the Pom34p membrane topology and address the Pom34p functional relationship with Nups. We provide evidence here that Pom34p is important in maintaining normal NPC architecture and function. Our topology studies show that Pom34p is a double-pass transmembrane protein with both N- and C-terminal regions exposed to the cytosol/pore. Further analysis reveals roles for the Pom34p N- and C-terminal regions with specific peripheral Nups. We also document perturbations in the NPC association of FG Nups and nuclear transport in a *pom34*Δ*N nup188*Δ mutant. These results provide further insight into the roles for membrane proteins in the structural organization of the NPC.

We have found that Pom34p inserts with a hairpin-like structure into the nuclear membrane, effectively generating multiple functional domains: a cytosolic/pore N-terminal domain, a cytosolic/pore C-terminal domain, a lumenal loop domain, and two transmembrane domains (TM1 and TM2). As commonly observed in other integral membrane proteins, positively charged amino acid residues are positioned at the cytoplasmic sides flanking both hydrophobic transmembrane domains (MULUGETA and BEERS 2003). Our results suggest that the multiple Pom34p domains are independently necessary for its function. First, we note that both TM1 and TM2 are required for Pom34p membrane integration (Figure 2-2). Most multipass transmembrane proteins rely on the first transmembrane domain for membrane insertion and anchoring; however, the process can be more complicated (RAPOPORT *et al.* 2004). The requirement for both transmembrane regions to direct and/or anchor Pom34p into membranes might indicate that the two TMs work cooperatively during translocation into the NE/ER membrane. Structural analysis of the archaebacterium protein-conducting channel suggests that two TMs can be accommodated at one time in the ER Sec61 channel (RAPOPORT *et al.* 2004; VAN DEN BERG *et al.* 2004). Alternatively, both TMs might be required for stable membrane association. Second, the lumenal loop region might form a second, necessary, functional domain that appears to be essential for Pom34p stability. Proteins from deletion constructs that encoded the N-terminal domain plus TM1, the C-terminal domain plus TM2, or an internal deletion of the loop region could not be detected by Western analysis (data not shown). Finally, the N-terminal and C-terminal domains have nonoverlapping functions, as their ability to complement the different *pom34*Δ double

mutants differs (Figure 2-3). This suggests that protein–protein interactions on the cytosolic/pore side are important for Pom34p function.

The Pom34p N- and C-terminal regions may have distinct protein–protein interaction partners in the NPC. The schematic model shown in Figure 2-9 incorporates our findings with the insights from prior NPC structural analyses. Extensive prior biochemical studies have characterized NPC subcomplexes with distinct nucleoporin compositions (reviewed in SUNTHARALINGAM and WENTE 2003). Each subcomplex might represent a specific substructure of the NPC architecture. Our genetic studies have linked *POM34* with genes encoding Nups in the Nup84, Nup188, Nup170, and Nup82 subcomplexes. The complementation analysis with *pom34* deletion mutants indicates specific connections for (1) the Nup170 subcomplex with the Pom34p N domain and (2) the Nup188 subcomplex and the Nup82 subcomplex with the Pom34p C domain. The Nup170 subcomplex and Nup188 subcomplex are both symmetrically localized in the NPC with respect to the NE (ROUT *et al.* 2000). These two subcomplexes are thought to form a fundamental NPC framework as evidenced by an extensive genetic and biochemical interaction network among their components (AITCHISON *et al.* 1995; MARELLI *et al.* 1998; NEHRBASS *et al.* 1996; ZABEL *et al.* 1996). In contrast, the Nup82 subcomplex is localized exclusively on the cytoplasmic NPC face (ROUT *et al.* 2000). The model depicted in Figure 2-9 also takes into account estimates of the Pom34p stoichiometry being at least twice that of Pom152p and Ndc1p (ROUT *et al.* 2000). Overall, Pom34p might be a central hub at the core of the pore and serve to assist in anchoring different NPC subcomplexes to the NE.

Recently, studies on the molecular evolution of the NPC have proposed that subunits of the Nup84 subcomplex are structurally related to transport vesicle coat proteins. It has

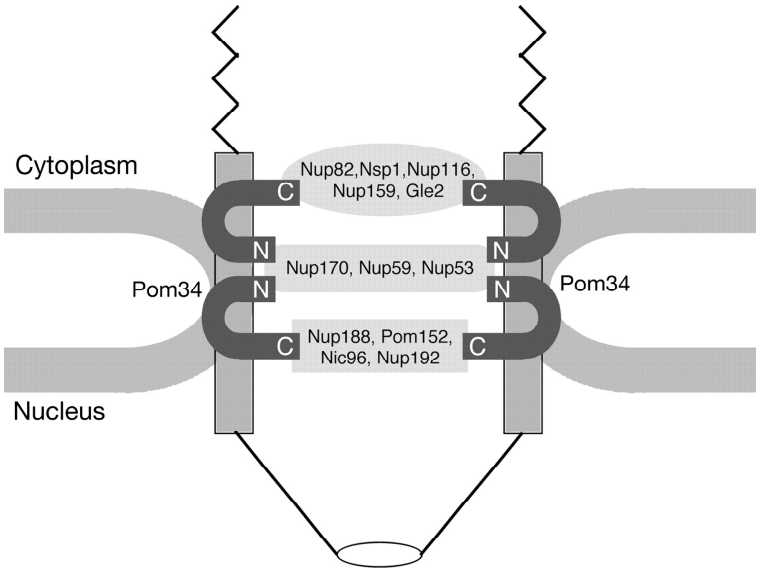

Figure 2-9: Model for Pom34p in NPC structural organization. The schematic diagram is based on information from published biochemical studies and the results in this chapter. Connections are shown between the N-terminal region of Pom34p and the Nup170 subcomplex and between the C-terminal Pom34p region and both the Nup188 subcomplex and the Nup82 subcomplex. Pom34p, the Nup170 subcomplex, and the Nup188 subcomplex are all found symmetrically localized on both faces of the NPC (ROUT *et al.* 2000). The predicted relative stoichiometries of Pom34p and the Nup170 subcomplex are 32 copies/NPC vs. 16 copies/NPC for the Nup188 subcomplex (ROUT *et al.* 2000). Nic96p and Nsp1p have been isolated in multiple biochemical subcomplexes and are also abundant NPC components at 32 copies/NPC [Nic96p in the Nup188 subcomplex and the Nic96 subcomplex (not shown); Nsp1p in the Nup82 subcomplex and the Nic96 subcomplex (not shown) [reviewed in (SUNTHARALINGAM and WENTE 2003)]. The Nup82 complex is exclusively cytoplasmic and predicted to be present in only 8 or 16 copies/NPC. Three peripheral FG Nups are shown assembled in the Nup82 subcomplex (Nsp1p, Nup116p, and Nup159p). Other FG Nups likely assemble by association with these core subcomplexes and the Nup84 subcomplex (not shown).

been suggested that this similarity could indicate a common function in membrane deformation wherein the Nup84 subcomplex contributes to the stabilization of the membrane curvature at the nuclear pore in much the same way that coat proteins contribute to membrane budding during vesicular transport (DEVOS *et al.* 2004; MANS *et al.* 2004). However, neither the Nup84 subcomplex nor its vertebrate ortholog, the Nup107–160 subcomplex, has been previously connected to the integral membrane proteins or the nuclear membrane (ANTONIN and MATTAJ 2005). The enhanced lethality observed in the *pom34*Δ *nup120*Δ double mutant provides the first evidence that the Nup84 subcomplex is intimately linked to the pore membrane.

Our genetic results suggest that the global NPC structure is weakened in the absence of both one cytoplasmic/pore domain of Pom34p (the N- or the C-terminal region) and one major soluble Nup. The *pom34*Δ*N nup188*Δ double mutant has perturbations in the function of specific FG Nups. Our immunofluorescence microscopy and biochemical fractionation results document the cytoplasmic mislocalization of at least five FG Nups: Nup116p, Nup100p, Nup57p, Nup49p, and Nup2p. Interestingly, Nsp1p is not significantly altered. Diminished FG Nup function in the *pom34*Δ*N nup188*Δ double mutant is also reflected by a defect in karyopherin nuclear transport pathways. Whereas Kap95p and Xpo1p transport is not changed at steady state in the *pom34*Δ*N nup188*Δ mutant, we observe specific inhibition of the Kap121p and Kap104p transport pathways. This transport phenotype correlates directly with results from our recent study of FG Nup function (STRAWN *et al.* 2004). We found that Kap121p and Kap104p import is more sensitive than Kap95p import to deletions of the FG domains. For example, a *nup100*Δ*GLFG nup49*Δ*GLFG nup57*Δ*GLFG* mutant has robust Kap95p import but a

markedly diminished capacity for Kap104p import (STRAWN *et al.* 2004). Taken together, this suggests a role for Pom34p either in maintaining the association of FG Nups in NPCs or in the assembly of FG Nups into new NPCs.

In the NPC architecture, the FG Nups are assembled into the NPC by associations with Nup82p (including Nsp1p, Nup116p, and Nup159p) and Nic96p (including Nsp1p, Nup49p, and Nup57p) and by potential connections between Nup42p, Nup57p, and Nup145N to the Nup84 subcomplex (ALLEN *et al.* 2001; BAILER *et al.* 2000; BAILER *et al.* 1998; BELGAREH *et al.* 1998; GRANDI *et al.* 1995a; HO *et al.* 2000; HURWITZ *et al.* 1998; LUTZMANN *et al.* 2005; ROUT *et al.* 2000). There is no evidence that Pom34p interacts directly with an FG Nup. In the *pom34*Δ*N nup188*Δ mutant, we predict that the FG Nups are perturbed via a secondary effect on the Nup170 and the Nup188 subcomplexes that are anchored in part by Pom34p (Figure 2-9).

As described in the Introduction, there are partial differences in Pom composition between vertebrates and fungi. However, the Poms likely share common roles across species in stabilizing the assembled core structure of the intact NPC by interacting with soluble structural Nups. We predict that the Pom compositional distinctions are linked to the contrasting mitotic mechanisms across species. During the open mitosis of vertebrates, the NE fragments and the NPC disassembles at the beginning of mitosis followed by reassembly in anaphase (BURKE and ELLENBERG 2002). Recent work in *Aspergillus nidulans* has shown that during its closed mitosis several FG Nups are disassembled from the NPC and nuclear transport is altered (DE SOUZA *et al.* 2004). However, during mitosis, the Aspergillus *POM152* homolog and the structural non-FG peripheral Nups tested maintain their NE and likely NPC association. Interestingly, our

*pom34*Δ*N nup188*Δ mutant shows decreased association of some of the same FG Nups and diminished nuclear transport by specific karyopherins. This suggests that there may be features of Pom152p and Pom34p that are critical for maintaining the pore/NE and anchorage of the major structural Nups during a closed mitosis. As such, the Poms may form the mechanistic basis for the differences between NPC dynamics in vertebrate and budding yeast cells.

Extensive NPC-specific proteomics studies have revealed only one other *S. cerevisiae* pore membrane protein, Ndc1p (ROUT *et al.* 2000). *NDC1* might compensate for the loss of both *POM34* and *POM152* in the double null strain. NPC structure in budding yeast is also influenced by several integral membrane proteins that are not specifically or exclusively localized at NPCs. Mutations in the genes encoding the NE/ER membrane proteins Brr6p, Spo7p, and Nem1p have synthetic lethal interactions with peripheral Nups, as well as perturb NE morphology and the incorporation of Nups into the NPC (DE BRUYN KOPS and GUTHRIE 2001; SINIOSSOGLOU *et al.* 1998). Snl1p is a membrane-anchored Bag domain cochaperone that might recruit Hsp70p to the NE/ER and assist with Nup folding and assembly (HO *et al.* 1998; SONDERMANN *et al.* 2002). The involvement of nonsubunit assembly factors has been well established in the biosynthesis of another macromolecular machine, the vacuolar H+-ATPase complex (GRAHAM and STEVENS 1999). We speculate that multiple integral membrane proteins, either within the nuclear pore domain or in the NE, execute coordinated functions in NPC assembly and function. Future studies will be required to identify the key integral membrane proteins that mediate NPC assembly into the intact NE in closed mitotic organisms and during interphase of all eukaryotic cells.

Table 2-1 Yeast strains used in Chapter II

References for the parental strains used in the double-mutant strain construction include: (AITCHISON *et al.* 1995; BAILER *et al.* 1998; BELANGER *et al.* 1994; BELANGER *et al.* 2004; BUCCI and WENTE 1998; EMTAGE *et al.* 1997; GOLDSTEIN *et al.* 1996; GORSCH *et al.* 1995; MURPHY and WENTE 1996; SAAVEDRA *et al.* 1997; WENTE and BLOBEL 1994; WENTE *et al.* 1992; ZABEL *et al.* 1996), and the Research Genetics collection.

Strain	Genotype	Source
PMY17	*MAT**a** pom152-2::HIS3 ade2-1 ura3-1 his3-11,15 trp1-1 leu2-3,112 can1-100*	(WOZNIAK *et al.* 1994)
psl21	*MATα pom152-2::HIS3 nup170-21 ade2 ade3 ura3 his3 trp1 leu2 can1* + p*CH1122-POM152 (ADE3-URA3)*	(AITCHISON *et al.* 1995)
SWY518	*MAT**a** ade2-1::ADE2 ura3-1 his3-11,15 trp1-1 leu2-3,112 can1-100*	(BUCCI and WENTE 1997)
SWY595	*MAT**a**/MATα ade2-1::ADE2/ade2-1::ADE2 ura3-1/ura3-1 his3-11,15/his3-11,15 trp1-1/trp1-1 leu2-3,112/leu2-3,112 can1-100/can1-100*	(BUCCI and WENTE 1997)
SWY2565	*MATα pom34::spHIS5 ade2-1::ADE2 ura3-1 his3-11,15 trp1-1 leu2-3,112 can1-100*	This study
SWY2566	*MAT**a** pom34::spHIS5 ade2-1::ADE2 ura3-1 his3-11,15 trp1-1 leu2-3,112 can1-100*	This study
SWY3093	*MATα pom34::spHIS5 pom152::HIS3 ura3-1 his3-11,15 trp1-1 leu2-3,112 can1-100 ade2-1*	This study
SWY3125	*MAT**a** pom34::spHIS5 nup188::KAN^R his3 ura3 trp1 leu2 lys2* + pSW1516	This study
SWY3132	*MAT**a** pom34::spHIS5 nup170::KAN^R his3 ura3 trp1 leu2 met15* + pSW1516	This study
SWY3139	*MAT**a** pom34::spHIS5 nup59::KAN^R his3 ura3 leu2 met15* + pSW1516	This study
SWY3142	*MATα pom34::spHIS5 nup53::KAN^R his3 ura3 trp1 leu2 met15*	This study
SWY3149	*MATα pom34::spHIS5 nup157::URA3 his3 ura3 trp1 leu2 lys2*	This study
SWY3153	*MAT**a** pom34::spHIS5 nic96:::HIS3 ade2 his3 ura3 trp1 leu2 lys2* + pUN100-*LEU2-nic96-1[P332L, L260P]*	This study
SWY3219	*MATα pom152::HIS3 nup188::KAN^R his3 ade2 lys2 ura3 leu2* + p*CH1122-POM152(ADE3-URA3)*	This study
SWY3305	*MATα pom34::spHIS5 gle2::HIS3 ade2 his3 trp1 leu2 ura3* + pSW1516	This study
SWY3309	*MATα pom34::spHIS5 gle1-2 his3 ura3 leu2 trp1*	This study
SWY3313	*MATα pom34::spHIS5 nup159-1(rat7-1) his3 ura3 leu2* + pSW1516	This study

Table 2-1 continued		
SWY3326	*MAT**a** pom34::spHIS5 nup82-3(nle4-1) ade2 his3 ura3 trp1 leu2* + pSW1516	This study
SWY3328	*MATα pom34::spHIS5 nup120::HIS3 his3 ura3 leu2*	This study
SWY3334	*MATα pom34::spHIS5 nup42::HIS3 his3 ura3 leu2*	This study
SWY3336	*MATα pom34::spHIS5 seh1::HIS3 his3 ura3 trp1 leu2*	This study
SWY3337	*MATα pom34::spHIS5 nup2::KAN^R his3 ura3 leu2*	This study
SWY3341	*MATα pom34::spHIS5 nup145ΔN::LEU his3-11,15 ura3-1 trp1-1 leu2-3,112 can1-100*	This study
SWY3348	*MAT**a** pom34::spHIS5 nup60::KAN^R his3 ura3 leu2*	This study
SWT3352	*MATα pom34::spHIS5 nup100-1::URA3 ade2-1 his3-11,15 ura3-1 trp1-1 leu2-3,112 can1-100*	This study
SWY3380	*MAT**a** pom34::spHIS5 nup57-E17 his3-11,15 ura3-1 leu2-3,112 trp1-1*	This study
SWY3382	*MAT**a** pom34::spHIS5 nup1-2::LEU2 ade2 his3 ura3 leu2 trp1 lys2*	This study
SWY3384	*MATα pom34::spHIS5 nup116-5::HIS3 ade2-1 his3-11,15 ura3-1 leu2-3,112 trp1-1*	This study
SWY3387	*MATα pom34::spHIS5 nup133::HIS3 ade2 his3 ura3 leu2 trp1 lys2*	This study
SWY3488	*MATα pom152::HIS3 nup59::KAN^R his3 ade2 lys2 ura3 leu2* + p*CH1122-POM152(ADE3-URA3)*	This study
SWY3489	*MAT**a** pom34::spHIS5 nup188::KAN^R his3 ura3 trp1 leu2 lys2* + pSW3044	This study
SWY3490	*MAT**a** pom34::spHIS5 nup188::KAN^R his3 ura3 trp1 leu2 lys2* + pSW3042	This study
SWY3581	*MAT**a** pom34::spHIS5 nup145::LEU2 his3-11,15 ura3-1 leu2-3,112 can1-100* + p*nup145-L2/URA3/CEN*	This study

Table 2-2 Plasmids used in Chapter II

All the *POM34* constructs are downstream of the endogenous promoter (360 bp). Additional vectors used include pFA6a-CTAP-MX6 (TASTO *et al.* 2001), pGAD-GFP (SHULGA *et al.* 1996), pKW430 (STADE *et al.* 1997), pEB0836 (ROMANO and MICHAELIS 2001), and pNS167 (SHULGA *et al.* 2000).

Plasmid	Description	Source
	pRS316 backbone	(SIKORSKI and HIETER 1989)
pSW1516	Full-length *POM34*	This study
	pRS315 backbone	(SIKORSKI and HIETER 1989)
pSW939	Full-length *SNL1* with *SUC2* located at *Nsi*I site	(HO *et al.* 1998)
pSW1517	Full-length *POM34*	This study
pSW3186	Fragment containing endogenous *POM34* promoter and the codons for the first three amino acid residues	This study
pSW3188	Full-length *POM34* with *Spe*I and *Xba*I sites inserted between amino acids 3 and 4, and *Sac*II/*Sac*I site inserted before stop codon	This study
pSW3189	Full-length *POM34* with *myc-SUC2* inserted at *Spe*I site of pSW3193	This study
pSW3190	Full-length *POM34* with *myc-SUC2-myc* inserted at *Sac*I site of pSW3188	This study
pSW3191	Full-length *POM152* at *Pst*I site	This study
pSW3192	Fragment of *POM152* with the codons for residues from 1026 to 1337 replaced by *myc-SUC2-myc*	This study
pSW3193	Full length *POM34* with *c-myc* inserted between codons for residues 3 and 4	
pSW3195	Full-length *POM34* with protein A inserted at *Sac*II/*Sac*I site of pSW3188	This study
pSW3196	Fragment of *pom34* with coding region for amino acids 62-85 replaced by codons for proline and glycine, for TM1Δ, derived from pSW3195	This study
pSW3197	Fragment of *pom34* with coding region for amino acids 129-153 replaced by codons for proline and glycine, for TM2Δ, derived from pSW3195	This study
	pRS425 backbone	(CHRISTIANSON *et al.* 1992)
pSW863	Full-length *POM152* in *Pst*I site	This study
pSW3036	Fragment encoding amino acids 1-160 of Pom34p	This study

Table 2-2 continued		
pSW3042	Fragment encoding amino acids 1-3, 55-299 of Pom34p	This study
pSW3044	Full length *POM34*	This study
pSW3187	Fragment containing endogenous *POM34* promoter and the codons for the first three amino acids	This study
pSW3198	Fragment encoding amino acids 1-3, 55-160 of Pom34p	This study
pSW3199	Fragment of *pom34* with coding region for amino acids 62-153 replaced by codons for proline and glycine	This study

Table 2-3 Growth of *pom34*Δ double mutants

Strains showing no enhanced growth defect in *pom34*Δ double mutants included *nup2*Δ, *nup42*Δ, *nup100*Δ, *nup145*Δ*N*, *nup60*Δ, *nic96-1*, *nup53*Δ, *nup157*Δ, *nup1*Δ, *nup133*Δ, *seh1*Δ, *nup145-L2*, and *gle1-2*. All synthetic lethal strains were rescued by a *URA3/CEN* plasmid carrying a wild-type copy of *POM34*, with lethality confirmed on 5-FOA media. All double-mutant strains were tested on YPD medium. +, growth at the indicated temperature; -, no growth at the indicated temperature.

Gene/strain	Temperature					Genetic interaction
	16.5˚C	23˚C	30˚C	34˚C	37˚C	
*pom34*Δ	+	+	+	+	+	
*nup188*Δ	+	+	+	+	+	Synthetic
*nup188*Δ *pom34*Δ	-	-	-	-	-	lethal
*nup170*Δ	+	+	+	+	+	Synthetic
*nup170*Δ *pom34*Δ	-	-	-	-	-	lethal
*nup59*Δ	+	+	+	+	+	Synthetic
*nup59*Δ *pom34*Δ	-	-	-	-	-	lethal
*gle2*Δ	+	+	+	+	-	Synthetic
*gle2*Δ *pom34*Δ	-	-	-	-	-	lethal
nup159-1(*rat7-1*)	+	+	+	+	-	Synthetic
*nup159-1 pom34*Δ	-	-	-	-	-	lethal
nup82-3(*nle4-1*)	+	+	+	+	-	Synthetic
*nup82-3 pom34*Δ	-	-	-	-	-	lethal
*nup120*Δ	+	+	+	+	-	Enhanced
*nup120*Δ *pom34*Δ	+	+	+	-	-	lethality
*nup116*Δ	+	+	+	+	-	Enhanced
*nup116*Δ *pom34*Δ	+	+	+	-	-	lethality
nup57-E17	+	+	+	+	-	Enhanced
*nup57-E17 pom34*Δ	+	+	+	-	-	lethality

CHAPTER III

IDENTIFICATION OF POTENTIAL NPC ASSEMBLY FACTORS THROUGH A SYNTHETIC LETHAL SCREEN APPROACH

Introduction

As discussed in Chapter I and II, the integral membrane Nups are important for assembling a functional NPC. yNdc1p is the only Pom in *S. cerevisiae* that shares primary sequence homology to higher eukaryotes. It is a multipass membrane protein with 6 transmembrane domains (LAU *et al.* 2006). And its unique membrane orientation presumably provides a platform to interact with other assembly factors. Experiments with a series of truncation mutants have shown that the majority of its sequence is required for the correct intracellular localization and function (LAU *et al.* 2004). Pom152p and Pom34p both have genetic interactions with other soluble Nups. Although they are encoded by nonessential genes, the NPC and/or NE morphology are perturbed in *pom152*Δ or *pom34*Δ related synthetic lethal mutants (AITCHISON *et al.* 1995 and this study).

The function of the above three Poms in budding yeast cell relies on the interaction with structural Nups, particularly the Nup170 subcomplex and Nup188 subcomplex (AITCHISON *et al.* 1995; NEHRBASS *et al.* 1996). These two subgroups of Nups are speculated to form a core framework of NPC. The genetic or physical connections between them and Poms implicate a coordinated role in anchorage of the NPC to the nuclear membrane. In agreement with this, a physical connection has been observed

This chapter is partially adapted from "The integral membrane protein Pom34p functionally links nucleoporin subcomplexes. Miao M, Ryan KJ, Wente SR. Genetics 2006 172(3): 1441-57"

between vNdc1 and Nup53-Nup93 subcomplex, a vertebrate homolog to Nup170 and Nup188 subcomplexes in budding yeast, suggesting that this mechanism is evolutionarily conserved (MANSFELD *et al.* 2006).

A recent report has used an inducible promoter to repress the expression of *yNDC1* in budding yeast cells (MADRID *et al.* 2006). Several Nups, including Nup159p, Nup59p and Nup60p are mislocalized from the nuclear rim and distributed into the cytosol. Codeletion of *POM152* has an additive effect on Nups mislocalization. However, electron microscopy examination revealed that nuclear pores still form in the NE. Further study showed that normal mRNA export is maintained even when three Poms are all depleted in budding yeast. These observations suggested that there might be other membrane factors involved in the nuclear pore generation and NPC assembly process.

Considering the dynamic organization of NPC structure and high mobility of lipids in the membrane bilayer, it is possible that membrane proteins outside of the NPC may play a transient role in NPC assembly, *e.g.*, inducing the fusion event between ONM and INM, stabilizing the membrane curvature, and enriching the assembly intermediates. Although NPC is the only path for nucleocytoplasmic transport, the "peri-pore" domain of the nuclear membrane may assist the pre-transport or after-transport processes to make the cargo movement more efficient. The continuity of ER/NE structure and a shared membrane protein composition suggest that molecular events underlying NPC structure and function may be more complicated than what is known for Poms. In support to this, multiple NE/ER membrane proteins in *S. cerevisiae* have been reported to have a role in NPC structure maintenance and nuclear transport.

The mutant *brr6-1* was discovered in an *in situ* hybridization screen aimed at identifying *S. cerevisiae* mRNA export mutants (DE BRUYN KOPS and GUTHRIE 2001). *BRR6* encodes a membrane protein predominantly localized to the nuclear rim. Although Brr6p has a punctate localization pattern at the NE, it does not cocluster with the NPCs, suggesting that it is not a bona fide NPC component. However, the *brr6-1* mutant has wide synthetic lethal relationships with several *nup* mutants. Repression of the *BRR6* expression by an inducible promoter leads to the NPCs clustering and the NE herniations. It is hypothesized that Brr6p is distributed to the "peri-pore" nuclear membrane domain, and acts to restrain the lateral movement of the NPCs or helps to dock the transport cargo as well as assembly intermediates. In *S. cerevisiae*, Brr6p has sequence homology with Brl1p, and *brl1* mutants show similar nuclear transport and NPC clustering defects (SAITOH *et al.* 2005).

NEM1 and *SPO7* were identified in a synthetic lethal screen with *nup84*Δ mutant (SINIOSSOGLOU *et al.* 1998). Both encode membrane proteins localized to NE/ER membranes. Although they are dispensable for cell viability individually or in combination, TEM observations have revealed heavy NE overproliferation in *spo7*Δ or *nem1*Δ cells. There is a defect in assembling Nup49p-GFP fusion protein to the NPCs in *spo7*Δ cells. Further studies showed that these two proteins form a complex and have phosphatase activity (SANTOS-ROSA *et al.* 2005). The enzymatic activity is involved in recruitment of Smp2p onto promoters of phospholipid biosynthetic genes. Overexpressing *SMP2* is able to restore the normal nuclear membrane morphology in *spo7*Δ or *nem1*Δ mutants. These observations suggested that Nem1p and Spo7p may play roles in the NE/NPC structure maintenance by affecting the membrane lipid composition.

Overexpression of *SNL1* suppresses the lethal phenotype of *nup116-C* expression, or temperature sensitivity of mutants allelic to *GLE2* and *NIC96* (HO et al. 1998). *SNL1* encodes an integral membrane protein localized to the NE/ER membranes, which serves as a Bag domain co-chaperone for cytosolic Hsp70 proteins (SONDERMANN *et al.* 2002). The Hsp70 proteins function in appropriate protein folding, clathrin uncoating, synaptic vesicle fusion, and protein targeting (reviewed in YOUNG *et al.* 2003). The NE/ER localization of Snl1p and the genetic relationship between *SNL1* overexpression and several *nup*s suggests that Snl1p is involved in specific cellular processes, probably the NPC biogenesis or Nup degradation pathways. Based on the observations of functional effect of NE/ER membrane proteins on the NPC structure, it is conceivable that more factors may be involved in the NPC assembly process.

As a powerful genetic model system, *S. cerevisiae* provides a unique advantage to revealing novel factors in subcellular processes. The relative small genome size and high efficiency of homologous recombination have made all kinds of manipulation possible. The strength of the yeast genetic approach is evidenced by the fact that about two thirds of Nups were identified through genetic analysis, *e.g.*, the synthetic lethal screens with *pom152*Δ, *nup1*Δ, and *nup100*Δ mutants (AITCHISON *et al.* 1995; KENNA *et al.* 1996; MURPHY *et al.* 1996). Several NE/ER membrane proteins as well as the cytoplasmic soluble factors have also been identified in the previous genetic experiments. In our laboratory a Nup-GFP based visual screen has been successfully conducted and a battery of *S. cerevisiae* NPC assembly mutants (*npa* mutants) have been obtained (RYAN and WENTE 2002). These mutants are all conditional alleles and present dramatic Nup-GFP mislocalization at the nonpermissive temperature. As discussed in Chapter I, several

mutant alleles have been characterized, including the genes encoding RanGTPase cycle components, karyopherins, and trafficking vesicle coatomers. These discoveries suggested that the NPC assembly is a complicated process which involves multiple pathways inside of the cell.

The NPC in *S. cerevisiae* features broad internal genetic interactions among *NUP*s and external connections with either membrane or soluble factors. Its crucial role in nucleocytoplasmic transport makes cell growth vulnerable to even a subtle structural abnormality of the NPC. This favors the use of synthetic lethal screens to identify novel factors involved in NPC structure maintenance. Synthetic lethality often represents the relationship between genes involved in parallel signaling pathways or forming a complex structure. In *S. cevevisiae*, there are a significant number of uncharacterized ORFs. For instance, *YDL089W*, *YPR174C*, and *YDR458C* encode proteins localized to the nuclear periphery but with unknown function (HUH *et al.* 2003). Moreover, some ORFs may have multiple roles in various intracellular processes, *e.g.*, *PRP20* encodes a *S. cerevisiae* homolog of RanGEF which mediates NPC assembly, nuclear transport, and mitotic spindle formation (as reviewed in SAZER and DASSO 2000). Therefore, a well designed genetic screen with an appropriate strain is likely to reveal novel factors in NPC assembly.

In a continuing effort to dissect the mechanism of NPC assembly, the studies in this chapter investigated the genetic relationship between *POM34* and *POM152*. A *pom34*Δ *pom152*Δ double mutant was generated, and strikingly, no detectable phenotype of NPC structure and function was discovered. To seek novel factors compensating for the

functional loss of two Poms, a synthetic lethal screen was performed and several mutant alleles of *NUP188*, *NUP170*, and *NUP192* were identified.

Materials and methods

Yeast strains and plasmids

The *S. cerevisiae* strains were grown in either rich (YPD: 1% yeast extract, 2% peptone, 2% glucose) or synthetic minimal (SM) media lacking appropriate amino acids and supplemented with 2% glucose. 5-Fluoroorotic acid (5-FOA; United States Biological) was used at a concentration of 1.0 mg/ml. Yeast transformations were performed using the lithium acetate method (ITO *et al.* 1983) or a modified lithium sorbitol method (Stratagene CytoTrap protocol). General yeast manipulations were conducted as described elsewhere (Sherman et al. 1986). *Escherichia coli* host for all plasmids was DH5α. The bacteria were propagated in TB or LB media with appropriate antibiotics, *i.e.*, either ampicillin (75mg/ml) or kanamycin (30mg/ml). All *S. cerevisiae* strains and plasmids used in this work are listed in Table 3-1 and 3-2.

Fluorescence microscopy

Indirect immunofluorescence experiments were performed as described previously (WENTE *et al.* 1992), following a 10-min fixation in 3.7% formaldehyde and 10% methanol. The fixed cells were incubated for 16 hr at 4˚C with mAb414 (1:2 tissue culture supernatant, DAVIS and BLOBEL 1986), mouse monoclonal mAb118C3 against Pom152p (1:2 tissue culture supernatant, STRAMBIO-DE-CASTILLIA *et al.* 1995), or

affinity-purified rabbit polyclonal against the Nup116GLFG region (1:800, BUCCI and WENTE 1998). Bound antibody was detected by incubation with Alexa 594-conjugated goat anti-mouse IgG (1:400 dilution) or Alexa 594-conjugated goat anti-rabbit IgG (1:300) for 60 min at room temperature. The cells were stained with 0.05 μg/ml 4′,6-diamidino-2-phenylindole (DAPI) before visualizing under the fluorescence microscope (model BX50; Olympus, Lake Success, NY) using an Uplan 100×/1.3 objective. Images were captured using a digital camera (Photometrics Cool Snap HQ; Roper Scientific) with MetaVue software (Universal Imaging, West Chester, PA). Images were processed using Adobe Photoshop 7.0.

3,3′-Dihexyloxacarbocyanineiodide ($DiOC_6$) staining: $DiOC_6$ staining was performed as described elsewhere (KONING *et al.* 1993). Budding yeast cells in midlog phase growth were stained for 5 min with 1 μg/ml $DiOC_6$ (Molecular Probes), using a 0.1 mg/ml ethanol stock. Stained cells were viewed by direct fluorescence microscopy as described above.

Synthetic lethal screen to identify the pos mutants

A full length *POM34* segment including 360 bp endogeous promoter region was PCR amplified from the pSW1516 template. After *Sal*I/*Sma*I digestion, it was inserted into pSW611 (*GLE1/ADE3/URA3/CEN*) to replace the full length *GLE1* gene and hence obtained sectoring plasmid pSW3283 (*POM34/ADE3/URA3/CEN*). The *pom34*Δ *pom152*Δ (SWY3093) strain was crossed with YCH 130 (gift of C. Hardy) to generate SWY3450. The SWY3450 was further backcrossed with SWY3093 once. The haploid progeny was transformed with sectoring plasmid pSW3283 to generate parental strains

SWY3500 and SWY3501. These parental strains were tested for sectoring capacity at various temperatures, a 34˚C was chosen as the optimal temperature for synthetic lethal screen and the subsequent color-sectoring capacity test.

Ethylmethane sulfunate (EMS) mutagenesis was conducted as described previously (RYAN and WENTE 2002). In detail, the SWY3500 and SWY3501 were grown in SM -ura until stationary phase. The cells were harvested and washed in 50 mM KPi, pH 7.0, twice before treatment of EMS at 30˚C with a final concentration of 3%. After 45 min of mutagenesis, the EMS solution was quenched with 5% sodium thiosulfate. The resulting mutagenized cells were extensively washed and diluted in water, and stored at 4˚C for 3 days before plated on YPD media to reach 300~340 colony forming units (cfu) per 100mm plate. EMS-treated SWY3500 and SWY3501 strains grew at 18% and 33% viability at 34˚C, respectively, in the pilot experiment.

After 5 days of incubation at 34˚C, the sectoring phenotype of budding yeast colonies was scored visually. The non-sectoring (Sec^-) colonies were restreaked onto YPD media twice and subsequently onto 5-FOA containing media once to verify the growth dependence of pSW3283. 100,000 cfu from each mating type was screened, and 62 mutants with Sec^- and 5-FOA sensitive phenotype were finally obtained. These 62 mutants were then crossed in a pairwise manner at 30˚C. After assessing the Sec^- and 5-FOA sensitivity of resulting diploids, the mutants were sorted into 12 complementation groups. pSW186 (*ADE3/LEU2/CEN*), pSW1023 (*URA3/LEU2/CEN*), pSW1517 (*POM34/LEU2/CEN*), and CP25 (*LEU2/CEN*) were transformed into members of each complementation group to identify *POM34*-dependent mutants. Only three

complementation groups depended on pSW1517 to restore sectoring ability and growth on 5-FOA containing media, which were named Pom synthetic lethal (*pos*) mutants.

The above *pos* mutants from three complementation groups were backcrossed with parental strain SWY3500 and SWY3501. A mutation at single chromosome locus is confirmed by the 2:2 segregation of Sec^- phenotype in their progeny. The backcrossed progeny of *pos3*, *pos4*, and *pos7* mutants were tested for temperature sensitivity at 23˚C and 37˚C. To identify the potential *NUP* mutations in three complementation groups, a battery of plasmids containing full length Nups were tested for the ability to restore the sectoring phenotype. These plasmids are CP171 (*NDC1/LEU2/CEN*), CP162 (*NUP188/LEU2/CEN*), CP161 (*NUP170/LEU2/CEN*), CP163 (*NUP59/LEU2/CEN*), CP109 (*NUP159/LEU2/CEN*), CP120 (*NUP42/LEU2/CEN*), CP94 (*NUP2/LEU2/CEN*), CP164 (*NUP53/LEU2/CEN*), pSW278 (*NIC96/LEU2/CEN*), pSW787 (*NUP82/LEU2/CEN*), pSW406 (*GLE2/LEU2/CEN*), pSW222 (*NSP1/LEU2/CEN*), pSW226 (*NUP133/LEU2/CEN*), pSW229 (*POM152/LEU2/CEN*), pSW408 (*NUP157/LEU2/CEN*), pSW812 (*NUP1/LEU2/CEN*), pSW806 (*NUP57/LEU2/CEN*), pSW711 (*NUP85/LEU2/CEN*), pSW821 (*NUP49/LEU2/CEN*), pSW75 (*NUP116/LEU2/CEN*), pSW78 (*NUP100/LEU2/CEN*), and CP25 (*LEU2/CEN*). Two complementation groups sector in the presence of CP162 (*NUP188/LEU2/CEN*) and CP161 (*NUP170/LEU2/CEN*), respectively (Table 3-3). The mutant, *pos7*, in the last complementation group was not complemented by any of the above Nup-bearing plasmids.

Cloning of *pos7*

The *S. cerevisiae* genomic library (American Type Culture Collection, VA) carried in the vector p366 (*LEU2/CEN*) was transformed into *pos7*. Approximately 5800 cfu were visually screened for sectoring ability at SM –leu media after extended growth at 34˚C. The library plasmids were then extracted from sectoring yeast cells and electroporated into DH5α *E. coli*. After propagation in DH5α, the plasmids were retransformed into *pos7* to verify the sectoring phenotype on SM -leu media at 34˚C. A total of 5 plasmids were verified in rescuing the sectoring capacity of *pos7*. These plasmids were analyzed with restriction enzyme *HindIII/NheI/EcoRI* and yielded a similar digestion pattern. Two plasmids were sequenced and both were shown to contain three complete ORFs, namely *NUP192*, *YJL037W*, and *YJL038C*. *YJL037W* and *YJL038C* were individually subcloned into pRS315. The resulting two plasmids as well as a plasmid containing full length *NUP192* (CP3138, from Ed Hurt, KOSOVA *et al.* 1999) were then transformed into *pos7* to define the mutation.

Results

POM152 overexpression partially suppresses the loss of *POM34* function

The overlapping synthetic lethal profile for *pom34*Δ and *pom152*Δ mutants, as described in Chapter II, suggested that the two proteins might have common function(s). Thus, we investigated whether overexpressing one would rescue the viability of a synthetic lethal combination for the other. Double-mutant *pom nup* strains that required the respective *POM/URA3* plasmid for viability were transformed with a high-copy

plasmid (*LEU2/2μ*) harboring wild-type *POM34* or *POM152*. The resulting budding yeast transformants were grown on SM–leu to maintain the high-copy *LEU2/2μ* plasmid and then assayed for colony formation after replica plating to media containing 5-FOA. If the *LEU2* plasmid rescued the mutant, the strain would be viable in the absence of the *URA3* plasmid and grow in the presence of 5-FOA. As a control, an empty *LEU2* plasmid did not rescue growth (Figure 3-1). Overexpressing *POM34* did not rescue any of the *pom152*Δ *nup* mutants (Figure 3-1 B). However, the *pom34*Δ *nup59*Δ and *pom34*Δ *nup170*Δ double mutants were viable with the *POM152/LEU2/2μ* plasmid (Figure 3-1 A). This suggested that overexpressing *POM152* suppressed the loss of *POM34* in the *nup59*Δ and *nup170*Δ genetic backgrounds. The suppression was, however, partial as reflected by diminished growth compared to the strains with a *POM34/LEU2* plasmid. In addition, overexpressing *POM152* did not complement the *pom34*Δ *nup188*Δ mutant. We concluded that these two integral membrane proteins have some level of functional redundancy but are not completely interchangeable.

The *pom34*Δ *pom152*Δ double mutant has no growth or morphology defects

Pom34p and Pom152p are the only two integral membrane proteins known to localize exclusively to the NPC in *S. cerevisiae*. Since each is encoded by a nonessential gene (GIAEVER *et al.* 2002; WOZNIAK *et al.* 1994), we generated a double null strain and tested the viability and growth of cells lacking both of these Poms. In comparison to wild-type or single-mutant strains, the *pom34*Δ *pom152*Δ cells had no apparent growth defect when tested at a range of temperatures from 23˚C to 37˚C (Figure 3-2). At 17˚C, the *pom152*Δ mutant was slightly cold sensitive, as was the *pom34*Δ *pom152*Δ mutant.

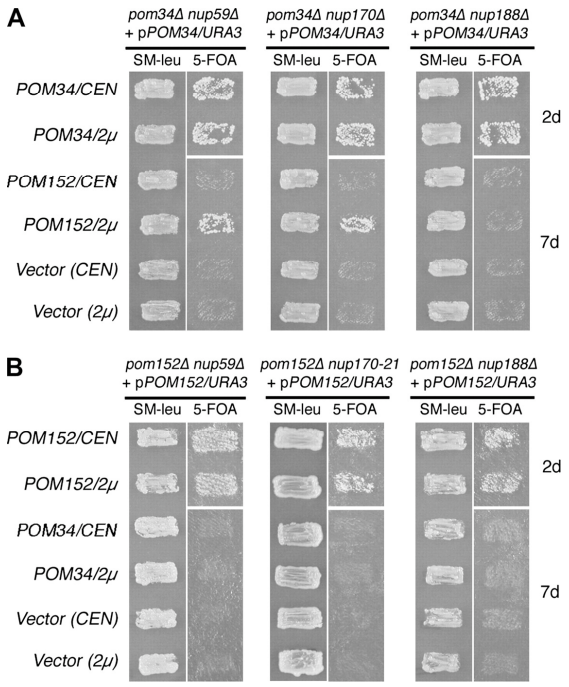

Figure 3-1: Multicopy suppression analysis of respective double mutants with *POM34* and *POM152* expression. (A) *pom34*Δ *nup* double-mutant strains harboring a *POM34/URA3/CEN* plasmid (SWY3139, SWY3132, and SWY3125) were transformed with *POM152/LEU2/CEN* (low copy), *POM152/LEU2/2μ* (high copy), *POM34/LEU2/CEN*, *POM34/LEU2/2μ*, or empty vectors. The resulting strains were patched on SM-leu and grown at 30˚C for 2 days before replica plating to 5-FOA medium. The cells on 5-FOA were incubated at 30˚C for 2 or 7 days (d). (B) *pom152*Δ *nup* double-mutant strains harboring a *POM152/URA3/CEN* plasmid (SWY3488, psl21, SWY3219) were transformed with the same *LEU2* plasmids, patched, and grown as in A.

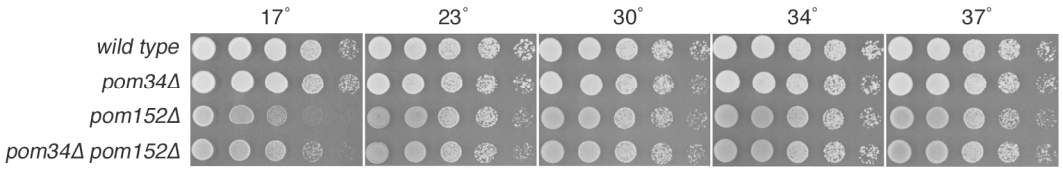

Figure 3-2: The *pom34*Δ *pom152*Δ double mutant has no significant growth defect. Fivefold serial dilutions of equal cell numbers from wild type (SWY518), *pom34*Δ (SWY2565), *pom152*Δ (PMY17), or *pom34*Δ *pom152*Δ (SWY3093) strains were spotted on YPD medium. Growth was compared after incubation at the designated temperature.

To directly examine Nup localization and general NPC structure, indirect immunofluorescence (IIF) microscopy was performed for staining with mouse monoclonal antibody mAb414 and rabbit affinity-purified anti-Nup116GLFG antibodies. These two antibodies both recognize epitopes in Nups that harbor phenylalanine–glycine (FG) repeats (BUCCI and WENTE 1998; DAVIS and BLOBEL 1986). In wild-type cells, the FG Nups exhibit concentrated, punctate nuclear rim localization (Figure 3-3 A). The *pom34*Δ *pom152*Δ double-mutant staining was identical to that of wild type, indicating that there is no defect in FG-Nups assembly.

To evaluate intracellular membrane content, cells in log phase growth were stained with a lipophilic fluorescent dye $DiOC_6$. $DiOC_6$ has been routinely used to assess intracellular membrane proliferation, including that from the ER/NE (KONING *et al.* 1993). The overproliferation of nuclear membranes has been reported in *pom152*Δ *nup170*Δ synthetic lethal mutant, and several other NPC assembly mutants (AITCHISON *et al.* 1995; RYAN and WENTE 2002). However, the membrane staining in *pom34*Δ *pom152*Δ cells was not different from that in wild type (Figure 3-3 B).

Finally, in order to exclude the possibility of subtle NPC structural alteration that may affect nucleocytoplasmic transport, two import cargos Pho4-NLS-GFP_3 and Nab2-NLS-GFP were tested for steady state localization in *pom34*Δ *pom152*Δ mutant. Both import reporters, representing Kap121p and Kap104p-mediated transport pathways respectively (CHOOK and BLOBEL 2001), were found to accumulate inside of the nucleus as in wild type cell (Figure 3-4). Overall, no significant defects in cell growth, Nup localization, membrane structures, and nuclear transport were detected in *pom34*Δ *pom152*Δ cells.

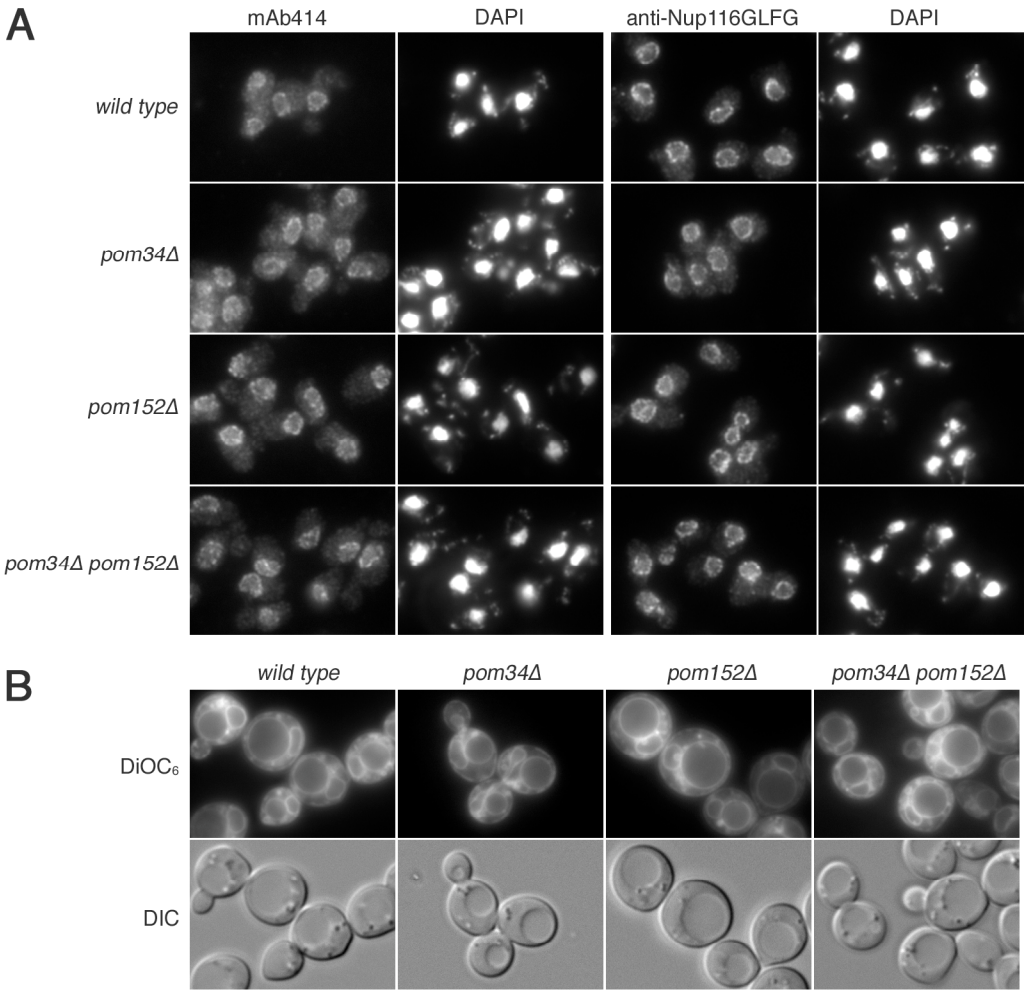

Figure 3-3: The *pom34*Δ *pom152*Δ double mutant has no detectable NPC and NE morphology defect. (A) Indirect immuofluorescence microscopy was performed as described in MATERIALS AND METHODS with either mouse monoclonal mAb414 or rabbit anti-Nup116GLFG antibodies. Nuclei were detected by DAPI staining. (B) Direct fluorescence microscopy of live cells stained with $DiOC_6$ to visualize membranes. Corresponding DIC pictures are shown.

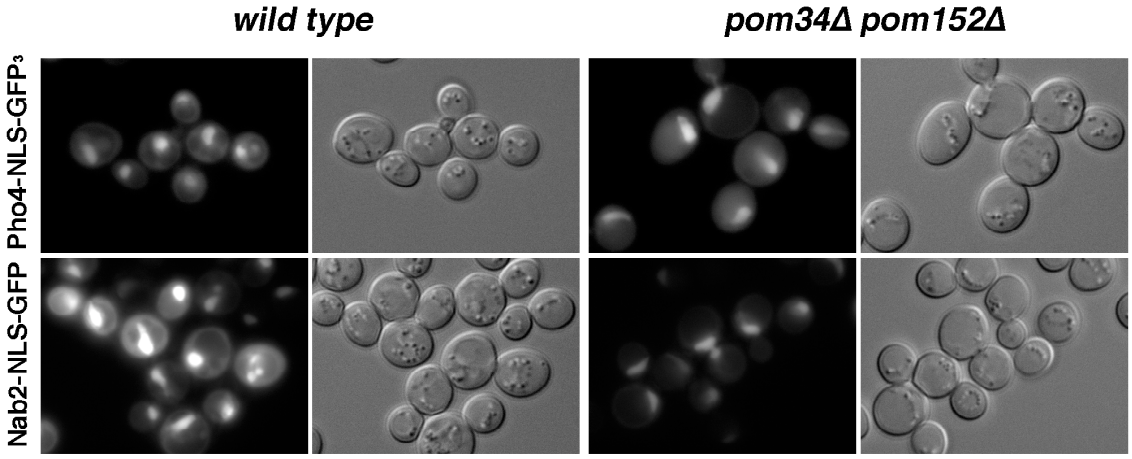

Figure 3-4: The *pom34*Δ *pom152*Δ mutant has no defect in Kap121p and Kap104p–mediated import. Pho4-NLS-GFP_3 (for Kap121p) or Nab2-NLS-GFP (for Kap104p) transport reporter plasmids were transformed into wild type or *pom34*Δ *pom152*Δ cells. Steady-state localization of GFP fluorescence was visualized in cells growing at early to mid-log phase at 30˚C. The corresponding DIC images are shown.

Synthetic lethal screen to identify the potential NPC assembly factors

Since there was no growth or NPC morphology defect observed in the *pom34*Δ *pom152*Δ mutant, we hypothesized that other unidentified Poms, or even NE/ER membrane proteins, may compensate for the functional loss of Pom34p and Pom152p. To reveal the potential factors involved in this process, a color-sectoring based, synthetic lethal screen was performed (outlined in Figure 3-5). The *pom34*Δ *pom152*Δ double mutant was crossed with an *ade2*Δ *ade3*Δ strain to generate parental strains for the screen. The disrupted *pom34*Δ and *pom152*Δ alleles were verified by PCR, as well as by IIF against Pom152p. The parental strains were tested for growth at various temperatures from 23˚C to 34˚C and no apparent retardation was observed. Their sectoring ability was tested in the presence of plasmid *POM34/ADE3/URA3/CEN* at temperatures from 23˚C to 34˚C. The strain showed a full capacity for sectoring at 34˚C on non-selective media, suggesting that there is no intrinsic pressure for retention of the *POM34/ADE3/URA3/CEN* plasmid in the parental strains at this condition. Therefore 34˚C was selected for the incubation condition for synthetic lethal mutants.

The *pom34*Δ *pom152*Δ *ade2 ade3* + *pPOM34/ADE3/URA3/CEN* strain was grown to stationary phase (OD_{600} >1.5). A total of $5x10^8$ cells were treated with 3% EMS for 45 minutes. This treatment led to 33% and 18% viability for *MATα* and *MATa* strains respectively, which is likely to result in at least one point mutation per genome. After visual screening for color sectoring and growth testing on 5-FOA containing media, as well as the subsequent complementation test, 12 complementation groups were obtained. They included two groups which were synthetic lethal with the *ura3-1* allele, and one group synthetic lethal with *ade3*. Five groups sectored independently of the

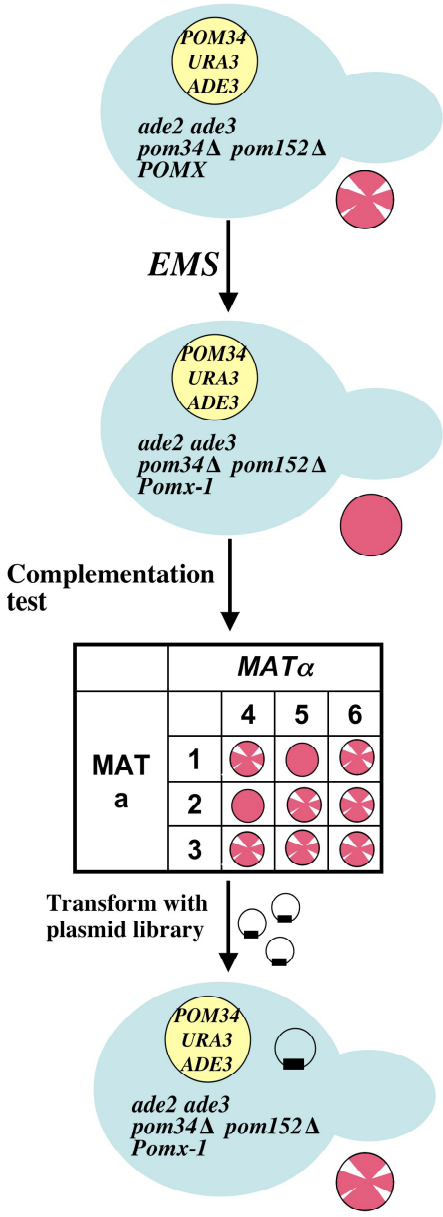

Figure 3-5: Flow chart of synthetic lethal screen process. A *pom34*Δ *pom152*Δ *ade2 ade3* strain carrying the sectoring plasmid *POM34/ADE3/URA3/CEN* showed a strong sectoring capacity at 34˚C. These parental strains, *MAT**a*** and *MAT*α, were treated with 3% EMS for 45 minutes and then plated on YPD. After incubation at 34˚C, the synthetic lethal mutants grew as Sec$^-$ colonies due to the dependence of *POM34* harbored in the sectoring plasmid. Sec$^-$ mutants from each mating type were crossed in a pairwise manner to be sorted into complementation groups. *POM34*-related synthetic lethal mutants were transformed with *S. cerevisiae* chromosome library harbored in *LEU2/CEN* vector to clone the mutated ORF.

POM34/ADE3/URA3/CEN plasmid, and therefore were omitted. One group showed resistance to plasmid transformation, therefore was also omitted. The remaining three groups of synthetic lethal mutants that relied on the *POM34/ADE3/URA3/CEN* for sectoring are defined as *pos* (Pom synthetic lethal) mutants. After direct tests with genes encoding the candidate Nups, or transforming with a *S. cerevisiae* genomic library, these *pos* mutants were complemented by *NUP188*, *NUP170*, and *NUP192* (Figure 3-6). To test for conditional growth, they were backcrossed and there was no linkage of temperature sensitivity at 23˚C or 37˚C with sectoring ability of *pos3*, *pos4*, and *pos7* progeny. The backcross of *1pos* and *pos12* mutants did not yield four viable spores for all tetrads dissected, therefore the effort to test temperature sensitivity was abandoned.

Although *POM34* was used to restore the sectoring ability of *pos* mutants, we wondered whether *POM152* has the equal capacity in restoring sectoring phenotype of the *pos* mutants as well. Low copy or high copy plasmids bearing *POM152* were tested in all 5 *pos* strains. As seen in Figure 3-7, *POM152* restored the full sectoring capacity of *pos12* when overexpressed, but not any other *pos* strains. This suggested that although *pos* strains were obtained through a screen against a *pom34*Δ *pom152*Δ double mutant, the mutant *nup* alleles identified were biased to the function of *POM34*.

Discussion

To investigate the relationship between Poms comprising the NPC, experiments were conducted to show that *POM34* and *POM152* have partially overlapping but nonessential function. Using a *pom34*Δ *pom152*Δ strain, a synthetic lethal screen was performed and mutant alleles of *NUP192*, *NUP188* and *NUP170* were identified.

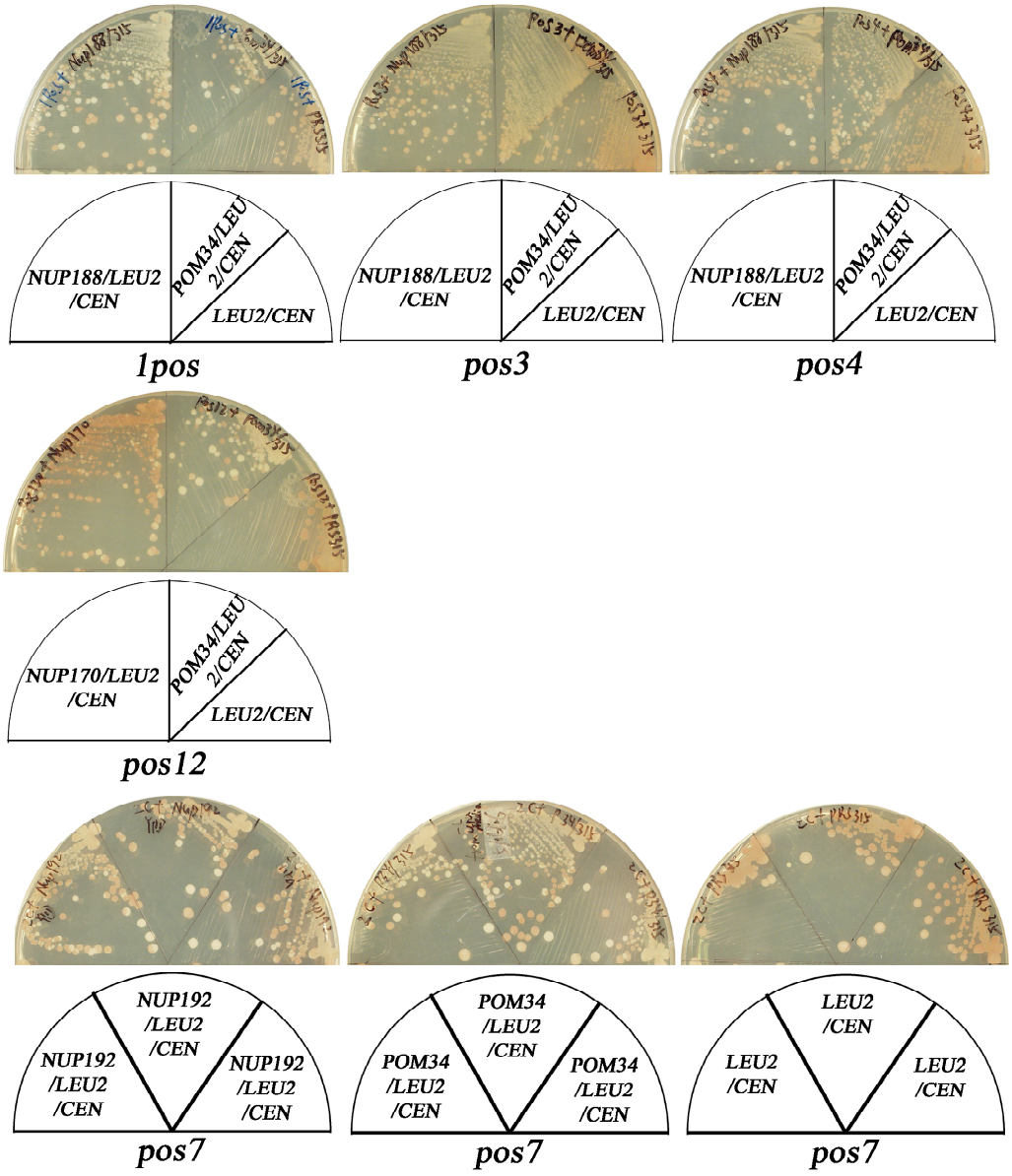

Figure 3-6: *NUP*s restore the sectoring phenotype to *pos* mutants. *NUP188/LEU2/CEN* plasmid was transformed into *1pos*, *pos3*, and *pos4* mutants. *NUP170/LEU2/CEN* plasmid was transformed into *pos12* mutant. *NUP192/LEU2/CEN* plasmid was transformed into *pos7* mutant. The sectoring ability of the transformants is observed after incubation at 34˚C on YPD media. The control plasmid *POM34/LEU2/CEN* and empty vector *LEU2/CEN* were included as well in each *pos* mutant.

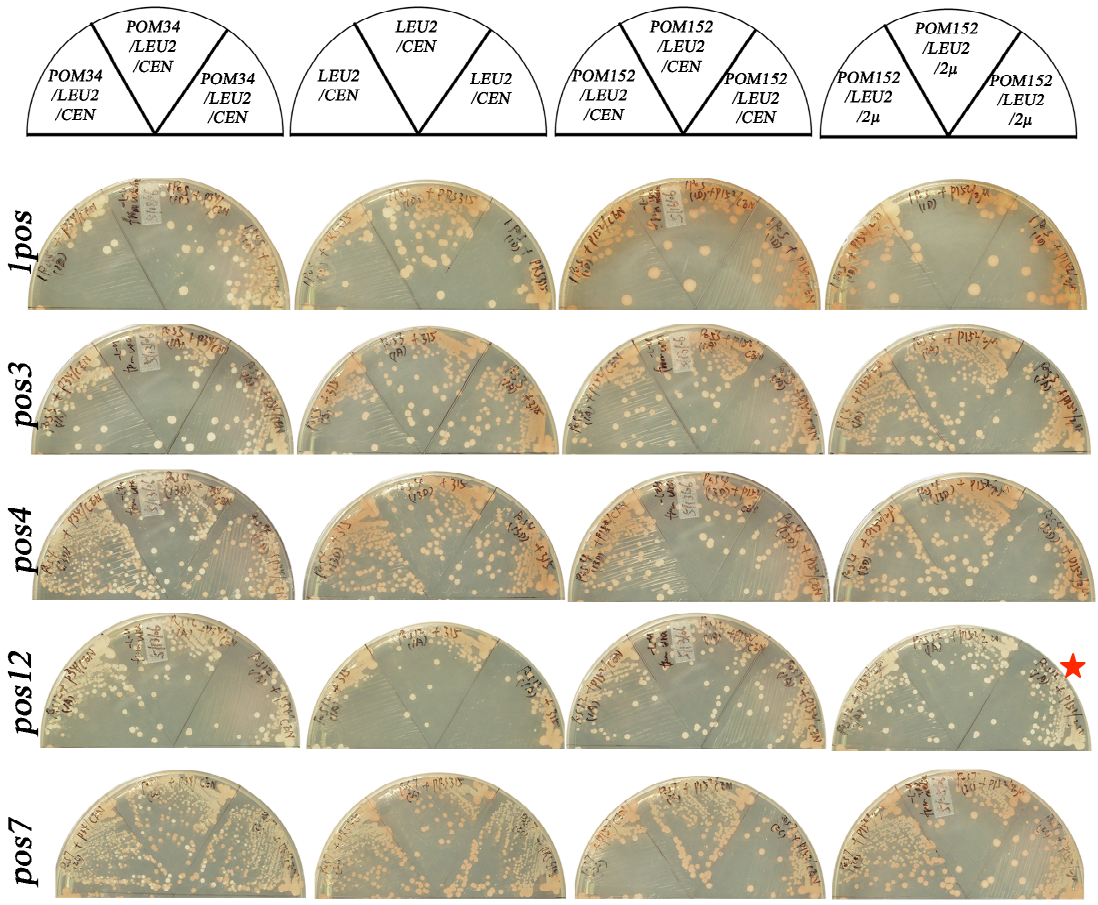

Figure 3-7: Overexpression of *POM152* restores *pos12* sectoring phenotype. All 5 *pos* mutants were transformed with *POM152/LEU2/CEN* (low copy), *POM152/LEU2/2μ* (high copy), *POM34/LEU2/CEN*, or empty vector and tested for sectoring ability at 34˚C on YPD media. Only *pos12* restored Sec^{+} phenotype in the presence of *POM152/LEU2/2μ* after incubation (showed by star).

In *S. cerevisiae*, we have found that the pattern of genetic connections for *POM34* and *POM152* with *NUP*s is quite similar. Like Pom34p, Pom152p has genetic and physical connections with components of the Nup170p and the Nup188p subcomplexes. Pom34p and Pom152p also have some level of functional overlap based on our genetic suppression results (Figure 3-1). Overexpression of *POM152* rescued the lethality of certain *pom34*Δ *nup* double mutants whereas overexpression of *POM34* did not rescue any of the tested *pom152*Δ *nup* mutants. Although we do not know if the respective POM overexpression levels are comparable, this suggests that Pom152p has a function distinct from Pom34p. In addition, the *pom34*Δ *nic96-1* mutant showed no enhanced lethality whereas a *pom152*Δ *nic96-7* mutant is synthetically lethal (AITCHISON *et al.* 1995; TCHEPEREGINE *et al.* 1999). This might reflect allele specificity for the *nic96* mutants, and/or these results might be further evidence of distinct roles for Pom152p and Pom34p. Work revealing the direct physical interaction partners for Pom152p and Pom34p will be needed to further resolve their distinct and shared functions.

Despite a potential complementary role for Pom34p and Pom152p in NPC structural maintenance, it is intriguing that the *pom34*Δ *pom152*Δ double mutant is viable and shows no detectable NPC defects. The same observation is also reported in another independent study (MADRID *et al.* 2006). There are several possible explanations. Firstly, it is possible that the *S. cerevisiae NDC1* will compensate the functional loss of two Poms in *pom34*Δ *pom152*Δ cells. However, the role of yNdc1p in NPC assembly is still not clear. Secondly, there might be an unidentified Pom playing a role in the *pom34*Δ *pom152*Δ double mutant. Thirdly, since the NPC/NE morphology has been reported to be affected by multiple factors outside of the NPC, it is also plausible that NE/ER membrane

proteins play a transient role in the NPC assembly process. In all conditions, a synthetic lethal relationship is likely to exist between the potential factors and the Poms. We speculated that the *pom34*Δ *pom152*Δ double null strain provided a sensitive genetic background to reveal those novel factors.

To fully address this, a synthetic lethal screen with EMS-treated *pom34*Δ *pom152*Δ cells was conducted. The sectoring plasmid *POM34/ADE3/URA3/CEN* was fully functional as shown from the complementation capacity in synthetic lethal mutants that rely on wild type *POM34* for viability. Previous experience suggested that the cell viability below 30% after EMS treatment would allow a successful synthetic lethal screen (MURPHY *et al.* 1996). The total number of 200,000 colonies analyzed was likely to saturate the screen. Taking dual standards of color sectoring on YPD media and growth inhibition on 5-FOA containing media, the mutants were stringently selected. The screen temperature, 34˚C, was higher than the classical budding yeast growth condition and might favor the lateral diffusion of integral membrane proteins along NE/ER surface, and hence increase the possibility of revealing factors that have a transient role in NPC assembly.

Despite cautious design and execution, the synthetic lethal screen did not reveal any ORFs encoding integral membrane proteins. There could be several explanations to this result. Firstly, the genetic screen was not saturated as evidenced by five *pos* mutants in three complementation groups. This is probably due to the stringent cutoff used in the visual screen. The sectoring phenotype and growth on 5-FOA containing media were not always distinct for each individual mutant. The standards used in the screen might be overstringent. After two rounds of visual screening and one round of testing for 5-FOA

sensitivity, several mutants with weak phenotypes might have been discarded. Secondly, there might exist a complex network of integral membrane proteins that compensates for the functional loss of Poms in the *pom34*Δ *pom152*Δ double mutant strain. It is a low chance to target all of them in one cell by EMS mutagenesis. Thirdly, the major function of Poms may be related to docking and organizing soluble Nups. The membrane fusion and "porogenic" events are possibly mediated through a completely different set of proteins. Therefore it is less likely to reveal those factors through a synthetic lethal screen with the *pom34*Δ *pom152*Δ stain. Fourthly, the potential membrane proteins acting in NPC biogenesis might play roles in multiple cellular processes. The mutation of the genes encoding these factors could lead to irreversible impairment of other essential cell functions, which ultimately eliminates their presence in the genetic screen.

Nup188p, Nup170p, and Nup192p are all major structural components of the NPC. These Nups together with other structural Nups, such as Nup157p, Nup59p, Nup53p, and Nic96p, form a fundamental framework for the NPC through their bulky molecular size. There exists a great level of functional redundancy between them, as evidenced by the fact that most individual structural Nups are dispensable for cell viability. Nup192p is the largest molecule and is encoded by an essential gene. Others have shown that the *nup192-15* allele causes a defect in assembling the Nup49-GFP into NPCs. Computer analysis of 3-D NE reconstruction revealed that the *nup192-15* mutant has fewer NPCs in the nuclear membrane at the restrictive temperature (GOMEZ-OSPINA *et al.* 2000). In preliminary studies, I found that the *nup192-15* allele was unable to complement the sectoring capacity of *pos7* mutant (data not shown). This suggests that the full function of Nup192p is critical for the cell lacking the two Poms. The identification of these Nups

further confirmed the concept that NPC structure is maintained by the coordination between Poms and large structural Nups.

Table 3-1 Yeast strains used in Chapter III

Strain	Genotype	Source
YCH130	*MAT**a** ade2 ade3 ura3 leu2 his3 lys2*	Gift from C. Hardy
SWY3500	*MAT**a** pom34::spHIS5 pom152::HIS3 ura3-1 his3-11,15 lys2 leu2-3,112 can1-100 ade2 ade3* +p*POM34/ADE3/URA3/CEN*	This study
SWY3501	*MATα pom34::spHIS5 pom152::HIS3 ura3-1 his3-11,15 trp1-1 leu2-3,112 can1-100 ade2 ade3* +p*POM34/ADE3/URA3/CEN*	This study
SWY3450	*MAT**a** pom34::spHIS5 pom152::HIS3 ura3-1 his3-11,15 leu2-3,112 can1-100 lys2 ade2 ade3*	This study
SWY518	*MAT**a** ade2-1::ADE2 ura3-1 his3-11,15 trp1-1 leu2-3,112 can1-100*	(BUCCI and WENTE 1997)
SWY2565	*MATα pom34::spHIS5 ade2-1::ADE2 ura3-1 his3-11,15 trp1-1 leu2-3,112 can1-100*	This study
SWY3093	*MATα pom34::spHIS5 pom152::HIS3 ura3-1 his3-11,15 trp1-1 leu2-3,112 can1-100 ade2-1*	This study
SWY3139	*MAT**a** pom34::spHIS5 nup59::KAN^R his3 ura3 leu2 met15* + pSW1516	This study
PMY17	*MAT**a** pom152-2::HIS3 ade2-1 ura3-1 his3-11,15 trp1-1 leu2-3,112 can1-100*	(WOZNIAK *et al.* 1994)
SWY3132	*MAT**a** pom34::spHIS5 nup170::KAN^R his3 ura3 trp1 leu2 met15* + pSW1516	This study
SWY3125	*MAT**a** pom34::spHIS5 nup188::KAN^R his3 ura3 trp1 leu2 lys2* + pSW1516	This study
SWY3488	*MATα pom152::HIS3 nup59::KAN^R his3 ade2 lys2 ura3 leu2* + p*CH1122-POM152(ADE3-URA3)*	This study
SWY3219	*MATα pom152::HIS3 nup188::KAN^R his3 ade2 lys2 ura3 leu2* + p*CH1122-POM152(ADE3-URA3)*	This study
psl21	*MATα pom152-2::HIS3 nup170-21 ade2 ade3 ura3 his3 trp1 leu2 can1* + p*CH1122-POM152 (ADE3-URA3)*	(AITCHISON *et al.* 1995)
SWY3785 (1pos)	*MATα nup188 pom34::spHIS5 pom152::HIS3 ura3-1 his3-11,15 trp1-1 leu2-3,112 can1-100 ade2 ade3* +p*POM34/ADE3/URA3/CEN*	This study
SWY3786 (pos3)	*MAT**a** nup188 pom34::spHIS5 pom152::HIS3 ura3-1 his3-11,15 lys2 leu2-3,112 can1-100 ade2 ade3* +p*POM34/ADE3/URA3/CEN*	This study
SWY3787 (pos4)	*MAT**a** nup188 pom34::spHIS5 pom152::HIS3 ura3-1 his3-11,15 lys2 leu2-3,112 can1-100 ade2 ade3* +p*POM34/ADE3/URA3/CEN*	This study
SWY3788 (pos7)	*MAT**a** nup192 pom34::spHIS5 pom152::HIS3 ura3-1 his3-11,15 lys2 leu2-3,112 can1-100 ade2 ade3* +p*POM34/ADE3/URA3/CEN*	This study

Table 3-1 continued		
SWY3789 (pos12)	*MAT**a** nup170 pom34::spHIS5 pom152::HIS3 ura3-1 his3-11,15 lys2 leu2-3,112 can1-100 ade2 ade3* +p*POM34/ADE3/URA3/CEN*	This study
SWY3791	Progeny (1D) from backcross between SWY3785 (*1pos*) and SWY3500	This study
SWY3792	Progeny (1A) from backcross between SWY3786 (*pos3*) and SWY3501	This study
SWY3793	Progeny (9D) from backcross between SWY3786 (*pos3*) and SWY3501	This study
SWY3794	Progeny (14C) from backcross between SWY3787 (*pos4*) and SWY3501	This study
SWY3795	Progeny (13D) from backcross between SWY3787 (*pos4*) and SWY3501	This study
SWY3796	Progeny (2C) from backcross between SWY3788 (*pos7*) and SWY3501	This study
SWY3797	Progeny (15C) from backcross between SWY3788 (*pos7*) and SWY3501	This study
SWY3798	Progeny (1A) from backcross between SWY3789 (*pos12*) and SWY3501	This study
SWY3799	Progeny (4C) from backcross between SWY3789 (*pos12*) and SWY3501	This study

Table 3-2 Plasmids used in Chapter III

Plasmid	Description	Source
	pRS316 backbone	(SIKORSKI and HIETER 1989)
pSW1516	Full-length *POM34*	This study
pSW3283	Full-length *POM34* and *ADE3*, derived from pSW611	This study
pSW611	Full-length *GLE1* and *ADE3*	(YORK *et al.* 1999)
	pRS315 backbone	(SIKORSKI and HIETER 1989)
pSW1517	Full-length *POM34*	This study
pSW3191	Full-length *POM152*	This study
pSW3285	Full-length *YJL037W*	This study
pSW3286	Full-length *YJL038C*	This study
pSW1023	Full-length *URA3*	Gift from A. Ho
pSW186	Full-length *ADE3*	Gift from S. Wente
CP171	Full-length *NDC1*	Gift from M. Winey
CP162	Full-length *NUP188*	(NEHRBASS *et al.* 1996)
CP161	Full-length *NUP170*	(AITCHISON *et al.* 1995)
CP163	Full-length *NUP59*	(MARELLI *et al.* 1998)
pSW278	Full-length *NIC96*	Gift from J. Watkin
CP109	Full-length *NUP159*	(GORSCH *et al.* 1995)
pSW787	Full-length *NUP82*	Gift from M. Bucci
pSW406	Full-length *GLE2*	(MURPHY *et al.* 1996)
pSW222	Full-length *NSP1*	Gift from S. Wente
pSW226	Full-length *NUP133*	(MURPHY *et al.* 1996)
pSW229	Full-length *POM152*	(MURPHY *et al.* 1996)
pSW408	Full-length *NUP157*	(MURPHY *et al.* 1996)
pSW812	Full-length *NUP1*	Gift from M. Bucci
pSW806	Full-length *NUP57*	(BUCCI and WENTE 1998)
pSW711	Full-length *NUP85*	Gift from M. Bucci
CP94	Full-length *NUP2*	Gift from Loeb
pSW821	Full-length *NUP49*	Gift from M. Bucci

Table 3-2 continued		
pSW75	Full-length *NUP116*	(WENTE *et al.* 1992)
pSW78	Full-length *NUP100*	(WENTE *et al.* 1992)
CP164	Full-length *NUP53*	(MARELLI *et al.* 1998)
	pRS425 backbone	(CHRISTIANSON *et al.* 1992)
pSW863	Full-length *POM152* in *Pst*I site	Gift from A. Ho
pSW3044	Full length *POM34*	This study
	Others	
CP120	Full-length *NUP42*	Gift from F. Stutz
pSW3284	Full-length *NUP192*, *YJL037W*, and *YJL038C*, isolated from *S. cerevisiae CEN* library	This study
CP3138	Full-length *NUP192* harbored in pUN100 vector	(KOSOVA *et al.* 1999)
CP3140	*nup192-15* harbored in YCplac22 vector	(KOSOVA *et al.* 1999)

Table 3-3 Complementation table of *pom34*Δ *pom152*Δ synthetic lethal screen

Genetic			Molecular			
Group	*pos* mutants	Temperature sensitivity (23˚C and 37˚C)	*POM34*	*NUP188*	*NUP170*	*NUP192*
1	SWY3785 *(1pos)* SWY3786 (*pos3)* SWY3787 (*pos4)*	Undetermined Not Not	+	+		
2	SWY3789(*pos12)*	Undetermined	+		+	
3	SWY3788 (*pos7)*	Not	+			+

CHAPTER IV

SPLIT UBIQUITIN YEAST TWO HYBRID ASSAY AND FUTURE DIRECTIONS

Introduction

In Chapter II, a series of experiments have been conducted to address the role of Pom34p in NPC structural organization. The membrane orientation of Pom34p, its genetic connections with Nups, and the effect on NPC structure and function were investigated. In Chapter III, the genetic relationship between *POM34* and *POM152* was examined. A synthetic lethal screen with *pom34*Δ *pom152*Δ mutant revealed several mutant alleles of *NUP192*, *NUP188*, or *NUP170*. These discoveries shed insight into the molecular organization of NPCs. Meanwhile, several questions remain unanswered in the NPC assembly field. Firstly, considering the fact that Poms from vertebrates are playing critical roles in NPC/NE formation, it is intriguing that budding yeast cells still maintain nuclear pores and a normal mRNA export in the lack of one or more Poms (this study and MADRID *et al.* 2006). We speculate that other novel membrane factors are also involved in this process, probably through the transient or permanent interactions with Poms. Examining the potential interaction pattern between Poms and other integral membrane proteins will help pinpoint the mechanism of NPC assembly. Secondly, although *NDC1* is the only Pom in *S. cerevisiae* sharing sequence homology to a counterpart in vertebrates, its function in NPC assembly is still unclear. For example, the *ndc1-39* conditional allele is reported to have only a minor defect in NPC assembly (LAU *et al.* 2004). Further dissection of the role of Ndc1p in NPC assembly will be necessary to

provide a full picture of budding yeast Poms function. Thirdly, the nuclear pore is formed by the fusion of ONM and INM, causing the membrane lipid bilayer to make a 180˚ turn at the nuclear pore. The mechanism of deforming the flat nuclear membrane into a sharply curved membrane is still unknown. To analyze the molecular events occurring during membrane deformation will improve the understanding of the fundamental process in generating a membrane pore. Several efforts to address the above questions have been described and future directions are also included.

Detection of membrane proteins that physically interact with Poms

Split ubiquitin yeast two hybrid assay

The yeast two hybrid assay takes advantage of the fact that DNA binding domain (BD) and transcription activation domain (AD) of the Gal4p transcription factor can be experimentally separated and reconstituted through a flexible bridging sequence. An interaction complex formed by the bait and prey proteins, which are conjugated to either Gal4p-BD or Gal4p-AD, will reconstitute the proximity between AD and BD and hence activate reporter genes (YOUNG 1998). This powerful technique has been widely used in direct tests and large scale screens of protein-protein interactions, and it provides an approach to test physical interaction between proteins *in vivo*. Several modifications of this method, such as the use of multiple reporter genes, the reverse yeast two hybrid assay, protein or RNA three-hybrid system, and split ubiquitin yeast two hybrid assay, *etc*. have been developed to detect more complicated interaction patterns (VAN CRIEKINGE and BEYAERT 1999).

The classical yeast two hybrid assay relies on the intranuclear localization of bait and prey proteins. Poms that are targeted to the nuclear membranes cannot be relocated into the nucleus when conjugated with Gal4p-BD or Gal4p-AD domain. Furthermore, the interactions between Poms and other NE/NPC factors may require the coordination of both cytoplasmic and lumenal domains, and even the transmembrane segments. Therefore, there is a particular hindrance in applying traditional yeast two hybrid approach to NE/NPC integral membrane protein study. Others have developed a membrane-based split ubiquitin yeast two hybrid method to overcome this obstacle (FETCHKO and STAGLJAR 2004). In this assay, halves of ubiquitin are fused to the cytoplasmic termini of full-length membrane proteins to form the bait and prey (Fig 4-1). The bait protein is able to be targeted into the appropriate membrane compartment through a native pathway, interact with other membrane or soluble factors included in the prey protein, and hence reconstitute a functional ubiquitin molecule. An artificial transcription factor conjugated with the ubiquitin molecule is subsequently cleaved by a ubiquitin specific protease and imported into the nucleus to activate the reporter genes. This method has been successfully used to analyze integral membrane protein interactions in both a direct test and genome-wide screen mode (MCGEE *et al.* 2006; MILLER *et al.* 2005).

Split ubiquitin yeast two hybrid screen with *Cub-POM152* bait

The "porogenic" process of nuclear pore formation is thought to be mediated through the NE lumenal connection of membrane proteins localized to both the ONM and INM. Of the three Poms in *S. cerevisiae*, Pom152p uniquely contains a bulky hydrophilic

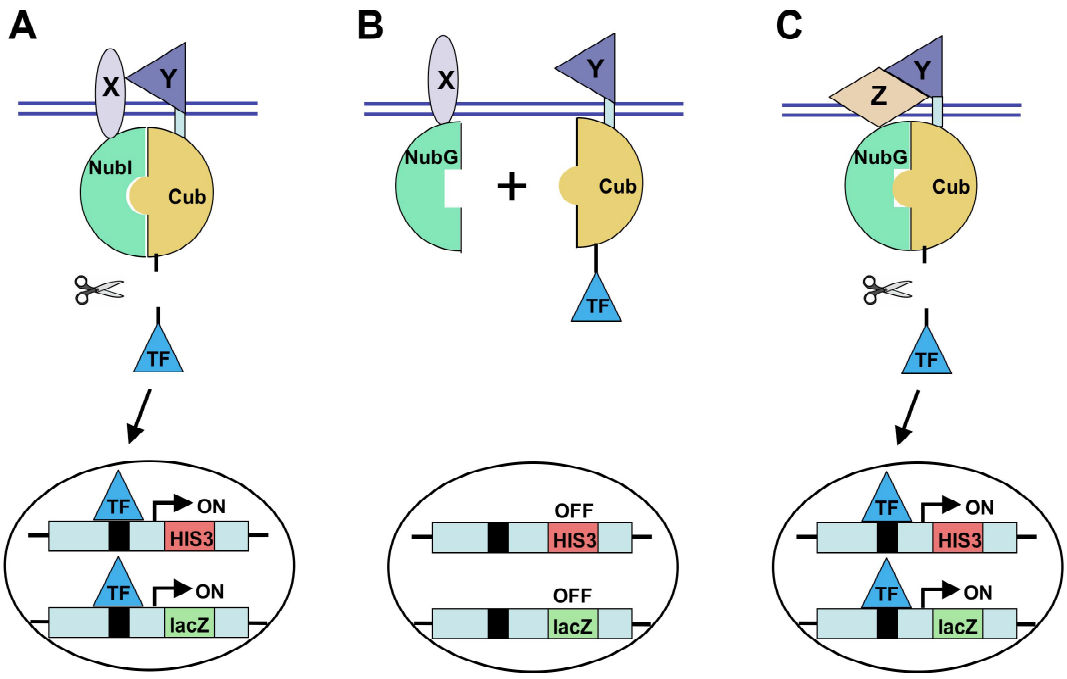

Figure 4-1 Outline of the split ubiquitin yeast two hybrid assay (adapted from FETCHKO and STAGLJAR 2004). (A) Two integral membrane proteins are conjugated with the N- or C-terminal moieties of ubiquitin in forming the bait and prey hybrid proteins. The N-terminal moiety of ubiquitin (NubI) has an ability to interact with C-terminal moiety of ubiquitin (Cub) to reconstitute a functional molecule. As a result, the artificial transcription factor (TF) conjugated to Cub will be cleaved by ubiquitin specific enzyme, and imported into the nucleus. The *HIS3*, *LacZ*, as well as *ADE2* (not shown) reporter genes will then be activated. (B) NubG harbors an I to G mutation to avoid spontaneous interaction with Cub. If there is no interaction between the bait and prey, the Cub and NubG moieties can not reconstitute a functional molecule. The reporter genes *HIS3*, *LacZ*, as well as *ADE2* (not shown) will not be activated. (C) The interaction between the bait and prey proteins will put the NubG and Cub moieties into close proximity and hence reconstitute a functional ubiquitin molecule. As a result, the TF will be released and transported into the nucleus to activate the reporter genes.

domain, about 1141 aa in length, sequestered inside of the NE lumen (TCHEPEREGINE *et al.* 1999). This feature is hypothetically favorable to lumenal interactions, which might play important roles in remodeling the nuclear membrane for NPC biogenesis. Therefore we choose this Pom for the split ubiquitin yeast two hybrid screen in an attempt to identify novel factors that may coordinate with Pom152p in generating a nuclear pore and maintaining a complete NPC architecture.

Based on the N_{cyto}-C_{lumen} membrane orientation of Pom152p, a Cub-TF cassette was fused to the N-terminus of full length Pom152p. The resulting fusion protein LexA-VP16-Cub-Pom152p (gift from D. Rexer) was used as a bait molecule to perform the prerequisite test against a negative control prey Alg5p-NubG or positive control prey Alg5p-NubI. Alg5p is an ER resident membrane protein involved in N-linked glycosylation. Its C-terminus is sequestered in the cytosol. These two prey testers were used to detect the correct membrane orientation of the bait proteins. Cub-Pom152p showed specific interaction with Alg5p-NubI, indicating that the Cub-TF cassette contained in Pom152p fusion protein bait was indeed exposed to the cytosol. To reduce nonspecific growth, a *pom152*Δ mutant strain (gift from D. Rexer) was used as the reporter host. The concentration of 3-aminotriazole (3-AT), a competitive inhibitor of *HIS3* gene product, required to suppress nonspecific activation of the reporter gene was optimized in pilot experiments. Complementation tests in several double mutant strains (SWY3800, SWY3219, and psl21) that rely on wild type *POM152* for viability suggested that the Pom152p bait is a partially functional protein (data not shown).

The *S. cerevisiae* NubG-ORF library (Dualsystems Biotech, Switzerland), a cDNA plasmid library carried on a *TRP1/2μ* vector, was cotransformed with *POM152* bait

plasmid into the host strain. In total, $1.1x10^6$ colonies were screened for growth on SM -leu-trp-his + 5mM 3-AT media. After 5 days of incubation at 30˚C, approximately 160 large colonies (diameter > 1mm) and 240 small colonies (diameter < 1mm) were obtained. These colonies were replica-plated onto SM -leu-trp-his-ade + 10mM 3-AT media. On SM -leu-trp-his-ade + 10mM 3-AT media, the growth of approximately 230 large colonies and 100 small colonies were observed. These colonies were further subjected to a β-galactosidase filter assay, which provides an additional screening criterion based on the *lacZ* reporter gene products. Most, if not all, colonies showed a blue color in the β-galactosidase filter test, and hence were retained for the next verification step.

In total, 112 colonies (100 large and 12 small) were randomly selected from SM -leu-trp-his + 5mM 3-AT media. The prey plasmids harbored in those colonies were tested with either experimental bait Cub-Pom152p or negative control bait Bves-Cub (gift from D. Bader). Growth was verified on SM -leu-trp-his + 5mM 3-AT media and SM –leu-trp-his-ade + 10mM 3-AT media. No Cub-Pom152p specific prey plasmid was obtained from these 112 colonies. Instead, most prey plasmids interacted with both Cub-Pom152p and Bves-Cub baits, or even appeared to interact only with Bves-Cub bait. To sample the molecular nature of these preys, seven of them were chosen for sequencing. The inserts were identified as *PHS1, YPR170W-B, EGD2, DPM1, TSC13, SCS2,* and *PHO88*. *TSC13* was selected to test the saturation of screen. Colony PCR was used to detect *TSC13*-bearing plasmids in the 160 large colonies on SM –leu-trp-his + 5mM 3-AT media, and it was discovered that 7 colonies harbored the same prey plasmid, indicating that the screen was saturated.

The above ORFs encode ER-resident membrane proteins or ER-associated soluble proteins. They function in lipid metabolism, protein sorting and targeting, and phosphate transport. However, all of them give rise to colonies with either Cub-Pom152p or Bves-Cub bait plasmids, arguing that ER localization *per se* is sufficient to drive interaction with bait, and these interactions are not specific to Pom152p function in NPC structural organization.

There are several explanations for why we did not obtain a *POM152* bait specific prey plasmid. Firstly, the epitope tagging with the Cub-TF cassette at the cytoplasmic N-terminus of Pom152p might alter its intracellular localization. The increased ER residence time, either persistent or temporary, might expose the bait protein to nonspecific interactors. Alternatively, the fusion of the Cub-TF cassette might interfere with its physical connections with native NPC/NE factors. R. Wozniak and coworkers reported that the cytoplasmic domain of Pom152p is essential for several double mutants that require wild type *POM152* for viability (TCHEPEREGINE *et al.* 1999). Secondly, the *S. cerevisiae* NubG-ORF library is constructed by a RT-PCR method. The technical challenges in establishing a cDNA library might impair the coverage of the budding yeast ORF pool, hence compromising the possibility to obtain a real physical interactor. Thirdly, membrane proteins encoded by N-terminal tagged NubG-ORF library plasmids might not adopt a native topological orientation, or the NubG epitope is concealed in protein folding process. As such, the NubG moiety of library prey might be inaccessible during the ubiquitin reconstitution-based screen. Fourthly, the prey plasmid is expressed in a high copy mode and might be susceptible to a nonspecific interaction with Pom152p bait. Fifthly, although the step-increased stringency test was applied in the screen, it was

unable to eliminate some false positives as seen in the pilot experiment. Therefore the highest stringency condition is recommended for the initial screen (personal communication with Dualsystems Biotech).

Several experiments could be performed to address the above concerns. An IIF experiment with anti-Pom152p antibody should be used to detect the subcellular localization of Cub-Pom152p bait. An abnormal localization to the cortical ER and/or other cytoplasmic compartments would explain the screen results. A linker sequence could be added in between the Cub-TF cassette and the Pom152p to reduce interference with Pom152p function. The quality of NubG-ORF cDNA library could be examined in terms of insert length, NubG moiety accessibility, nonspecific activation of reporter genes *etc*. A small pool of randomly selected NubG-ORF library plasmids could be used to assess the quality of the library.

Large scale test through the *S. cerevisiae* ORF-Cub collection of integral membrane proteins

Stanley Fields' group has fused the Cub or NubG moieties to a number of *S. cerevisiae* ORFs with putative TM domains. These ORF-Cub or ORF-NubG collections are particularly useful in overcoming the drawback of the cDNA prey library discussed above. The full length ORFs contained in the collections and the C-terminal tagging strategy introduce minimum perturbations to transmembrane protein topology. These tagged membrane protein ORF collections have been successfully applied to large scale yeast two hybrid assays, and an informative table of NE/NPC membrane protein interactions was obtained (MILLER *et al.* 2005). For instance, Pom34p is suggested to

interact with Elo2p and Elo3p, enzymes involved in very long chain fatty acid (VLCFA) biosynthesis, as well as Yop1p, a protein with unique "hairpin-like" membrane topology.

However, due to the N_{cyto}-C_{lumen} membrane orientation adopted by Pom152p, it was not included in the C-terminally tagged ORF-Cub collection. Similarly, there are other NE membrane proteins with the same topological orientation as Pom152p, such as Brr6p and Brl1p (DE BRUYN KOPS and GUTHRIE 2001; SAITOH *et al.* 2005), which are absent from the collection. Using the N-terminally tagged Cub-Pom152p as an effective bait for testing the ORF-NubG collection is likely to yield positive interaction factors. The same strategy could also be applied to Brr6p and Brl1p to complete the NE/NPC membrane protein interaction network.

Analyzing the specific role of Ndc1p in NPC assembly

The *pom34*Δ *pom152*Δ double mutant does not have any significant phenotype in terms of growth rate, FG-Nup localization, intracellular membrane structure, and nuclear transport. It is very likely that Ndc1p plays an essential role in the absence of the two Poms. However, besides the NPC, Ndc1p is also localized to the SPB and required for NE insertion of duplicated SPBs. Studying the function of Ndc1p in NPC assembly is limited by its role in SPB anchorage. Either increasing or decreasing the gene dosage compromises the function of *NDC1* in mitotic spindle formation (CHIAL *et al.* 1999). Previous efforts in isolating *ndc1* conditional alleles have not yielded many NPC specific mutants since the resulting SPB defect leads to a cell cycle arrest before causing relevant NPC phenotypes (CHIAL *et al.* 1998).

Instead of a genetic approach to isolate *ndc1* conditional alleles with particular NPC assembly defects, it might be possible to target Ndc1p exclusively to the SPB through an FKBP-FRB binding method and hence restrain its function to the SPB. The 12kD domain of FK506-binding protein (FKBP) has a specific binding affinity to the FKBP-rapamycin binding domain (FRB) upon the addition of rapamycin (CHEN *et al.* 1995; KLEMM *et al.* 1997; OHBA *et al.* 2004). After conjugating these two small domains to Ndc1p and a SPB component Nbp1p, the Ndc1p might be specifically trapped at the SPB upon rapamycin treatment (ARAKI *et al.* 2006). This would allow us to observe NPC assembly defects without perturbing the role of Ndc1p in SPB function.

The fusion site on Ndc1p would need to be tested and various rapamycin concentrations could be applied to ensure the effective binding between FKBP and FRB. However, tethering Ndc1p to a single SPB component might impair the potential dynamic function of Ndc1p in SPB organization. Therefore, various SPB protein or multiple components in combination could be tested for a maximum maintenance of SPB function. Moreover, increasing the level of Ndc1p molecules trapped at the SPB might interphere with its function. A *MET* repressible promoter could then be used to reduce the *NDC1* expression. Once Ndc1p is trapped at the SPB and correct cell cycle process is verified, the NPC structural integrity, nucleocytoplasmic transport efficiency, and necessity of other Poms or membrane factors in NPC function could be analyzed to pinpoint the effect of Ndc1p in NPC assembly.

Membrane curvature stabilization assay

The ONM and INM join at certain sites in the NE to form a nuclear pore wherein NPC assembly takes place. The initial pore is considered to be unstable due to the highly curved pore membrane, which is energetically unfavorable . The pore might be stabilized by assembling NPC components at the nascent pore, or alternatively, by specified protein and/or lipid composition around the pore membrane. The latter possibility is attracting more attention recently (ANTONNY 2006; DRIN *et al.* 2007). The connection between the ONM and INM results in a 180˚ turn of membrane. Considering the budding yeast NE is 25~30 nm in thickness, this sharply curved nuclear pore membrane is in even tighter conformation than that of trafficking vesicles. The 180˚ bend of the nuclear membrane generates an unbalanced array of two lipid leaflets, potentially leaving a bulky space between phospholipid headgroups. This vacancy is speculated to be occupied by membrane proteins with large transmembrane domains and/or VLCFA with long fatty acyl chains, which in turn stabilize the sharp curvature.

Several ER/NE integral membrane proteins contain unusually large hydrophobic stretches, about 35 amino acids in length. Rtn4C and DP1 in vertebrates are inserted into the lipid bilayer in a "wedge-like" topology (VOELTZ *et al.* 2006), which is predicted to fill in the extra space generated by membrane curvature. They predominantly localize to tubular ER membranes and function to shape the structure. The Rtn1p/Rtn2p/Yop1p complex in *S. cerevisiae* is also composed of large transmembrane domains and may adopt the similar topology as their vertebrate homologs (CALERO *et al.* 2001; DE CRAENE *et al.* 2006; VOELTZ *et al.* 2006). The study of their possible roles in nuclear pore formation and NPC assembly is ongoing in our laboratory.

The role of fatty acid synthesis in NE/NPC morphology maintenance is largely derived from the study of *ACC1*, which encodes an enzyme that functions at a rate limiting step during lipid synthesis. Its gene product catalyzes the biosynthesis of malonyl-CoA, an active two carbon-unit donor for the step-wise fatty acid side chain elongation process. A strain harboring the *acc1-7-1* conditional allele has mislocalized FG-Nups and defective mRNA export. Ultrastructural studies revealed that the ONM and INM are separated from each other in this mutant. The INM often protrudes into the lumenal space of the NE and sometimes forms vesicles in the intermembrane space, presumably resulting from the break of bended nuclear membranes at the nuclear pore (SCHNEITER *et al.* 1996). Biochemical tests suggested that levels of long chain (C_{18} atoms) and very long chain (C_{26} atoms) fatty acids are strikingly reduced in the *acc1-7-1* mutant, while at the same time myristic acid (C_{14} atoms) accumulates in the cell. These observations imply that fatty acid composition might have a role in NE/NPC structure and function (SCHNEITER *et al.* 1996). However, supplementation of malonyl-CoA, long chain, or VLCFA does not rescue the growth defect of *acc1*Δ, probably due to their poor uptake or lack of activation inside of cells.

VLCFAs are elongated from precursor long chain fatty acids through a membrane bound elongase system. This consecutive synthesis pathway involves four steps, and is repeated in four to five cycles. The enzyme complex consists of Elo2p/Elo3p, Ybr159wp, Tsc13p and at least one unknown factor (HAN *et al.* 2002; KOHLWEIN *et al.* 2001; OH *et al.* 1997). VLCFAs predominantly exist in sphingolipids and phosphatidylinositol, which are important components of lipid bilayers. Their large fatty acyl side chains are speculated to fill in the vacancy caused by a sharply curved membrane (SCHNEITER *et al.*

2004). Consistent with their crucial roles in cellular function, the genes encoding the elongase complex are either essential or show synthetic lethality relationships.

To examine the potential effect of VLCFA in NPC assembly, several experiments could be conducted. Firstly, NPC structure and function could be monitored in null or conditional allele mutants from the VLCFA synthesis pathway to gain a comprehensive picture of possible NPC perturbations. This would be largely performed by IIF against Nups and with nuclear transport assays. Ultrastructural studies would pinpoint any NE/NPC morphological defects. Secondly, an enriched NE membrane fraction from wild type and elongase mutant cells could be analyzed for fatty acid profiles. The reduction of VLCFA in the NE is expected along with NPC structural defects. Meanwhile, lipid synthesis inhibitors could be applied to phenocopy the elongase mutant defects. Thirdly, the genes encoding the fatty acid elongase complex could be expressed in a shuffle plasmid to rescue the potential NE/NPC structural defect. They could also be overexpressed to monitor if there is a dominant negative effect on NPC biogenesis. Such studies would help determine if VLCFA plays a direct role in the NPC assembly process.

It is plausible that NE fusion and NPC assembly events might involve factors outside of the NPC. Those factors might play an accessory role during NPC biogenesis and are not necessarily bona fide NPC components. For instance, Tsc13p is physically retained at nucleus-vacuole junction sites by the membrane protein Nvj1p, and hence affects the biogenesis of microautophagic vesicles through local VLCFA synthesis (KVAM *et al.* 2005; KVAM and GOLDFARB 2006). An analogous mechanism might also apply to the nuclear pore membrane. Interactions between Pom34p and Elo2p as well as Elo3p have been reported in the genome wide split ubiquitin yeast two hybrid assay (MILLER *et al.*

2005). Further biochemical experiments could be conducted to verify these interactions and examine other fatty acid elongase enzymes as well. Alternatively, an NPC clustering mutant could be used to observe the coenrichment of elongase complex with NPC clusters. This would help address the question of whether Poms recruit the fatty acid elongase to regions adjacent to the NPC and facilitate the local production of VLCFA.

In summary, the mechanism of NPC assembly might go far beyond what we know at this moment. Poms, as well as other membrane factors outside of the NPCs, are speculated to be involved in this process. Although an attempt to identify potential interaction factors through a Pom152p based genetic screen has not been successful, the genome wide yeast two hybrid analysis of full length integral membrane proteins reported a link between Pom34p and the integral membrane proteins with large transmembrane domains, or the VLCFA synthesis enzymes. These discoveries introduce a novel concept related to stabilizing the sharp membrane curvature of the nuclear pore, and also strongly suggest that membrane based NPC assembly involves various events in multiple genres. To keep seeking unknown factors and characterizing their function in NPC biogenesis will refine our understanding to this basic biological process.

APPENDIX

A. Yeast strains constructed and used

Strain	Genotype	Source
SWY3546	*MAT**a** his3D200 trp1-901 leu2-3,112 ade2 LYS2::(lexAop)4-HIS3 URA3::(lexAop)8-lacZ ade2::(lexAop)8-ADE2 GAL4 POM152::Kan*	Gift from D. Rexer
YOL387	*MAT**a** his3Δ200 trp1-901 leu2-3,112 ade2 LYS2::(lexAop)4-HIS3 URA3::(lexAop)8-lacZ ade2::(lexAop)8-ADE2 GAL4*	Dualsystem Biotech
SWY3790 (pos110)	*MAT**a** pos110 pom34::spHIS5 pom152::HIS3 ura3-1 his3-11,15 lys2 leu2-3,112 can1-100 ade2 ade3* +p*POM34/ADE3/URA3/CEN*	This study
YOL486	*MAT**a** nup192::HIS3 ade2 his3 leu2 trp1 ura3 can1+ YCplac33-URA3-NUP192*	(KOSOVA *et al.* 1999)
YOL487	*MAT**a** nup192::HIS3 ade2 his3 leu2 trp1 ura3 can1+ YCplac22-TRP1-nup192-15*	(KOSOVA *et al.* 1999)
YOL534	*GAL1(::URA3)-NDC1-GFP::HIS3*	(MADRID *et al.* 2006)
YOL535	*GAL1(::URA3)-NDC1-GFP::HIS3 pom34::Kan*	(MADRID *et al.* 2006)
YOL536	*GAL1(::URA3)-NDC1-GFP::HIS3 pom34::Kan pom152::Kan*	(MADRID *et al.* 2006)
YOL586	*GAL1(::URA3)-NDC1-GFP::HIS3 pom152::Kan*	(MADRID *et al.* 2006)
SWY3800	*pom152::HIS3 nup59::Kan^r his3 ura3 leu2 lys2* + p*CH1122-POM152(ADE3-URA3)*	This study
SWY3801	*TSC13-GFP nup133::HIS*	This study
SWY3802	*SCS2-GFP nup133::HIS*	This study
SWY3803	*EGD2-GFP nup133::HIS*	This study
SWY3804	*DPM1-GFP nup133::HIS*	This study
SWY3805	*YBR159W-GFP nup133::HIS*	This study
SWY3806	*SNL1-GFP nup133::HIS*	This study
SWY3807	*PHS1-GFP nup133::HIS*	This study

B. Plasmids constructed and used

Plasmid	Description	Source
pSW3271	*GST-pom34C*	This study
pSW3272	*MBP-pom34C*	This study
pSW3273	*GAD-pom34N*	This study
pSW3274	*GBDU-pom34N*	This study
pSW3275	*GAD-pom34C*	This study
pSW3276	*GBDU-pom34C*	This study
pSW3277	*GBD-pom34N*	This study
pSW3278	*GBD-pom34C*	This study
pSW3279	*GAD-NUP53*	This study
pSW3280	*GBDU-NUP53*	This study
pSW3281	*GAD-NUP59*	This study
pSW3282	*GBDU-NUP59*	This study
CP3149	*Bves-Cub*	Gift from D. Bader
CP3139	*YCplac33-NUP192*	(KOSOVA *et al.* 1999)
CP3105	*RCUP1-NUP53*	(MARELLI *et al.* 2001)
CP3103	*CUP1-NUP53*	(MARELLI *et al.* 2001)
CP3102	*BJ244-NUP53*	(MARELLI *et al.* 2001)
CP3076	*pAI-ALG5*	Dualsystem Biotech
CP3077	*pDL2-ALG5*	Dualsystem Biotech
CP3078	*pCCW-ALG5*	Dualsystem Biotech
pSW3200	*LexA-VP16-Cub-POM152*	Gift from D. Rexer
pSW3184	*LexA-VP16-Cub-POM34*	Gift from D. Rexer

REFERENCES

ADAM, S. A., 2001 The nuclear pore complex. Genome Biol **2:** REVIEWS0007.

AITCHISON, J. D., M. P. ROUT, M. MARELLI, G. BLOBEL and R. W. WOZNIAK, 1995 Two novel related yeast nucleoporins Nup170p and Nup157p: complementation with the vertebrate homologue Nup155p and functional interactions with the yeast nuclear pore-membrane protein Pom152p. J Cell Biol **131:** 1133-1148.

ALLEN, N. P., L. HUANG, A. BURLINGAME and M. REXACH, 2001 Proteomic analysis of nucleoporin interacting proteins. J Biol Chem **276:** 29268-29274.

ALLEN, T. D., J. M. CRONSHAW, S. BAGLEY, E. KISELEVA and M. W. GOLDBERG, 2000 The nuclear pore complex: mediator of translocation between nucleus and cytoplasm. J Cell Sci **113 (Pt 10):** 1651-1659.

ANTONIN, W., C. FRANZ, U. HASELMANN, C. ANTONY and I. W. MATTAJ, 2005 The integral membrane nucleoporin pom121 functionally links nuclear pore complex assembly and nuclear envelope formation. Mol Cell **17:** 83-92.

ANTONIN, W., and I. W. MATTAJ, 2005 Nuclear pore complexes: round the bend? Nat Cell Biol **7:** 10-12.

ANTONNY, B., 2006 Membrane deformation by protein coats. Curr Opin Cell Biol **18:** 386-394.

ARAKI, Y., C. K. LAU, H. MAEKAWA, S. L. JASPERSEN, T. H. GIDDINGS, JR. *et al.*, 2006 The Saccharomyces cerevisiae spindle pole body (SPB) component Nbp1p is required for SPB membrane insertion and interacts with the integral membrane proteins Ndc1p and Mps2p. Mol Biol Cell **17:** 1959-1970.

ARIS, J. P., and G. BLOBEL, 1988 Identification and characterization of a yeast nucleolar protein that is similar to a rat liver nucleolar protein. J Cell Biol **107:** 17-31.

BAILER, S. M., C. BALDUF, J. KATAHIRA, A. PODTELEJNIKOV, C. ROLLENHAGEN *et al.*, 2000 Nup116p associates with the Nup82p-Nsp1p-Nup159p nucleoporin complex. J Biol Chem **275:** 23540-23548.

BAILER, S. M., S. SINIOSSOGLOU, A. PODTELEJNIKOV, A. HELLWIG, M. MANN *et al.*, 1998 Nup116p and nup100p are interchangeable through a conserved motif which constitutes a docking site for the mRNA transport factor gle2p. Embo J **17:** 1107-1119.

BAUDIN, A., O. OZIER-KALOGEROPOULOS, A. DENOUEL, F. LACROUTE and C. CULLIN, 1993 A simple and efficient method for direct gene deletion in Saccharomyces cerevisiae. Nucleic Acids Res **21:** 3329-3330.

BECK, M., F. FORSTER, M. ECKE, J. M. PLITZKO, F. MELCHIOR *et al.*, 2004 Nuclear pore complex structure and dynamics revealed by cryoelectron tomography. Science **306:** 1387-1390.

BELANGER, K. D., M. A. KENNA, S. WEI and L. I. DAVIS, 1994 Genetic and physical interactions between Srp1p and nuclear pore complex proteins Nup1p and Nup2p. J Cell Biol **126:** 619-630.

BELANGER, K. D., L. A. SIMMONS, J. K. ROTH, K. A. VANDERPLOEG, L. B. LICHTEN *et al.*, 2004 The karyopherin Msn5/Kap142 requires Nup82 for nuclear export and performs a function distinct from translocation in RPA protein import. J Biol Chem **279:** 43530-43539.

BELGAREH, N., C. SNAY-HODGE, F. PASTEAU, S. DAGHER, C. N. COLE *et al.*, 1998 Functional characterization of a Nup159p-containing nuclear pore subcomplex. Mol Biol Cell **9:** 3475-3492.

BODOOR, K., S. SHAIKH, D. SALINA, W. H. RAHARJO, R. BASTOS *et al.*, 1999 Sequential recruitment of NPC proteins to the nuclear periphery at the end of mitosis. J Cell Sci **112 (Pt 13):** 2253-2264.

BUCCI, M., and S. R. WENTE, 1997 In vivo dynamics of nuclear pore complexes in yeast. J Cell Biol **136:** 1185-1199.

BUCCI, M., and S. R. WENTE, 1998 A novel fluorescence-based genetic strategy identifies mutants of Saccharomyces cerevisiae defective for nuclear pore complex assembly. Mol Biol Cell **9:** 2439-2461.

BURKE, B., and J. ELLENBERG, 2002 Remodelling the walls of the nucleus. Nat Rev Mol Cell Biol **3:** 487-497.

CALERO, M., G. R. WHITTAKER and R. N. COLLINS, 2001 Yop1p, the yeast homolog of the polyposis locus protein 1, interacts with Yip1p and negatively regulates cell growth. J Biol Chem **276:** 12100-12112.

CHEN, J., X. F. ZHENG, E. J. BROWN and S. L. SCHREIBER, 1995 Identification of an 11-kDa FKBP12-rapamycin-binding domain within the 289-kDa FKBP12-rapamycin-associated protein and characterization of a critical serine residue. Proc Natl Acad Sci U S A **92:** 4947-4951.

CHIAL, H. J., T. H. GIDDINGS, JR., E. A. SIEWERT, M. A. HOYT and M. WINEY, 1999 Altered dosage of the Saccharomyces cerevisiae spindle pole body duplication

gene, NDC1, leads to aneuploidy and polyploidy. Proc Natl Acad Sci U S A **96:** 10200-10205.

CHIAL, H. J., M. P. ROUT, T. H. GIDDINGS and M. WINEY, 1998 Saccharomyces cerevisiae Ndc1p is a shared component of nuclear pore complexes and spindle pole bodies. J Cell Biol **143:** 1789-1800.

CHOOK, Y. M., and G. BLOBEL, 2001 Karyopherins and nuclear import. Curr Opin Struct Biol **11:** 703-715.

CHRISTIANSON, T. W., R. S. SIKORSKI, M. DANTE, J. H. SHERO and P. HIETER, 1992 Multifunctional yeast high-copy-number shuttle vectors. Gene **110:** 119-122.

CRONSHAW, J. M., A. N. KRUTCHINSKY, W. ZHANG, B. T. CHAIT and M. J. MATUNIS, 2002 Proteomic analysis of the mammalian nuclear pore complex. J Cell Biol **158:** 915-927.

DAIGLE, N., J. BEAUDOUIN, L. HARTNELL, G. IMREH, E. HALLBERG *et al.*, 2001 Nuclear pore complexes form immobile networks and have a very low turnover in live mammalian cells. J Cell Biol **154:** 71-84.

DAMELIN, M., and P. A. SILVER, 2002 In situ analysis of spatial relationships between proteins of the nuclear pore complex. Biophys J **83:** 3626-3636.

DAVIS, L. I., and G. BLOBEL, 1986 Identification and characterization of a nuclear pore complex protein. Cell **45:** 699-709.

DE BRUYN KOPS, A., and C. GUTHRIE, 2001 An essential nuclear envelope integral membrane protein, Brr6p, required for nuclear transport. Embo J **20:** 4183-4193.

DE CRAENE, J. O., J. COLEMAN, P. ESTRADA DE MARTIN, M. PYPAERT, S. ANDERSON *et al.*, 2006 Rtn1p is involved in structuring the cortical endoplasmic reticulum. Mol Biol Cell **17:** 3009-3020.

DE SOUZA, C. P., A. H. OSMANI, S. B. HASHMI and S. A. OSMANI, 2004 Partial nuclear pore complex disassembly during closed mitosis in Aspergillus nidulans. Curr Biol **14:** 1973-1984.

DENNING, D., B. MYKYTKA, N. P. ALLEN, L. HUANG, B. AL *et al.*, 2001 The nucleoporin Nup60p functions as a Gsp1p-GTP-sensitive tether for Nup2p at the nuclear pore complex. J Cell Biol **154:** 937-950.

DEVOS, D., S. DOKUDOVSKAYA, F. ALBER, R. WILLIAMS, B. T. CHAIT *et al.*, 2004 Components of coated vesicles and nuclear pore complexes share a common molecular architecture. PLoS Biol **2:** e380.

DILWORTH, D. J., A. SUPRAPTO, J. C. PADOVAN, B. T. CHAIT, R. W. WOZNIAK *et al.*, 2001 Nup2p dynamically associates with the distal regions of the yeast nuclear pore complex. J Cell Biol **153:** 1465-1478.

DOYE, V., and E. HURT, 1997 From nucleoporins to nuclear pore complexes. Curr Opin Cell Biol **9:** 401-411.

DRIN, G., J. F. CASELLA, R. GAUTIER, T. BOEHMER, T. U. SCHWARTZ *et al.*, 2007 A general amphipathic alpha-helical motif for sensing membrane curvature. Nat Struct Mol Biol **14:** 138-146.

EMTAGE, J. L., M. BUCCI, J. L. WATKINS and S. R. WENTE, 1997 Defining the essential functional regions of the nucleoporin Nup145p. J Cell Sci **110 (Pt 7):** 911-925.

ERIKSSON, C., C. RUSTUM and E. HALLBERG, 2004 Dynamic properties of nuclear pore complex proteins in gp210 deficient cells. FEBS Lett **572:** 261-265.

FAHRENKROG, B., and U. AEBI, 2003 The nuclear pore complex: nucleocytoplasmic transport and beyond. Nat Rev Mol Cell Biol **4:** 757-766.

FAVREAU, C., H. J. WORMAN, R. W. WOZNIAK, T. FRAPPIER and J. C. COURVALIN, 1996 Cell cycle-dependent phosphorylation of nucleoporins and nuclear pore membrane protein Gp210. Biochemistry **35:** 8035-8044.

FELDHERR, C. M., D. AKIN and R. J. COHEN, 2001 Regulation of functional nuclear pore size in fibroblasts. J Cell Sci **114:** 4621-4627.

FETCHKO, M., and I. STAGLJAR, 2004 Application of the split-ubiquitin membrane yeast two-hybrid system to investigate membrane protein interactions. Methods **32:** 349-362.

GALY, V., I. W. MATTAJ and P. ASKJAER, 2003 Caenorhabditis elegans nucleoporins Nup93 and Nup205 determine the limit of nuclear pore complex size exclusion in vivo. Mol Biol Cell **14:** 5104-5115.

GIAEVER, G., A. M. CHU, L. NI, C. CONNELLY, L. RILES *et al.*, 2002 Functional profiling of the Saccharomyces cerevisiae genome. Nature **418:** 387-391.

GOLDBERG, M. W., and T. D. ALLEN, 1996 The nuclear pore complex and lamina: three-dimensional structures and interactions determined by field emission in-lens scanning electron microscopy. J Mol Biol **257:** 848-865.

GOLDBERG, M. W., C. WIESE, T. D. ALLEN and K. L. WILSON, 1997 Dimples, pores, star-rings, and thin rings on growing nuclear envelopes: evidence for structural intermediates in nuclear pore complex assembly. J Cell Sci **110 (Pt 4):** 409-420.

GOLDSTEIN, A. L., C. A. SNAY, C. V. HEATH and C. N. COLE, 1996 Pleiotropic nuclear defects associated with a conditional allele of the novel nucleoporin Rat9p/Nup85p. Mol Biol Cell **7:** 917-934.

GOMEZ-OSPINA, N., G. MORGAN, T. H. GIDDINGS, JR., B. KOSOVA, E. HURT *et al.*, 2000 Yeast nuclear pore complex assembly defects determined by nuclear envelope reconstruction. J Struct Biol **132:** 1-5.

GORLICH, D., and U. KUTAY, 1999 Transport between the cell nucleus and the cytoplasm. Annu Rev Cell Dev Biol **15:** 607-660.

GORSCH, L. C., T. C. DOCKENDORFF and C. N. COLE, 1995 A conditional allele of the novel repeat-containing yeast nucleoporin RAT7/NUP159 causes both rapid cessation of mRNA export and reversible clustering of nuclear pore complexes. J Cell Biol **129:** 939-955.

GRAHAM, L. A., and T. H. STEVENS, 1999 Assembly of the yeast vacuolar proton-translocating ATPase. J Bioenerg Biomembr **31:** 39-47.

GRANDI, P., V. DOYE and E. C. HURT, 1993 Purification of NSP1 reveals complex formation with 'GLFG' nucleoporins and a novel nuclear pore protein NIC96. Embo J **12:** 3061-3071.

GRANDI, P., S. EMIG, C. WEISE, F. HUCHO, T. POHL *et al.*, 1995a A novel nuclear pore protein Nup82p which specifically binds to a fraction of Nsp1p. J Cell Biol **130:** 1263-1273.

GRANDI, P., N. SCHLAICH, H. TEKOTTE and E. C. HURT, 1995b Functional interaction of Nic96p with a core nucleoporin complex consisting of Nsp1p, Nup49p and a novel protein Nup57p. Embo J **14:** 76-87.

GREBER, U. F., A. SENIOR and L. GERACE, 1990 A major glycoprotein of the nuclear pore complex is a membrane-spanning polypeptide with a large lumenal domain and a small cytoplasmic tail. Embo J **9:** 1495-1502.

HALLBERG, E., R. W. WOZNIAK and G. BLOBEL, 1993 An integral membrane protein of the pore membrane domain of the nuclear envelope contains a nucleoporin-like region. J Cell Biol **122:** 513-521.

HAN, G., K. GABLE, S. D. KOHLWEIN, F. BEAUDOIN, J. A. NAPIER *et al.*, 2002 The Saccharomyces cerevisiae YBR159w gene encodes the 3-ketoreductase of the microsomal fatty acid elongase. J Biol Chem **277:** 35440-35449.

HAREL, A., R. C. CHAN, A. LACHISH-ZALAIT, E. ZIMMERMAN, M. ELBAUM *et al.*, 2003a Importin beta negatively regulates nuclear membrane fusion and nuclear pore complex assembly. Mol Biol Cell **14:** 4387-4396.

HAREL, A., A. V. ORJALO, T. VINCENT, A. LACHISH-ZALAIT, S. VASU *et al.*, 2003b Removal of a single pore subcomplex results in vertebrate nuclei devoid of nuclear pores. Mol Cell **11:** 853-864.

HAWRYLUK-GARA, L. A., E. K. SHIBUYA and R. W. WOZNIAK, 2005 Vertebrate Nup53 interacts with the nuclear lamina and is required for the assembly of a Nup93-containing complex. Mol Biol Cell **16:** 2382-2394.

HO, A. K., G. A. RACZNIAK, E. B. IVES and S. R. WENTE, 1998 The integral membrane protein snl1p is genetically linked to yeast nuclear pore complex function. Mol Biol Cell **9:** 355-373.

HO, A. K., T. X. SHEN, K. J. RYAN, E. KISELEVA, M. A. LEVY *et al.*, 2000 Assembly and preferential localization of Nup116p on the cytoplasmic face of the nuclear pore complex by interaction with Nup82p. Mol Cell Biol **20:** 5736-5748.

HUH, W. K., J. V. FALVO, L. C. GERKE, A. S. CARROLL, R. W. HOWSON *et al.*, 2003 Global analysis of protein localization in budding yeast. Nature **425:** 686-691.

HURWITZ, M. E., C. STRAMBIO-DE-CASTILLIA and G. BLOBEL, 1998 Two yeast nuclear pore complex proteins involved in mRNA export form a cytoplasmically oriented subcomplex. Proc Natl Acad Sci U S A **95:** 11241-11245.

IMREH, G., and E. HALLBERG, 2000 An integral membrane protein from the nuclear pore complex is also present in the annulate lamellae: implications for annulate lamella formation. Exp Cell Res **259:** 180-190.

IMREH, G., D. MAKSEL, J. B. DE MONVEL, L. BRANDEN and E. HALLBERG, 2003 ER retention may play a role in sorting of the nuclear pore membrane protein POM121. Exp Cell Res **284:** 173-184.

ITO, H., Y. FUKUDA, K. MURATA and A. KIMURA, 1983 Transformation of intact yeast cells treated with alkali cations. J Bacteriol **153:** 163-168.

KENNA, M. A., J. G. PETRANKA, J. L. REILLY and L. I. DAVIS, 1996 Yeast N1e3p/Nup170p is required for normal stoichiometry of FG nucleoporins within the nuclear pore complex. Mol Cell Biol **16:** 2025-2036.

KIM, H., K. MELEN and G. VON HEIJNE, 2003 Topology models for 37 Saccharomyces cerevisiae membrane proteins based on C-terminal reporter fusions and predictions. J Biol Chem **278:** 10208-10213.

KISELEVA, E., M. W. GOLDBERG, B. DANEHOLT and T. D. ALLEN, 1996 RNP export is mediated by structural reorganization of the nuclear pore basket. J Mol Biol **260:** 304-311.

KISELEVA, E., S. RUTHERFORD, L. M. COTTER, T. D. ALLEN and M. W. GOLDBERG, 2001 Steps of nuclear pore complex disassembly and reassembly during mitosis in early Drosophila embryos. J Cell Sci **114:** 3607-3618.

KLEMM, J. D., C. R. BEALS and G. R. CRABTREE, 1997 Rapid targeting of nuclear proteins to the cytoplasm. Curr Biol **7:** 638-644.

KOHLWEIN, S. D., S. EDER, C. S. OH, C. E. MARTIN, K. GABLE *et al.*, 2001 Tsc13p is required for fatty acid elongation and localizes to a novel structure at the nuclear-vacuolar interface in Saccharomyces cerevisiae. Mol Cell Biol **21:** 109-125.

KONING, A. J., P. Y. LUM, J. M. WILLIAMS and R. WRIGHT, 1993 DiOC6 staining reveals organelle structure and dynamics in living yeast cells. Cell Motil Cytoskeleton **25:** 111-128.

KOSOVA, B., N. PANTE, C. ROLLENHAGEN and E. HURT, 1999 Nup192p is a conserved nucleoporin with a preferential location at the inner site of the nuclear membrane. J Biol Chem **274:** 22646-22651.

KVAM, E., K. GABLE, T. M. DUNN and D. S. GOLDFARB, 2005 Targeting of Tsc13p to nucleus-vacuole junctions: a role for very-long-chain fatty acids in the biogenesis of microautophagic vesicles. Mol Biol Cell **16:** 3987-3998.

KVAM, E., and D. S. GOLDFARB, 2006 Structure and function of nucleus-vacuole junctions: outer-nuclear-membrane targeting of Nvj1p and a role in tryptophan uptake. J Cell Sci **119:** 3622-3633.

KYTE, J., and R. F. DOOLITTLE, 1982 A simple method for displaying the hydropathic character of a protein. J Mol Biol **157:** 105-132.

LAU, C. K., V. A. DELMAR and D. J. FORBES, 2006 Topology of yeast Ndc1p: predictions for the human NDC1/NET3 homologue. Anat Rec A Discov Mol Cell Evol Biol **288:** 681-694.

LAU, C. K., T. H. GIDDINGS, JR. and M. WINEY, 2004 A novel allele of Saccharomyces cerevisiae NDC1 reveals a potential role for the spindle pole body component Ndc1p in nuclear pore assembly. Eukaryot Cell **3:** 447-458.

LENART, P., G. RABUT, N. DAIGLE, A. R. HAND, M. TERASAKI *et al.*, 2003 Nuclear envelope breakdown in starfish oocytes proceeds by partial NPC disassembly followed by a rapidly spreading fenestration of nuclear membranes. J Cell Biol **160:** 1055-1068.

LIU, J., A. J. PRUNUSKE, A. M. FAGER and K. S. ULLMAN, 2003 The COPI complex functions in nuclear envelope breakdown and is recruited by the nucleoporin Nup153. Dev Cell **5:** 487-498.

LUSK, C. P., T. MAKHNEVYCH, M. MARELLI, J. D. AITCHISON and R. W. WOZNIAK, 2002 Karyopherins in nuclear pore biogenesis: a role for Kap121p in the assembly of Nup53p into nuclear pore complexes. J Cell Biol **159:** 267-278.

LUTZMANN, M., R. KUNZE, A. BUERER, U. AEBI and E. HURT, 2002 Modular self-assembly of a Y-shaped multiprotein complex from seven nucleoporins. Embo J **21:** 387-397.

LUTZMANN, M., R. KUNZE, K. STANGL, P. STELTER, K. F. TOTH *et al.*, 2005 Reconstitution of Nup157 and Nup145N into the Nup84 complex. J Biol Chem **280:** 18442-18451.

MACAULAY, C., and D. J. FORBES, 1996 Assembly of the nuclear pore: biochemically distinct steps revealed with NEM, GTP gamma S, and BAPTA. J Cell Biol **132:** 5-20.

MADRID, A. S., J. MANCUSO, W. Z. CANDE and K. WEIS, 2006 The role of the integral membrane nucleoporins Ndc1p and Pom152p in nuclear pore complex assembly and function. J Cell Biol **173:** 361-371.

MANS, B. J., V. ANANTHARAMAN, L. ARAVIND and E. V. KOONIN, 2004 Comparative genomics, evolution and origins of the nuclear envelope and nuclear pore complex. Cell Cycle **3:** 1612-1637.

MANSFELD, J., S. GUTTINGER, L. A. HAWRYLUK-GARA, N. PANTE, M. MALL *et al.*, 2006 The conserved transmembrane nucleoporin NDC1 is required for nuclear pore complex assembly in vertebrate cells. Mol Cell **22:** 93-103.

MARELLI, M., J. D. AITCHISON and R. W. WOZNIAK, 1998 Specific binding of the karyopherin Kap121p to a subunit of the nuclear pore complex containing Nup53p, Nup59p, and Nup170p. J Cell Biol **143:** 1813-1830.

MARELLI, M., C. P. LUSK, H. CHAN, J. D. AITCHISON and R. W. WOZNIAK, 2001 A link between the synthesis of nucleoporins and the biogenesis of the nuclear envelope. J Cell Biol **153:** 709-724.

MAUL, G. G., H. M. MAUL, J. E. SCOGNA, M. W. LIEBERMAN, G. S. STEIN *et al.*, 1972 Time sequence of nuclear pore formation in phytohemagglutinin-stimulated lymphocytes and in HeLa cells during the cell cycle. J Cell Biol **55:** 433-447.

MAUL, G. G., J. W. PRICE and M. W. LIEBERMAN, 1971 Formation and distribution of nuclear pore complexes in interphase. J Cell Biol **51:** 405-418.

MCGEE, M. D., R. RILLO, A. S. ANDERSON and D. A. STARR, 2006 UNC-83 IS a KASH protein required for nuclear migration and is recruited to the outer nuclear membrane by a physical interaction with the SUN protein UNC-84. Mol Biol Cell **17:** 1790-1801.

MILLER, J. P., R. S. LO, A. BEN-HUR, C. DESMARAIS, I. STAGLJAR *et al.*, 2005 Large-scale identification of yeast integral membrane protein interactions. Proc Natl Acad Sci U S A **102:** 12123-12128.

MULUGETA, S., and M. F. BEERS, 2003 Processing of surfactant protein C requires a type II transmembrane topology directed by juxtamembrane positively charged residues. J Biol Chem **278:** 47979-47986.

MURPHY, R., J. L. WATKINS and S. R. WENTE, 1996 GLE2, a Saccharomyces cerevisiae homologue of the Schizosaccharomyces pombe export factor RAE1, is required for nuclear pore complex structure and function. Mol Biol Cell **7:** 1921-1937.

MURPHY, R., and S. R. WENTE, 1996 An RNA-export mediator with an essential nuclear export signal. Nature **383:** 357-360.

NEHRBASS, U., H. KERN, A. MUTVEI, H. HORSTMANN, B. MARSHALLSAY *et al.*, 1990 NSP1: a yeast nuclear envelope protein localized at the nuclear pores exerts its essential function by its carboxy-terminal domain. Cell **61:** 979-989.

NEHRBASS, U., M. P. ROUT, S. MAGUIRE, G. BLOBEL and R. W. WOZNIAK, 1996 The yeast nucleoporin Nup188p interacts genetically and physically with the core structures of the nuclear pore complex. J Cell Biol **133:** 1153-1162.

OH, C. S., D. A. TOKE, S. MANDALA and C. E. MARTIN, 1997 ELO2 and ELO3, homologues of the Saccharomyces cerevisiae ELO1 gene, function in fatty acid elongation and are required for sphingolipid formation. J Biol Chem **272:** 17376-17384.

OHBA, T., E. C. SCHIRMER, T. NISHIMOTO and L. GERACE, 2004 Energy- and temperature-dependent transport of integral proteins to the inner nuclear membrane via the nuclear pore. J Cell Biol **167:** 1051-1062.

OLSSON, M., S. SCHEELE and P. EKBLOM, 2004 Limited expression of nuclear pore membrane glycoprotein 210 in cell lines and tissues suggests cell-type specific nuclear pores in metazoans. Exp Cell Res **292:** 359-370.

ONISCHENKO, E. A., N. V. GUBANOVA, E. V. KISELEVA and E. HALLBERG, 2005 Cdk1 and okadaic acid-sensitive phosphatases control assembly of nuclear pore complexes in Drosophila embryos. Mol Biol Cell **16:** 5152-5162.

OSMANI, A. H., J. DAVIES, H. L. LIU, A. NILE and S. A. OSMANI, 2006 Systematic deletion and mitotic localization of the nuclear pore complex proteins of Aspergillus nidulans. Mol Biol Cell **17:** 4946-4961.

PANTE, N., and U. AEBI, 1996 Sequential binding of import ligands to distinct nucleopore regions during their nuclear import. Science **273:** 1729-1732.

PANTE, N., and M. KANN, 2002 Nuclear pore complex is able to transport macromolecules with diameters of about 39 nm. Mol Biol Cell **13:** 425-434.

PRUNUSKE, A. J., J. LIU, S. ELGORT, J. JOSEPH, M. DASSO *et al.*, 2006 Nuclear envelope breakdown is coordinated by both Nup358/RanBP2 and Nup153, two nucleoporins with zinc finger modules. Mol Biol Cell **17:** 760-769.

PYHTILA, B., and M. REXACH, 2003 A gradient of affinity for the karyopherin Kap95p along the yeast nuclear pore complex. J Biol Chem **278:** 42699-42709.

RABUT, G., V. DOYE and J. ELLENBERG, 2004 Mapping the dynamic organization of the nuclear pore complex inside single living cells. Nat Cell Biol **6:** 1114-1121.

RAPOPORT, T. A., V. GODER, S. U. HEINRICH and K. E. MATLACK, 2004 Membrane-protein integration and the role of the translocation channel. Trends Cell Biol **14:** 568-575.

ROMANO, J. D., and S. MICHAELIS, 2001 Topological and mutational analysis of Saccharomyces cerevisiae Ste14p, founding member of the isoprenylcysteine carboxyl methyltransferase family. Mol Biol Cell **12:** 1957-1971.

ROUT, M. P., J. D. AITCHISON, A. SUPRAPTO, K. HJERTAAS, Y. ZHAO *et al.*, 2000 The yeast nuclear pore complex: composition, architecture, and transport mechanism. J Cell Biol **148:** 635-651.

RYAN, K. J., J. M. MCCAFFERY and S. R. WENTE, 2003 The Ran GTPase cycle is required for yeast nuclear pore complex assembly. J Cell Biol **160:** 1041-1053.

RYAN, K. J., and S. R. WENTE, 2002 Isolation and characterization of new Saccharomyces cerevisiae mutants perturbed in nuclear pore complex assembly. BMC Genet **3:** 17.

RYAN, K. J., Y. ZHOU and S. R. WENTE, 2006 The Karyopherin Kap95 Regulates Nuclear Pore Complex Assembly into Intact Nuclear Envelopes In Vivo. Mol Biol Cell.

SAAVEDRA, C. A., C. M. HAMMELL, C. V. HEATH and C. N. COLE, 1997 Yeast heat shock mRNAs are exported through a distinct pathway defined by Rip1p. Genes Dev **11:** 2845-2856.

SAITOH, Y. H., K. OGAWA and T. NISHIMOTO, 2005 Brl1p -- a novel nuclear envelope protein required for nuclear transport. Traffic **6:** 502-517.

SANTOS-ROSA, H., J. LEUNG, N. GRIMSEY, S. PEAK-CHEW and S. SINIOSSOGLOU, 2005 The yeast lipin Smp2 couples phospholipid biosynthesis to nuclear membrane growth. Embo J **24:** 1931-1941.

SAZER, S., and M. DASSO, 2000 The ran decathlon: multiple roles of Ran. J Cell Sci **113 (Pt 7):** 1111-1118.

SCHLAICH, N. L., M. HANER, A. LUSTIG, U. AEBI and E. C. HURT, 1997 In vitro reconstitution of a heterotrimeric nucleoporin complex consisting of recombinant Nsp1p, Nup49p, and Nup57p. Mol Biol Cell **8:** 33-46.

SCHNEITER, R., B. BRUGGER, C. M. AMANN, G. D. PRESTWICH, R. F. EPAND *et al.*, 2004 Identification and biophysical characterization of a very-long-chain-fatty-acid-substituted phosphatidylinositol in yeast subcellular membranes. Biochem J **381:** 941-949.

SCHNEITER, R., M. HITOMI, A. S. IVESSA, E. V. FASCH, S. D. KOHLWEIN *et al.*, 1996 A yeast acetyl coenzyme A carboxylase mutant links very-long-chain fatty acid synthesis to the structure and function of the nuclear membrane-pore complex. Mol Cell Biol **16:** 7161-7172.

SCHNELL, D. J., and D. N. HEBERT, 2003 Protein translocons: multifunctional mediators of protein translocation across membranes. Cell **112:** 491-505.

SENGSTAG, C., 2000 Using SUC2-HIS4C reporter domain to study topology of membrane proteins in Saccharomyces cerevisiae. Methods Enzymol **327:** 175-190.

Sherman, F., G. R. Fink and J. B. Hicks, 1986. *Methods in Yeast Genetics*. Cold Spring Harbor Laboratory Press, Cold Spring Harbor, NY.

SHULGA, N., N. MOSAMMAPARAST, R. WOZNIAK and D. S. GOLDFARB, 2000 Yeast nucleoporins involved in passive nuclear envelope permeability. J Cell Biol **149:** 1027-1038.

SHULGA, N., P. ROBERTS, Z. GU, L. SPITZ, M. M. TABB *et al.*, 1996 In vivo nuclear transport kinetics in Saccharomyces cerevisiae: a role for heat shock protein 70 during targeting and translocation. J Cell Biol **135:** 329-339.

SIKORSKI, R. S., and P. HIETER, 1989 A system of shuttle vectors and yeast host strains designed for efficient manipulation of DNA in Saccharomyces cerevisiae. Genetics **122:** 19-27.

SINIOSSOGLOU, S., M. LUTZMANN, H. SANTOS-ROSA, K. LEONARD, S. MUELLER *et al.*, 2000 Structure and assembly of the Nup84p complex. J Cell Biol **149:** 41-54.

SINIOSSOGLOU, S., H. SANTOS-ROSA, J. RAPPSILBER, M. MANN and E. HURT, 1998 A novel complex of membrane proteins required for formation of a spherical nucleus. Embo J **17:** 6449-6464.

SMYTHE, C., H. E. JENKINS and C. J. HUTCHISON, 2000 Incorporation of the nuclear pore basket protein nup153 into nuclear pore structures is dependent upon lamina assembly: evidence from cell-free extracts of Xenopus eggs. Embo J **19:** 3918-3931.

SODERQVIST, H., and E. HALLBERG, 1994 The large C-terminal region of the integral pore membrane protein, POM121, is facing the nuclear pore complex. Eur J Cell Biol **64:** 186-191.

SONDERMANN, H., A. K. HO, L. L. LISTENBERGER, K. SIEGERS, I. MOAREFI *et al.*, 2002 Prediction of novel Bag-1 homologs based on structure/function analysis identifies Snl1p as an Hsp70 co-chaperone in Saccharomyces cerevisiae. J Biol Chem **277:** 33220-33227.

STADE, K., C. S. FORD, C. GUTHRIE and K. WEIS, 1997 Exportin 1 (Crm1p) is an essential nuclear export factor. Cell **90:** 1041-1050.

STAVRU, F., B. B. HULSMANN, A. SPANG, E. HARTMANN, V. C. CORDES *et al.*, 2006a NDC1: a crucial membrane-integral nucleoporin of metazoan nuclear pore complexes. J Cell Biol **173:** 509-519.

STAVRU, F., G. NAUTRUP-PEDERSEN, V. C. CORDES and D. GORLICH, 2006b Nuclear pore complex assembly and maintenance in POM121- and gp210-deficient cells. J Cell Biol **173:** 477-483.

STOFFLER, D., B. FEJA, B. FAHRENKROG, J. WALZ, D. TYPKE *et al.*, 2003 Cryo-electron tomography provides novel insights into nuclear pore architecture: implications for nucleocytoplasmic transport. J Mol Biol **328:** 119-130.

STRAMBIO-DE-CASTILLIA, C., G. BLOBEL and M. P. ROUT, 1995 Isolation and characterization of nuclear envelopes from the yeast Saccharomyces. J Cell Biol **131:** 19-31.

STRAWN, L. A., T. SHEN, N. SHULGA, D. S. GOLDFARB and S. R. WENTE, 2004 Minimal nuclear pore complexes define FG repeat domains essential for transport. Nat Cell Biol **6:** 197-206.

STRAWN, L. A., T. SHEN and S. R. WENTE, 2001 The GLFG regions of Nup116p and Nup100p serve as binding sites for both Kap95p and Mex67p at the nuclear pore complex. J Biol Chem **276:** 6445-6452.

SUNTHARALINGAM, M., and S. R. WENTE, 2003 Peering through the pore: nuclear pore complex structure, assembly, and function. Dev Cell **4:** 775-789.

TASTO, J. J., R. H. CARNAHAN, W. H. MCDONALD and K. L. GOULD, 2001 Vectors and gene targeting modules for tandem affinity purification in Schizosaccharomyces pombe. Yeast **18:** 657-662.

TCHEPEREGINE, S. E., M. MARELLI and R. W. WOZNIAK, 1999 Topology and functional domains of the yeast pore membrane protein Pom152p. J Biol Chem **274:** 5252-5258.

VAN CRIEKINGE, W., and R. BEYAERT, 1999 Yeast Two-Hybrid: State of the Art. Biol Proced Online **2:** 1-38.

VAN DEN BERG, B., W. M. CLEMONS, JR., I. COLLINSON, Y. MODIS, E. HARTMANN *et al.*, 2004 X-ray structure of a protein-conducting channel. Nature **427:** 36-44.

VOELTZ, G. K., W. A. PRINZ, Y. SHIBATA, J. M. RIST and T. A. RAPOPORT, 2006 A class of membrane proteins shaping the tubular endoplasmic reticulum. Cell **124:** 573-586.

WALTHER, T. C., A. ALVES, H. PICKERSGILL, I. LOIODICE, M. HETZER *et al.*, 2003a The conserved Nup107-160 complex is critical for nuclear pore complex assembly. Cell **113:** 195-206.

WALTHER, T. C., P. ASKJAER, M. GENTZEL, A. HABERMANN, G. GRIFFITHS *et al.*, 2003b RanGTP mediates nuclear pore complex assembly. Nature **424:** 689-694.

WENTE, S. R., and G. BLOBEL, 1993 A temperature-sensitive NUP116 null mutant forms a nuclear envelope seal over the yeast nuclear pore complex thereby blocking nucleocytoplasmic traffic. J Cell Biol **123:** 275-284.

WENTE, S. R., and G. BLOBEL, 1994 NUP145 encodes a novel yeast glycine-leucine-phenylalanine-glycine (GLFG) nucleoporin required for nuclear envelope structure. J Cell Biol **125:** 955-969.

WENTE, S. R., M. P. ROUT and G. BLOBEL, 1992 A new family of yeast nuclear pore complex proteins. J Cell Biol **119:** 705-723.

WINEY, M., D. YARAR, T. H. GIDDINGS, JR. and D. N. MASTRONARDE, 1997 Nuclear pore complex number and distribution throughout the Saccharomyces cerevisiae cell cycle by three-dimensional reconstruction from electron micrographs of nuclear envelopes. Mol Biol Cell **8:** 2119-2132.

WOZNIAK, R. W., E. BARTNIK and G. BLOBEL, 1989 Primary structure analysis of an integral membrane glycoprotein of the nuclear pore. J Cell Biol **108:** 2083-2092.

WOZNIAK, R. W., G. BLOBEL and M. P. ROUT, 1994 POM152 is an integral protein of the pore membrane domain of the yeast nuclear envelope. J Cell Biol **125:** 31-42.

YANG, L., T. GUAN and L. GERACE, 1997 Integral membrane proteins of the nuclear envelope are dispersed throughout the endoplasmic reticulum during mitosis. J Cell Biol **137:** 1199-1210.

YANG, Q., M. P. ROUT and C. W. AKEY, 1998 Three-dimensional architecture of the isolated yeast nuclear pore complex: functional and evolutionary implications. Mol Cell **1:** 223-234.

YORK, J. D., A. R. ODOM, R. MURPHY, E. B. IVES and S. R. WENTE, 1999 A phospholipase C-dependent inositol polyphosphate kinase pathway required for efficient messenger RNA export. Science **285:** 96-100.

YOUNG, J. C., J. M. BARRAL and F. ULRICH HARTL, 2003 More than folding: localized functions of cytosolic chaperones. Trends Biochem Sci **28:** 541-547.

YOUNG, K. H., 1998 Yeast two-hybrid: so many interactions, (in) so little time. Biol Reprod **58:** 302-311.

ZABEL, U., V. DOYE, H. TEKOTTE, R. WEPF, P. GRANDI *et al.*, 1996 Nic96p is required for nuclear pore formation and functionally interacts with a novel nucleoporin, Nup188p. J Cell Biol **133:** 1141-1152.